

Lawrence Berkeley National Laboratory

Recent Work

Title

THERMODYNAMIC STUDIES OF Ga-In, Ga-Sb AND Ga-In-Sb LIQUID ALLOYS BY SOLID STATE ELECTROCHEMISTRY WITH OXIDE ELECTROLYTES

Permalink

<https://escholarship.org/uc/item/60q2752b>

Author

Pong, Raymond.

Publication Date

1975-04-01

c. 2

RECEIVED
JUL 23 1975
RADIATION LABORATORY

JUL 23 1975

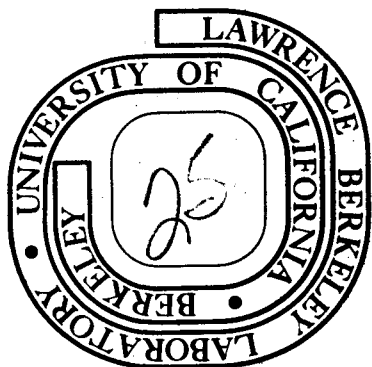
LAWRENCE BERKELEY
DEVELOPMENT DIVISION

**THERMODYNAMIC STUDIES OF Ga-In, Ga-Sb AND Ga-In-Sb
LIQUID ALLOYS BY SOLID STATE ELECTROCHEMISTRY
WITH OXIDE ELECTROLYTES**

Raymond Pong
(M.S. thesis)

April 1975

Prepared for the U.S. Energy Research and
Development Administration under Contract W-7405-ENG-48



TWO-WEEK LOAN COPY
This is a Library Circulating Copy
which may be borrowed for two weeks.
For a personal retention copy, call
Tech. Info. Division.

DISCLAIMER

This document was prepared as an account of work sponsored by the United States Government. While this document is believed to contain correct information, neither the United States Government nor any agency thereof, nor the Regents of the University of California, nor any of their employees, makes any warranty, express or implied, or assumes any legal responsibility for the accuracy, completeness, or usefulness of any information, apparatus, product, or process disclosed, or represents that its use would not infringe privately owned rights. Reference herein to any specific commercial product, process, or service by its trade name, trademark, manufacturer, or otherwise, does not necessarily constitute or imply its endorsement, recommendation, or favoring by the United States Government or any agency thereof, or the Regents of the University of California. The views and opinions of authors expressed herein do not necessarily state or reflect those of the United States Government or any agency thereof or the Regents of the University of California.

THERMODYNAMIC STUDIES OF Ga-In, Ga-Sb and Ga-In-Sb
LIQUID ALLOYS BY SOLID STATE ELECTROCHEMISTRY WITH OXIDE ELECTROLYTES

Contents

Abstract	v
I. General Introduction	1
References	4
II. Theory	6
A. Introduction	6
B. The Nernst Equation	6
C. Solid Oxide Electrolytes	8
D. P_{O_2} Range of CSZ and YDT	9
References	12
Figures	14
III. Experimental Apparatus and Procedures	15
A. Introduction	15
B. Ga-In Cell	15
1. Apparatus	15
2. Procedures	19
C. Ga-Sb, Ga-In-Sb Cells	21
1. Apparatus	21
2. Procedures	23
References	25
Figures	26
IV. The Ga-In System	33
A. Results	33
B. Discussion	36

I. GENERAL INTRODUCTION

Solid state electrochemical methods were applied to the study of the thermodynamic properties of Ga-In-Sb liquid alloys. The experimental investigations on the ternary required that the available data on two of the corresponding binaries be verified. The In-Sb system has been investigated quite thoroughly by Terpilowsky,¹ Hoshino et al.,² and Chatterji and Smith³ using liquid and solid electrolyte techniques. Also, the Ga-Sb system has been experimentally explored on a limited basis by Danilin and Yatsenko⁴ using an electrolyte technique, adding to the earlier study by Schottky and Bever⁵ through liquidus measurements. The Ga-In system has been somewhat more thoroughly explored by Klinedinst et al.⁶ using a solid state electrolyte technique, by Svirbely et al.⁷ using studies of the liquidus as determined by resistivity measurements, and by Denny et al.⁸ using cooling and melting studies of given alloy compositions followed by metallographic examination of the quenched alloy melts.

The liquidus in the Ga-In-Sb ternary system has been explored experimentally by Köster and Thomas.⁹ Component activities in the ternary system have been calculated by Blom and Plaskett¹⁰ using activity data for In-Sb, Ga-Sb, and In-Ga, activity data for the InSb-GaSb pseudo-binary, and liquidus data for the ternary. In this study, activities of gallium in the Ga-In and Ga-Sb systems were studied further and the gallium activities in the $Ga_x In_{1-x} Sb$ system studied for a gallium rich alloy.

Recent work on the Ga-In-Sb system was spurred on by the important semiconducting properties of the intermetallics GaSb and InSb and by Gunn-effect device applications of $\text{Ga}_x\text{In}_{1-x}\text{Sb}$ solid solutions. The semiconducting properties of GaSb are much like those of Ge or are superior. Also, both GaSb and InSb are good candidates for light emitting diode (LED) materials in the infrared region. The interest in InSb is mainly due to the Gunn effect exhibited when a magnetic field is applied. The greatest interest is in $\text{Ga}_x\text{In}_{1-x}\text{Sb}$ as a Gunn-effect device material.¹¹⁻¹³ Gunn-effect devices are useful for the amplification of small signals, generation of microwave signals, and generation of microwave power.

Studies of $\text{Ga}_x\text{In}_{1-x}\text{Sb}$ have shown the Gunn effect for the composition range $0.3 < x < 0.54$.¹⁶ The important characteristics of Gunn effect materials, such as the bandgap between the valence and conduction bands and the energy separation of the sub-bands of the conduction band, have been studied by a number of methods.¹⁷⁻²² From such data, as described above, and from Monte Carlo calculations of the characteristics important to the operation of Gunn-effect devices, Hilsum and Rees¹² have theorized that $\text{Ga}_x\text{In}_{1-x}\text{Sb}$ with $0.7 < x < 0.95$ will have very favorable Gunn-effect characteristics due to electron transfer between 3 sub-bands in the conduction band; in GaAs, the Gunn effect depends on transfer between two sub-bands. As of 1970 efforts to fabricate a Gunn-effect device from $\text{Ga}_x\text{In}_{1-x}\text{Sb}$ have failed for values of $x > 0.55$. The failures have been attributed to the lack of sufficiently lightly doped n-type $\text{Ga}_x\text{In}_{1-x}\text{Sb}$.¹²

Because of the interest shown recently in the quasi-chemical treatment, a closer examination was accorded this treatment and its derivation. By using mathematical procedures described by Guggenheim,²³ the quasi-chemical treatment was extended to next-nearest neighbors and third nearest neighbors for a simple cubic lattice. Though the mathematical procedures of Guggenheim were followed, a new method of bond counting was used. This difference led to a conclusion different from that reached by Guggenheim regarding the consolute temperature. In addition, by going to higher order approximations, the quasi-chemical model was shown to yield activity coefficients approaching those of the α -parameter model (i.e., 0th order quasi-chemical model).

REFERENCES

1. J. Terpilowsky, *Archiwam Hutnictwa* IV-4, 355 (1959).
2. H. Hoshino, Y. Nakamura, M. Shimoji, K. Niwa, *Berichte der Bunsengesellschaft* 69(2), 114 (1965).
3. D. Chatterji, J. V. Smith, *J. Electrochem. Soc.* 120(6), 770 (1973).
4. V. N. Danilin, S. P. Yatsonko, *Akad. Nauk, SSSR* 2, 145 (1970).
5. W. F. Schottky, M. B. Bever, *Acta Met.* 7, 322 (1958).
6. K. A. Klinedinst, M. V. Rao, D. A. Stevenson, *J. Electrochem. Soc.* 119, 1261 (1972).
7. W. J. Svirbely, S. M. Selis, *J. Phys. Chem.* 58, 33 (1954).
8. J. P. Denny, J. H. Hamilton, J. R. Lewis, *J. Metals*, p. 39 (1952).
9. V. W. Köster, B. Thoma, *Z. Metallkunde* 46, 293 (1955).
10. G. M. Blom, T. S. Plaskett, *J. Electrochem. Soc.* 118, 1832 (1971).
11. J. C. McGroddy, Negative Differential Conductivity in Semiconductors in Proceedings of the Tenth International Conference on the Physics of Semiconductors, U. S. Atomic Energy Commission, 1970, p. 31.
12. C. Hilsum, H. D. Rees, A Detailed Analysis of Three-Level Electron Transfer in Proceedings of the Tenth International Conference on the Physics of Semiconductors, U. S. Atomic Energy Commission, 1970, p. 45.
13. A. Joulie, J. Allegre, G. Bougnot, *Mater. Res. Bull.* 7, 1101 (1972).
14. J. C. McGroddy, M. R. Lorenz, T. S. Plaskett, *Solid State Comm.* 7, 901 (1969).
15. A. Van der Ziel, Solid State Physical Electronics (Prentice-Hall, Inc., N. J., 1968), 2nd ed.

16. L. P. Hunter, ed. Handbook of Semiconductor Electronics (McGraw-Hill Book Company, N. Y., 1970).
17. O. Madelung, Physics of III-V Compounds (John Wiley and Sons, Inc., N. Y., 1964).
18. I. Kudman, T. E. Seidel, J. Appl. Phys. 38, 4379 (1967).
19. B. Pistoulet, J. L. Robert, D. Barjon, Proceedings of the IX International Conference of Physical Semiconductors (Nauka, Leningrad, 1968), Vol. 2, p. 1222.
20. M. R. Lorenz, J. C. McGroddy, T. S. Plaskett, S. Porowski, IBM J. Res. Develop. 13, 583 (1969).
21. W. M. Coderre, J. C. Woolley, Can. J. Phys. 47, 2553 (1969).
22. S. A. Porowski, J. E. Smith, Jr., J. C. McGroddy, M. I. Nathan, W. Paul, Proc. CNRS Colloquium on the Properties of Solids under Pressure, Grenoble, CNRS No. 188, p. 217, 1969.
23. E. A. Guggenheim, Mixtures (Claredon Press, Oxford, 1952).

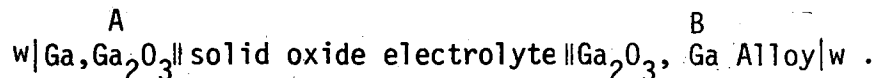
II. THEORY

A. Introduction

The study of the activity of Ga in Ga-In, Ga-Sb, and Ga-In-Sb melts was conducted with the use of solid oxide electrolyte. Use of such oxides for the purpose of determining Gibbs energies at elevated temperatures was pioneered by Kiukkola and Wagner.¹ These materials have since been used for the measurement of the Gibbs energies of formation of many oxides¹⁻⁹ and the partial molar Gibbs energies of components of alloys.^{1,2,10-15}

B. The Nernst Equation

As in emf measurements in aqueous electrolyte applications, the interpretation of high temperature solid oxide electrolyte emf measurements utilizes the Nernst equation. In the system used here, the relevant equilibrium for the development of the Nernst equation is the one that concerns the formation of Ga₂O₃ from O₂ and Ga_(s). The cell is the following:



The Gibbs energy of formation of Ga₂O₃ is expressed for either half-cell as:

$$\Delta G^\circ = \mu_{\text{Ga}_2\text{O}_3} + 6\mu_{e^-} - 2\mu_{\text{Ga}} - 3\mu_{\text{O}_2} \quad (1)$$

Thus,

$$6(\mu_{e_B^-} - \mu_{e_A^-}) = 2(\mu_{\text{Ga}_B} - \mu_{\text{Ga}_A}) + 3(\mu_{\text{O}_B^{2-}} - \mu_{\text{O}_A^{2-}}) - (\mu_{\text{Ga}_2\text{O}_3_B} - \mu_{\text{Ga}_2\text{O}_3_A}) \quad (2)$$

But

$$\mu_{e^-}_B - \mu_{e^-}_A = \Delta G_{e^-} = -FE \quad (3)$$

$$\mu_{\text{Ga}_B} - \mu_{\text{Ga}_A} = RT \ln \frac{a_{\text{Ga}_B}}{a_{\text{Ga}_A}} \quad (4)$$

Choosing pure Ga as the reference state gives:

$$a_{\text{Ga}_A} = 1 \quad (5)$$

In the experimental situation given, the Ga_2O_3 remains the only solid and the Ga and Ga-alloy are liquid so that the following holds: Since the electrolytes used are predominantly conductors of O^{2-} ions with transport numbers of O^{2-} better than 0.99, if the external circuit represented by the emf measurement circuit has a resistance greater than a factor of 10^3 of that of the internal resistance of the cell to minimize meter loading, then O^{2-} will equilibrate between the two half-cells giving: $\mu_{\text{O}^{2-}}_B = \mu_{\text{O}^{2-}}_A$. Under the above conditions, Eq. (2) reduces to:

$$\ln a_{\text{Ga}(\text{alloy})} = - \frac{3FE}{RT} \quad (6)$$

Thus, the gallium activities can be obtained from the measured concentration cell voltages.

C. Solid Oxide Electrolytes

Solid oxide electrolytes are materials which carry current predominately in the form of doubly negatively charged oxygen sublattice vacancies. The theory for the conductivity of these materials is presented in several other places,¹⁶⁻²⁰ and only a brief review of the material is presented here.

The crystals of interest for use as solid electrolytes are those ionic crystals with a large band gap between the valence and conduction bands, serving to minimize electronic conduction. The conduction in such cases is due to the existence of charged defects. Ionic conduction was first studied in pure crystals. In those crystals, the defects are created by thermodynamic equilibrium which result in either pairs of interstitial atom and lattice vacancies (Frenkel defects) or pairs of cationic and anionic sublattice vacancies (Schottky defects). The interstitials and vacancies are subject to diffusion and thermal motion. Thus, the motion of these defects is random. However, once charged and subjected to an external electric field these defects no longer move randomly but with the field, giving rise to the ionic current. In pure ionic crystals where Frenkel defects dominate, the ionic current can be due to charged interstitials, charged vacancies, or both, since the diffusivities of these defects are not in general equal. The same is true in crystals dominated by Schottky defects. These crystals, as ionic conductors, are normally highly dependent on the partial pressure of one of the components over the crystal and as such are ionic conductors over only a narrow range of partial pressure of that component, usually the anionic component.

To be useful for thermodynamic measurements, the charge carrier must not be ambiguous but rather a single species. In order to rid the electrolytes of ZrO_2 and ThO_2 of the objection of a narrow P_{O_2} range and to minimize the ambiguity of the current carrier, CaO and Y_2O_3 are used to dope the electrolytes. The effect is to replace the tetravalent Zr and Th with the divalent Ca and trivalent Y. The effect is to create oxygen sublattice vacancies. By so doing, the P_{O_2} range is broadened since the concentration of the oxygen vacancies is not dependent on the P_{O_2} over this range. Furthermore, the concentration of the one defect is increased greatly over that of the other of the defect pair, so that this defect when charged becomes the dominant defect for ionic conduction purposes.

D. P_{O_2} Range of CSZ and YDT

A number of investigations have been conducted on earlier stabilized zirconia and yttria-doped thoria to this date concerning the optimal compositions and accompanying P_{O_2} range.²¹⁻²⁵ The main feature of these studies is the fact that the conductivity of the electrolyte increases as the doping oxide content is increased until the doping content reaches about 15 cation percent, at which point the conductivity as a function of doping oxide begins to decline. This behavior is expected since the doping initially increases the anion vacancies available for ionization and conduction and at some point further doping destroys the crystallinity of the tetravalent oxide lattice leading to a decline in the conductivity.

Of itself, maximum conductivity is highly desirable in a solid electrolyte. However, increasing the doping oxide concentration has the added benefit of extending the useful P_{O_2} range of the electrolyte,

subject to the same upper dopant concentration limit. Thus

$Zr_{0.85}Ca_{0.15}O_{1.85}$ (CSZ) and $Th_{0.85}Y_{0.15}O_{1.925}$ (YDT) have been the most studied compositions and are the electrolytes used here.

Figure 1 shows the conservative and liberal lower oxygen partial pressure limits to the electrolytic domain of CSZ as derived from the data of Schmalzreid²⁶ and Patterson et al.²² by Patterson.²⁴ This figure shows that the P_{O_2} in equilibrium with Ga in the temperature range of interest ($T < 1000^\circ C$) does not lie within the electrolytic domain of CSZ as defined by the conservative lower limit. This limit is derived from the earlier work of Schmalzreid.²⁶ The later work of Patterson, Bogren and Rapp,²² Patterson,²⁴ and Tretyakov²⁵ define domain boundaries which place that part of the $Ga_2O_3 - Ga - O_2$ equilibrium of interest in the electrolytic domain of CSZ. Included in Fig. 1 is the lower P_{O_2} electrolytic domain boundary of YDT as derived from the data of Tretyakov and Muan,²⁸ Hardaway²⁹ et al., and Lavine and Kolodney³⁰ by Patterson.²⁴

Plotted also in Fig. 1 are the standard Gibbs energies of formation as a function of temperature of the various oxides of the species of interest based on a single mole of O_2 . The Gibbs energy of formation of the oxide of gallium and the oxide of indium are obtained from the data of Klinedinst and Stevenson.^{2,3} The data for gaseous suboxide of gallium, $Ga_2O(g)$, is derived by Seybolt.¹⁵ The data for the solid suboxide of gallium, $Ga_2O(s)$, and the most stable oxide of antimony are derived from Coughlin.³¹ From this graph it is obvious that for the temperature of interest ($600^\circ C < T < 1000^\circ C$), the sesquioxide of gallium, Ga_2O_3 is by far the most stable. This implies that the formation of the other oxides

is so heavily disfavored that Ga_2O_3 is the only solid to exist in the presence of the Ga and Ga-alloy melts studied here.

REFERENCES

1. K. Kiukkola and C. Wagner, J. Electrochem. Soc. 104, 379 (1957).
2. K. A. Klinedinst, D. A. Stevenson, J. Chem. Thermo. 4, 565 (1972).
3. K. A. Klinedinst, D. A. Stevenson, J. Chem. Thermo. 5, 21 (1973).
4. R. W. Headrick, Design Criteria for Solid Electrolyte Electrochemical Cells (M. S. Thesis), LBL-839, July 1972.
5. W. G. Bugden, J. N. Pratt, Trans. AIME 79, 221 (1970).
6. G. G. Charette, S. N. Flengas, J. Electrochem. Soc. 115, 796 (1968).
7. F. E. Rizzo, L. R. Bidwell, D. F. Frank, Trans. AIME 239, 593 (1967).
8. L. R. Bidwell, J. Electrochem. Soc. 114, 30 (1967).
9. R. A. Rapp, Trans. AIME 227, 371 (1963).
10. P. Chatterji, J. V. Smith, J. Electrochem. Soc. 120, 770 (1973).
11. K. A. Klinedinst, M. A. Rao, D. A. Stevenson, J. Electrochem. Soc. 119, 126 (1972).
12. W. G. Bugden, J. N. Pratt, J. Chem. Thermo. 1, 353 (1969).
13. A. Kubik, C. B. Alcock, Metal Science Journal 1, 19 (1967).
14. L. R. Bidwell, R. Speiser, Acta Met. 13, 61 (1965).
15. A. U. Seybolt, J. Electrochem. Soc. 111, 697 (1964).
16. N. F. Mott, R. W. Garney, Electronic Processes in Ionic Crystals (Clarendon Press, Oxford, 1948), 2nd ed.
17. Robert A. Rapp, David A. Shores, Solid Electrolyte Galvanic Cells in Physiochemical Measurements in Metals Research (Interscience Publishers, New York, 1970), pt. 2.
18. C. B. Alcock, Transport of Ions and Electrons in Ceramic Oxides in Electromotive Force Measurements in High Temperature Systems (American Elsevier Publishing Company, Inc., 1968).

19. F. A. Kröger, The Chemistry of Imperfect Crystals (North-Holland Publ., Amsterdam, 1964).
20. Motaaki Sato, Electrochemical Measurements and Control of Oxygen Fugacity and other Gaseous Fugacities with Solid Electrolyte Sensors in Research Techniques for High Pressure and High Temperature (Springer-Verlag, N. Y., 1971).
21. B. C. H. Steele, C. B. Alsack, Trans. AIME 233, 1359 (1965).
22. J. W. Patterson, C. C. Bogren, R. A. Rapp, J. Electrochem. Soc. 114, 752 (1967).
23. T. J. Salzano, H. S. Issacks, B. Miscushkin, J. Electrochem. Soc. 118, 412 (1971).
24. J. W. Patterson, J. Electrochem. Soc. 118, 1033 (1971).
25. T. H. Etsell, S. N. Flengas, J. Electrochem. Soc. 119, 1 (1972).
26. H. Schmalzreid, Z. Elektrochem. 66, 572 (1962).
27. J. D. Tretyakov, Neorg. Materials (USSR) 2, 501 (1966).
28. J. D. Tretyakov, M. Muan, J. Electrochem. Soc. 116, 331 (1969).
29. J. B. Hardaway, III, J. W. Patterson, D. R. Wilder and J. D. Schieltz, J. Am. Cer. Soc. 54, 94 (1971).
30. S. R. Levine and M. Kolodney, J. Electrochem. Soc. 116, 1420 (1969).
31. J. P. Coughlin, Contributions to the Data in Theoretical Metallurgy, XII Heats and Free Energies of Formation of Inorganic Oxides Bulletin 542, Bureau of Mines, United States Government Printing Office, Washington (1954).

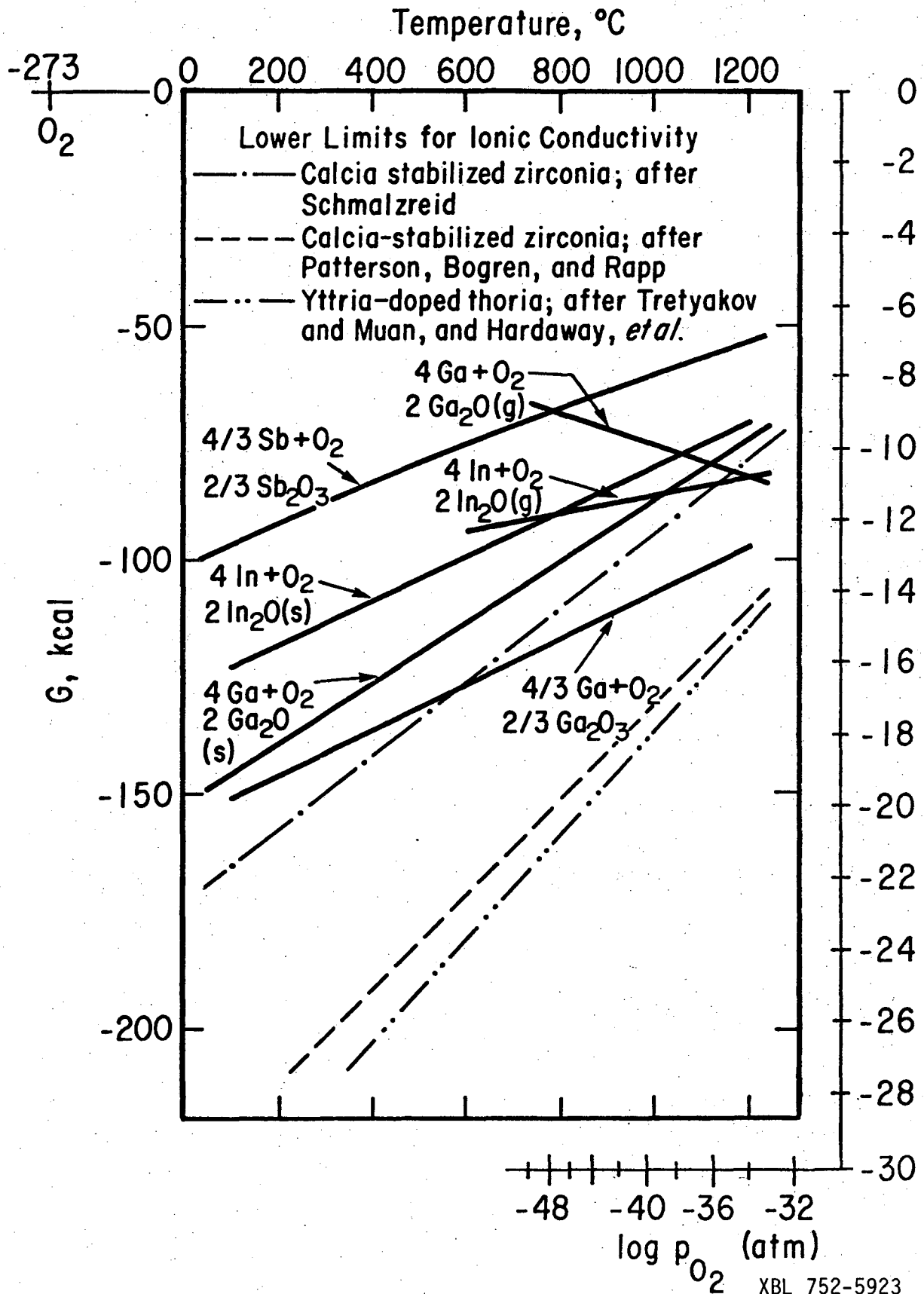


Fig. 1. Gibbs energies of formation on a molar O_2 basis are compared to the lower O_2 partial pressure limits for ionic conductivity of oxide electrolytes.

III. EXPERIMENTAL APPARATUS AND PROCEDURES

A. Introduction

In order to study the activity of Ga in high temperature melts using a solid oxide electrolyte technique it is necessary to exclude other sources of oxygen by making measurements either in a vacuum or in a high purity inert gas atmosphere. Since oxygen is the important component in electrochemical cells using the above technique, a very low oxygen partial pressure is necessary over the molten electrodes. Because of the simplicity of building and maintaining a gas tight system and purifying argon to the requisite purity as compared to an equivalent vacuum system, measurement under an inert atmosphere was chosen.

Complicating factors are the need to introduce electrical leads into the molten electrodes and the necessity to separate the atmospheres of the two molten electrodes.¹

B. Ga-In Cell

1. Apparatus

An unscaled schematic of the cell is shown in Fig. 1. The main cell body was an 18 in. long tube of high purity recrystallized alumina 1 1/2 in. OD, 1 1/4 in. ID, closed at one end. The open end was sealed to a water-cooled stainless steel head with a buna rubber O-ring. Three ceramic tubes were passed through the head at the vertices of an equilateral triangle inscribed in a 3/8 in. radius circle centered on the head. These ceramic tubes were sealed to the head with viton O-ring.

*Morganite refractories.

The inner ceramic tube, which served as the reference electrode compartment, was a slip cast high purity calcia stabilized zirconia, $Zr_{0.85}Ca_{0.15}O_{1.85}$, (CSZ) tube.* Centered in this tube was a 1/8 in. OD high purity alumina thermocouple insulator through which the high purity argon was introduced at a point near the closed bottom of the CSZ tube, as shown in Fig. 1. A tungsten electrode lead was also run through this insulator to the bottom of the CSZ tube. The open top of this CSZ tube was sealed to a 1/4 in. stainless steel Swagelok tee with a teflon front ferrule backed with a nylon back ferrule. The 1/8 in. tube was run through the tee and sealed also with teflon and nylon ferrules to a 1/8 in. Swagelok reducer swaged to the tee (see Fig. 1). The side port from the straight run of the tee was the gas outlet for the CSZ tube venting the gas to a mercury vapor trap. The 1/8 in. tube was sealed to a second 1/8 in. reducer swaged to a second 1/4 in. Swagelok stainless steel tee, then the 1/8 in. tube was run through the straight run of the tee. The second run of the straight run was sealed to a short length of pyrex tubing. The 1/8 in. pyrex tube was ended within the pyrex tube with the tungsten wire extending completely through the pyrex tube. The open end of the pyrex tube was then sealed with black sealing thus forming a seal through which the tungsten lead was extended but which did not seal the 1/8 in. tube. The inlet gas was introduced through the side port of the second tee, routed by the tee configuration to the pyrex tube and into the 1/8 in. alumina tube. This configuration allowed a positive gas circulation

* Zircoa Corporation.

in the CSZ tube electrode leads which were isolated from the stainless steel swagelok parts, and seals which were vacuum tight.

The second ceramic tube was made of high purity alumina.* This tube had both ends open and serves to transport the high purity argon blanket gas to a point near the bottom of the main cell body. In addition, the second electrode lead was threaded through this tube. The top end of this tube was sealed to one arm of the straight run of a 1/4 in. stainless steel swagelok tee. The other arm was sealed to a short piece of pyrex through which the tungsten lead was threaded. This pyrex tube was sealed as in the assembly of the CSZ electrode. The electrical lead for the sample electrode was warped around the tip of the CSZ tube to insure good electrical contact with the sample liquid alloy. The side arm of the tee was the inlet for introducing the high purity argon to the tube.

The third ceramic tube was similar to the second tube except that the bottom end was closed. This tube served as the thermocouple well.

The gas outlet for the main cell compartment was a 1/8 in. tube welded to the center of the lead. This also led to a mercury vapor trap.

As the bottom of the main cell body was hemispherical, a flat platform made of alumina was placed at the bottom. On this platform was placed a crucible made of high purity crystallized alumina,** 26 mm in height and 18 mm in diameter, containing the alloy electrode.

* McDanel Refractory Porcelain.

** Morganite Refractories.

The furnace was wound with Kanthal A-1 wire and powered by a proportional controller utilizing a triac gate, which controlled the temperature of the region of the sample to 0.5°C . The cell was maneuvered in a position such that with shunts across the appropriate section of the furnace windings, the region of the crucible had a vertical temperature variation of $\pm 0.5^{\circ}\text{C}$ in the sample region. In later runs to alleviate the lateral temperature variation which must exist in a cell of this geometry due to natural convection of the gas, two baffles were used. These created a small compartment for the crucible, a second small compartment above that compartment, and finally, a compartment which was the remainder of the main compartment. Also, initial runs indicated the necessity of a ground shield which was installed to alleviate pick-up of noise from the furnace windings.

The temperature was measured with a chromel-alumel thermocouple referenced to the melting point of ice. The thermocouple and cell emfs were read with a Leeds and Northrup K-3 potentiometer. Figures 2 and 3 show the temperature control and gas manifold systems.

The high purity argon gas was provided by purifying argon with a Centorr gettering furnace. This furnace purified argon at rates of 20 standard cubic feet per minute to less than 0.001 ppm by gettering the argon over titanium at 800°C . The total flow of argon through the gettering furnace for this experiment was less than 1 standard cubic feet per minute. Since the equilibrium partial pressure of O_2 over titanium at 800°C is 10^{-39} atmospheres, and the equilibrium partial pressures of other impurities are equally low, the argon purity is considerably lower than 0.001 ppm due to the increased residence time in the gettering furnace.

The distribution system for the argon was made of 1/4 in. stainless steel tubing using stainless steel Swagelok fittings where necessary. The gas flows were metered to the two electrode compartments. The gas flow-rates were 0.12 and 6.0 cc/min in the reference and sample compartments respectively, values selected to provide one compartment volume at 23°C per hour. The compartments were isolated from the gas source by Nupro bellows shut off valves. The final connections, from the shut-off valve to the compartment gas inlets, were made with corrugated, flexible stainless steel tubing with 1/2 in. nominal O.D.

2. Procedures

The reference electrode was formed by dropping first Ga_2O_3 powder of 4-9's purity* and second molten Ga of 6-9's purity** into the bottom of the CSZ tube. The reference electrode was placed in position in the head, and the gas delivery and lead feed-through assembly was sealed to the top of the tube.

The other two tubes were positioned similarly, with the sample electrode lead fed through the appropriate tube. The end of the sample electrode lead was wrapped around the tip of the CSZ tube. The tip of the CSZ tube was placed in the crucible containing carefully measured amounts of Ga_2O_3 and In of 5-9's purity.** To secure the positioning of the crucible, the crucible was wired to the thermocouple tube with a short piece of tungsten wire. This assembly was then placed in position in the main cell body and sealed to the main cell body by the O-ring seal.

* Ventron Corporation.

** Cominco American.

The assembled cell was positioned in the furnace, and the gas connections were made using teflon and nylon ferrules to alleviate the need for large torques on the ceramic tube. The cell compartments were then purged for 2 hr with the purified argon at rates of at least 50 compartment volumes per hour. Since argon is slightly denser than the major components of air, Ar was delivered to a point near the bottom of the respective compartments. Since the gas outlet was at the top of the compartments, the gas atmosphere at the end of the purge period had the purity of Ar delivered by the gettering furnace.

At this point the gas flows were reduced to values corresponding to a single compartment volume per hour and shut off. The cell temperature at this point was raised to the cell operating values.

Initially, the cell temperatures were raised and lowered rapidly, but problems due to the low value of thermal shock resistance of CSZ necessitated much lower temperature elevation rates.

No set procedure for making measurements was established since for this system there did not appear to be any dependence on the thermal state of the previous measurement. However, in order to facilitate comparison with the data of Klinedinst, cell emfs were measured at temperatures of 800°, 850°, 900°, and 950°. One difference was that in this study no gas flow was used except when initially purging the cell and when the cell temperature was being lowered. Thus, in general, all data points represented a condition of no gas flow in the system.

C. Ga-Sb, Ga-In-Sb Cells

1. Apparatus

The cells containing Ga-Sb and Ga-In-Sb differed from those for Ga-In alloy studies in several important details. The major problem, reported by Chatterji and Smith, was antimony reacting slowly with tungsten electrode contacts. That difficulty is minimized by allowing the tungsten to contact the alloy melt only when a measurement was being made. To accomplish this the pyrex and black wax feed-through of the alloy electrode lead feed-through assembly of the Ga-In cell was replaced with a sliding lead feed-through assembly. This assembly consisted of a 1/8 in. pyrex and black wax feed-through placed within a Swagelok union bored through to slightly over 1/8 in. This union was sealed to a length of 1/8 in. stainless steel tubing with the back ferrule inverted and the front ferrule replaced with an O-ring with a approximately 1/8 in. x 1/12 in. wall, greased with vacuum grease. This formed the sliding seal for moving the tungsten lead in and out of the stainless tubing. In order to prevent grounding of the tungsten lead, the 1/8 in. tubing was connected to a 1/4 in. pyrex tube with a 1/4 in. to 1/8 in. bored-through union. This 1/4 in. pyrex tube was then sealed to the port previously occupied by the pyrex and black wax feed-through (Fig. 4). The seal was tested with a He leak detector and was found not to leak within the detector range.

The tungsten lead was threaded through the alloy compartment gas inlet tube, now shortened to a point close to the cell head. The lead was then threaded through a 1/8 in. alumina insulator wired

to the electrolyte tubes. This 1/8 in. alumina tube was positioned just above the crucible so that when the sliding seal was pushed down the lead would move down through the tubes and into the alloy melt. When the seal was pushed up the tungsten lead was withdrawn from the melt.

Because it was generally desirable to minimize electrode lead and melt interactions, the sliding seal was also used on the reference electrode lead. Since the electrode lead path was straight in this case, no special changes were made in this electrode to insure that the lead contacted the melt.

A second change in the cell involved the change in solid oxide electrolyte material. Since the lower P_{O_2} limit of CSZ is not sufficiently lower than the $Ga_2O_3-Ga-O_2$ equilibrium, a YDT tube* 18 in. long and 1/4 in. in diameter was used as a solid oxide electrolyte.

Another difficulty encountered in the Ga-Sb cells was the high internal cell resistances. The internal resistances were measured to be as large as 10^4 ohms. For source impedances of this magnitude with potentiometers, small cell currents can flow. In order to minimize cell currents during measurements a Keithley electrometer with 10^{12} ohms input impedance was used in place of a potentiometer to determine the approximate cell emf as shown in Figs. 5 and 6a. Accurate measurements of the cell emf were made by using the potentiometer in series with the electrometer (Fig. 6b). This arrangement used the potentiometer as a source of bucking voltage to the cell and the electrometer as a null meter. The circuit impedance was essentially that of the electrometer.

* Zirconia Corporation

The final modifications on the system were in the gas delivery system (Fig. 7). Because of the shortening of the main compartment gas inlet tube and the greater reliability of vacuum evacuation, a mechanical vacuum pump was added to the system to purify the cell atmosphere. Additional bellows shutoff valves were added to isolate the two cell compartments, the argon source, the vacuum pump, and mercury gas traps from each other. The very fine metering valves were relocated in order that atmospheric gases might not be pulled into the system through packed seals. The last modification to the gas handling system was cold trapping the gas outlet lines in trichloroethylene and dry ice prior to the mercury vapor traps in order to minimize any possibility of back diffusion of mercury to the cell compartments.

2. Procedure

The reference and alloy electrode preparation was the same as in the Ga-In cells. The antimony used was 5-9's purity.*

The compartment atmospheres were purified by evacuation to 200 microns and back filling with purified argon five times.

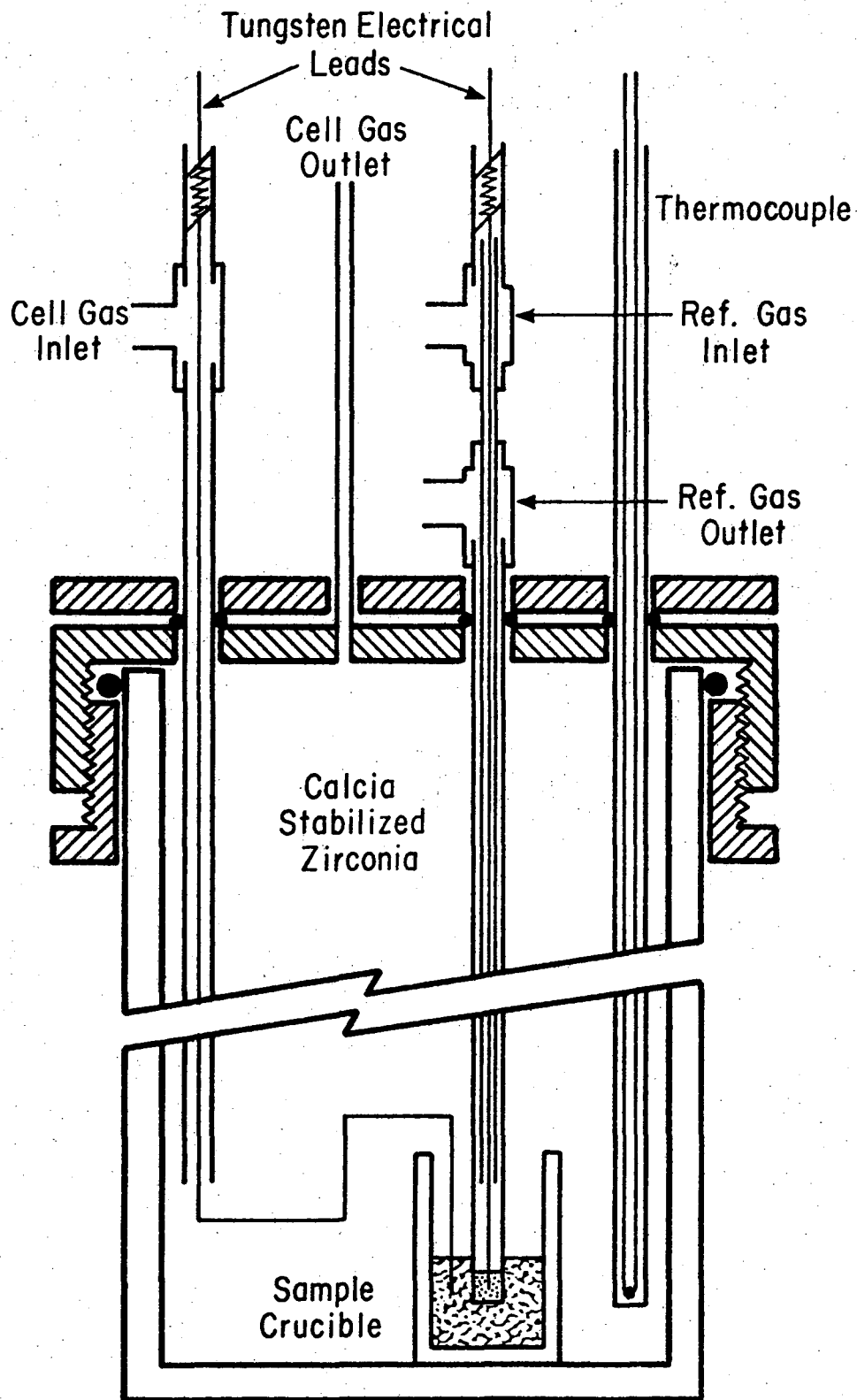
After purifying the cell atmospheres, the temperature of the cell was slowly raised to 800°C at the rate of 70°C per hour. This rate was convenient since a rate of 150°F per hour was recommended by Zircoa to avoid thermal stress cracking and recrystallization problems common in YDT.

*Cominco American.

Liquid alloys of Ga and Sb, and of Ga, In and Sb were found to equilibrate very slowly. Thus, once the cells reached 800°C it was necessary to monitor periodically the cell emf until a constant value was obtained. This typically required 2 to 3 days, though 5 days was necessary in some cases in order to obtain values constant to within 0.01 millivolt. This was in great contrast with the Ga-In alloys which equilibrated very quickly--in less than a day. After the cell emfs had stabilized in this fashion, the alloy melts were assumed to have become completely mixed, and data were then taken at various temperatures. Even the measurements at various temperatures required a great deal of time, the time required being a strong function of temperature, so that it was necessary to monitor periodically the emfs at each temperature until they stabilized in order to obtain the equilibrium values of the emfs. Again, the emfs at the various temperatures were independent of how the temperatures were reached.

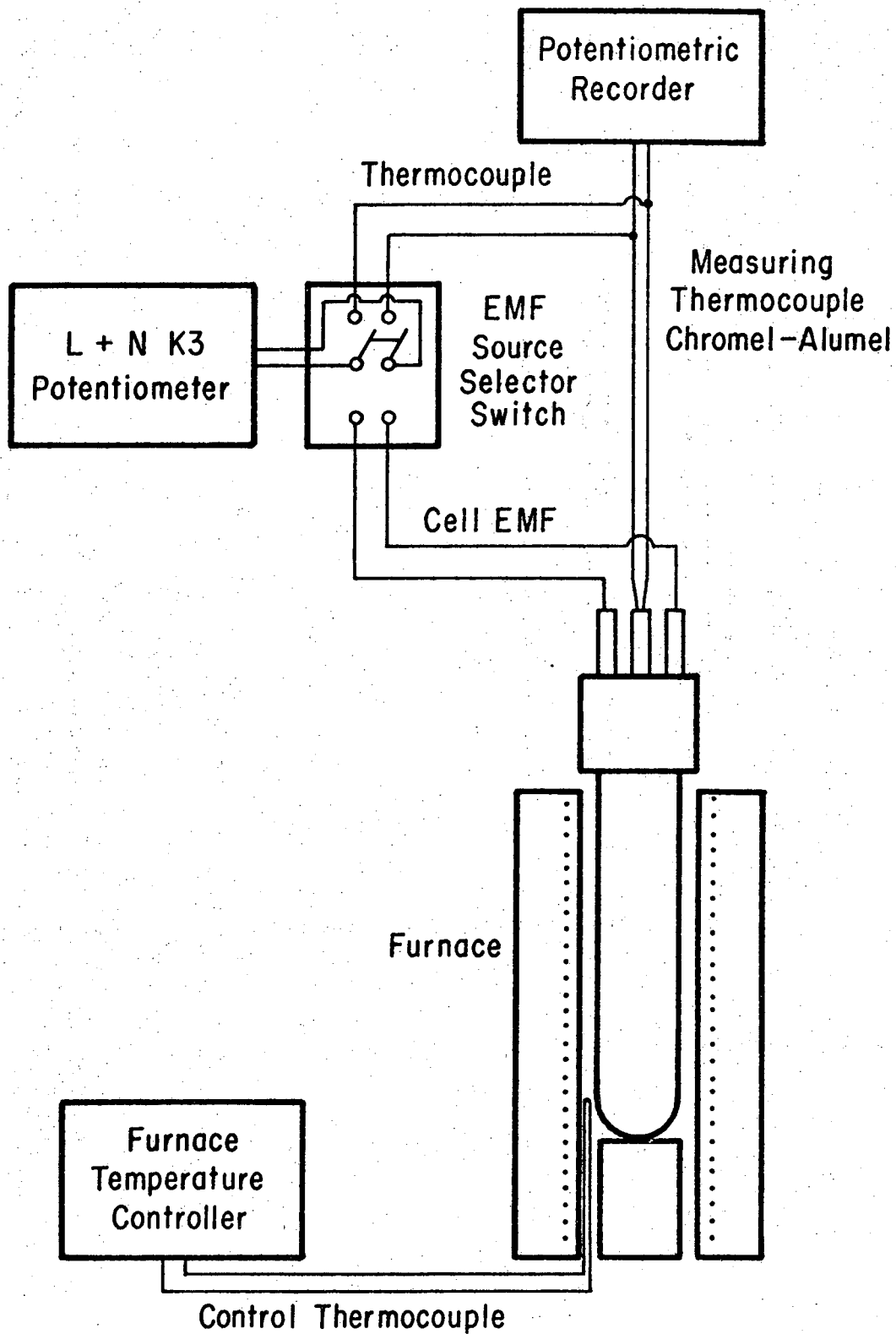
REFERENCE

1. T. A. Ramanarayanan, W. L. Worrell, Limitations in the Use of Solid State Electrochemical Cells for High-Temperature Equilibrium Measurements, to be published.



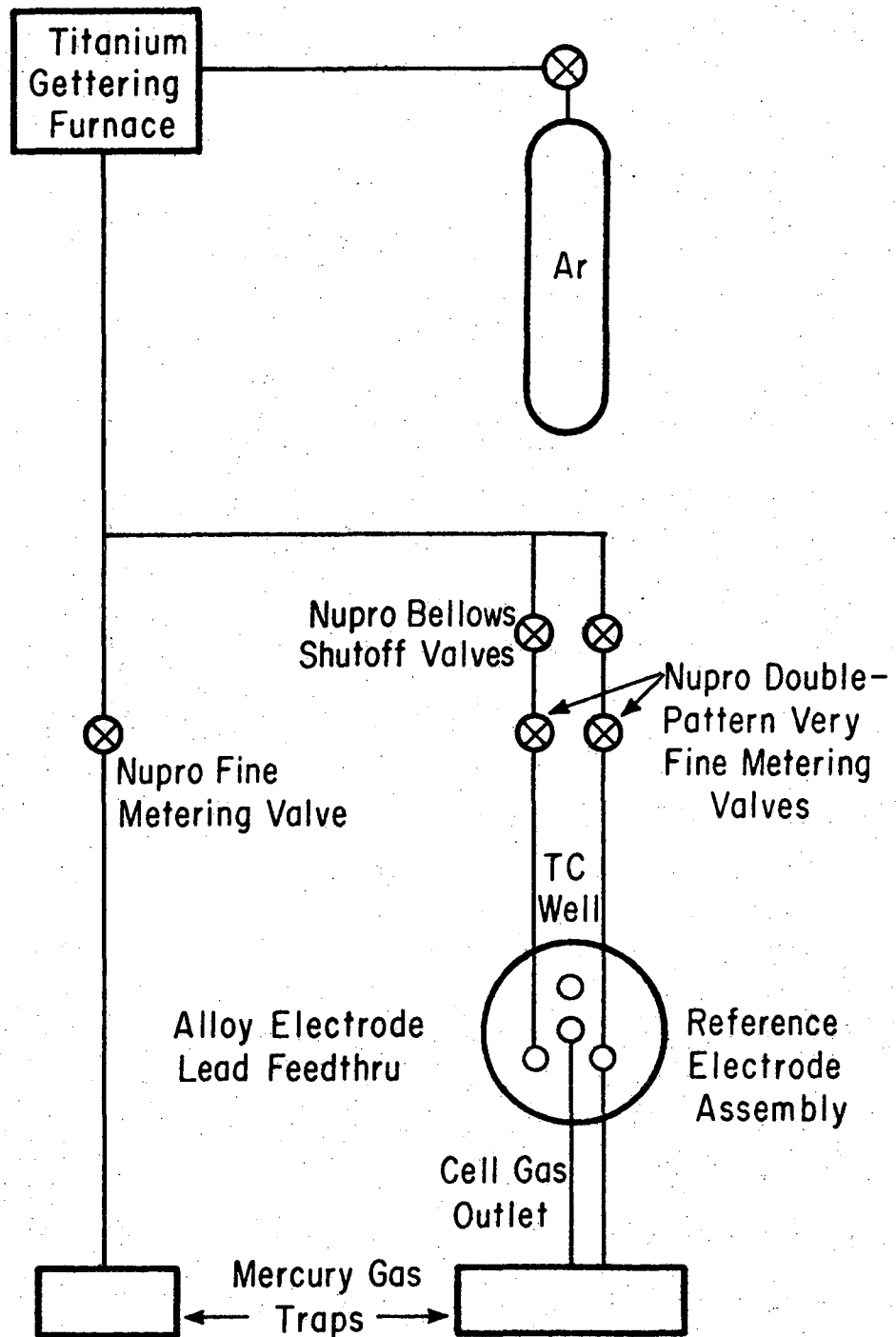
XBL 752-5724

Fig. 1. Schematic diagram of the experimental cell configuration for Ga-In, alloy activity studies.



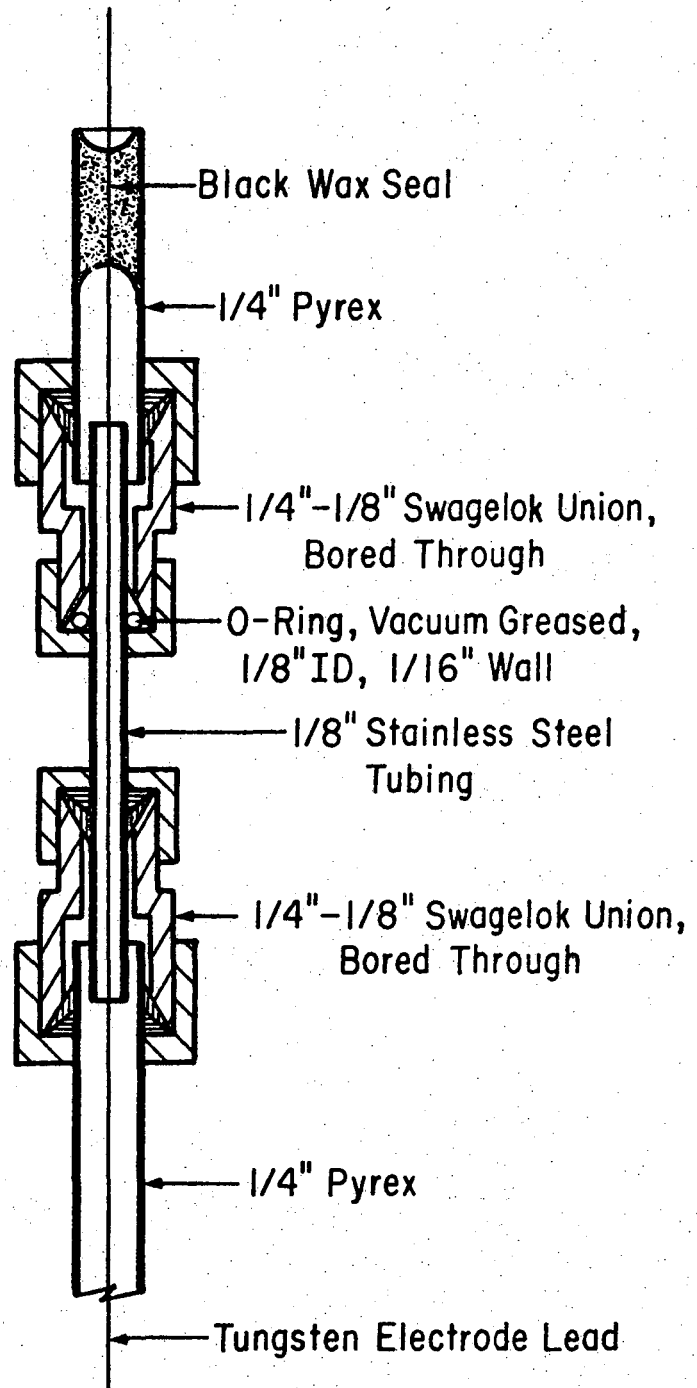
XBL 752-5725

Fig. 2. Temperature control and EMF measurement circuit for Ga-In alloy activity studies.



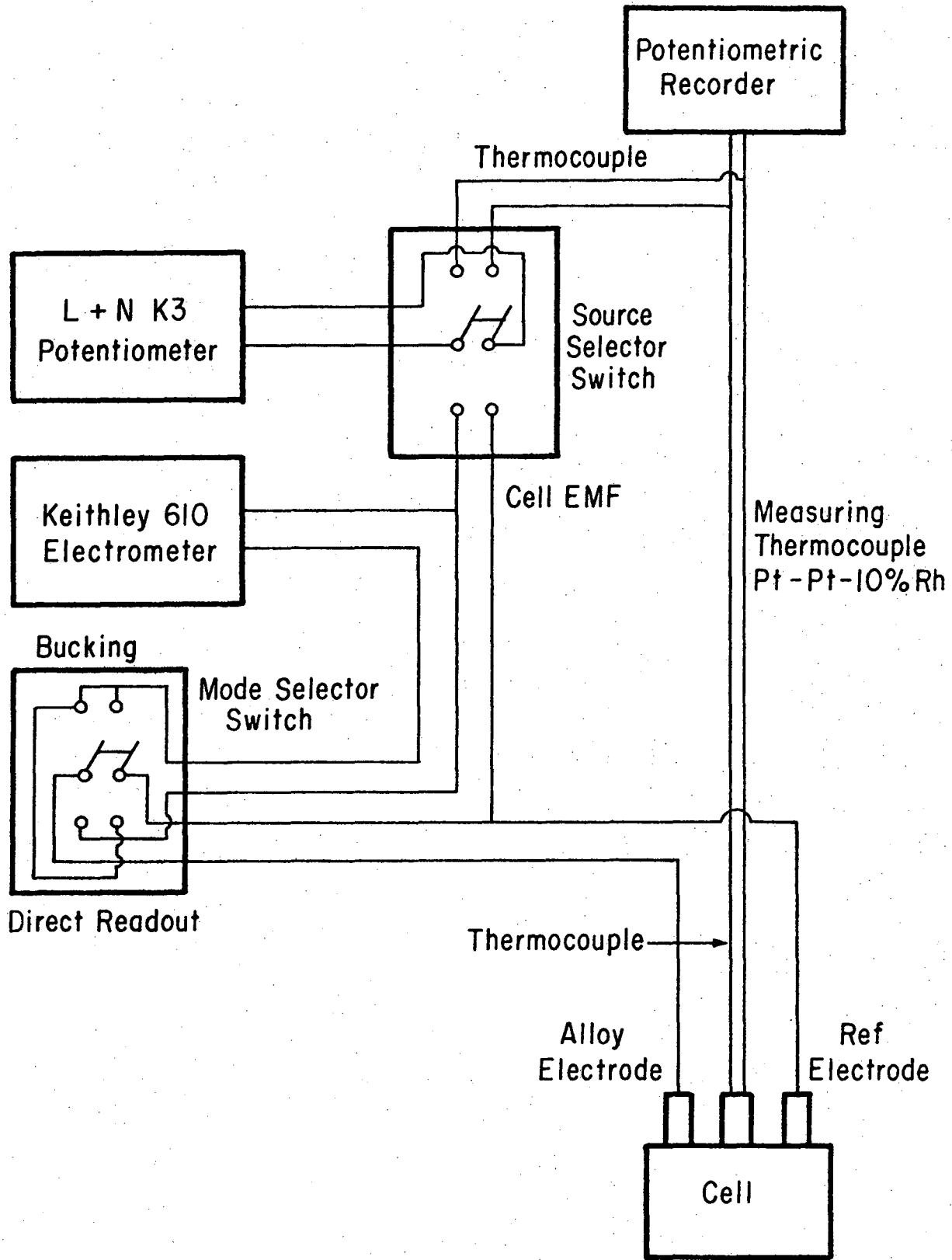
XBL 752-5726

Fig. 3. Gas flow system for the Ga-In alloy activity studies.



XBL 752-5727

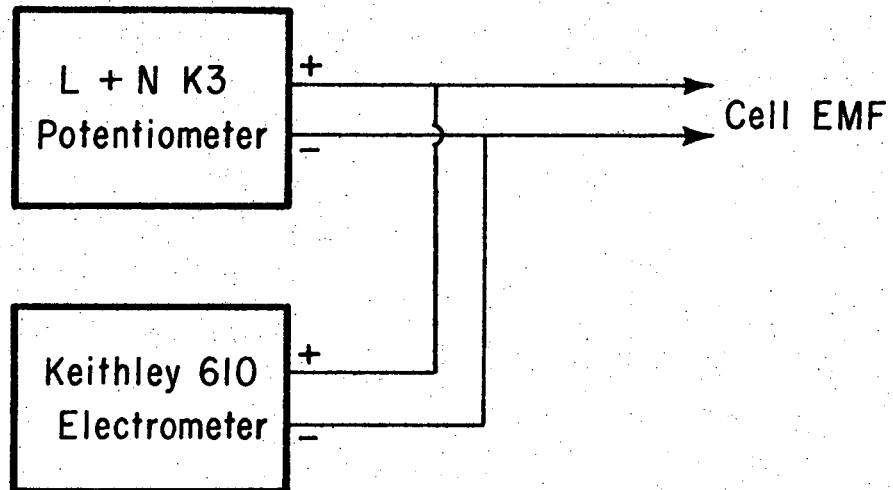
Fig. 4. Sliding electrode feedthrough used to insert and withdraw a tungsten lead into and from gas Ga-Sb and Ga-In-Sb melts.



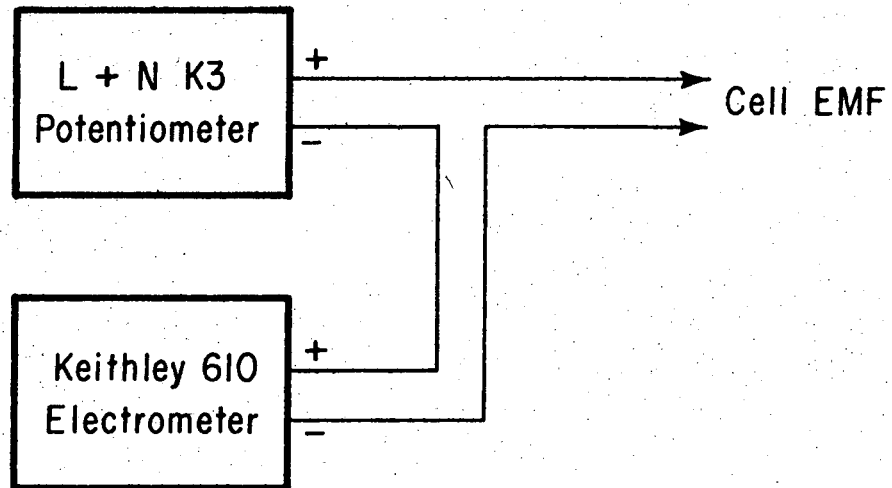
XBL 752-5728

Fig. 5. Temperature monitoring and emf measurement circuits for Ga-Sb and Ga-In-Sb alloy activity studies.

Direct Readout Mode — Potentiometer not used.

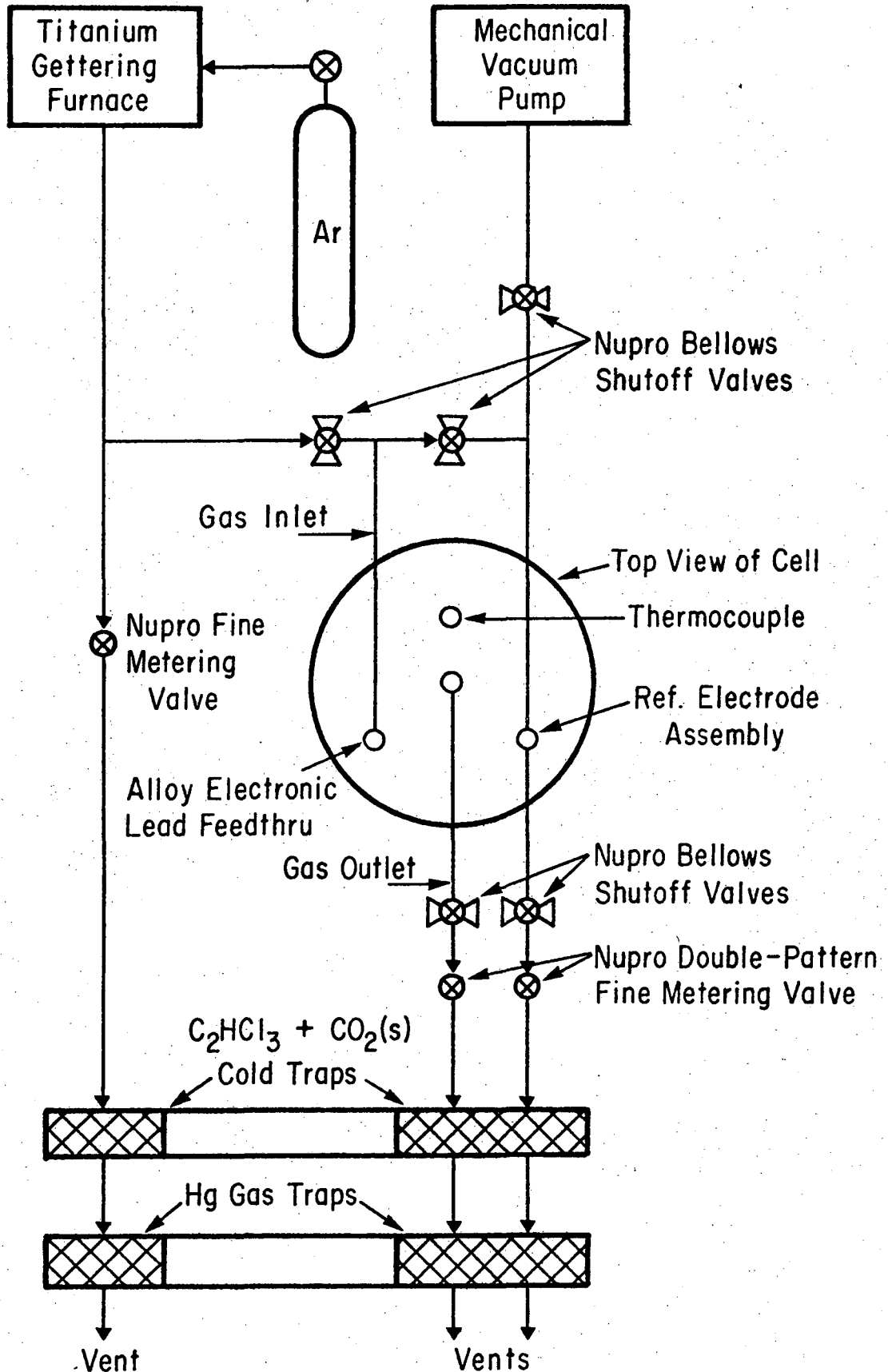


Bucking Mode — Potentiometer used as a bucking voltage source and the electrometer as a null meter.



XBL 752-5729

Fig. 6. The effective emf measurement circuits for the Ga-Sb and Ga-In-Sb studies.



XBL 752-5730

Fig. 7. Gas flow system for the Ga-Sb and Ga-In-Sb alloy activity studies.

IV. The Ga-In System

A. Results

The emf measured as a function of temperature in the Ga-In system is plotted in Fig. 1 for the compositions investigated, along with the comparable measurements of the study by Klinedinst et al.⁴ These results demonstrate the reproducibility of the emf method.

A number of sources of instabilities in cell emf were encountered. The main instability was characterized by a rapid drop-off in the cell emf with time. In runs showing this effect, measurements of the internal cell resistance before emf drop-off gave resistances of the order of 10,000 ohms and after emf drop-off resistances of the order of 10 ohms. This change suggests electrolyte failure. Thus, improvements in equipment and operating procedure were implemented to minimize this problem. Further improvements were implemented prior to the initiation of measurements on the Ga-Sb system based on experiences gained in the Ga-In system. These improvements have been outlined in the Equipment and Procedures Section III-C.

The emf data are reduced to α_{GaIn} s, defined by

$$\alpha_{\text{GaIn}} = (\ln \gamma_{\text{Ga}}) / (1 - x_{\text{Ga}})^2$$

This parameter can be expected to have the form⁶⁻⁹

$$\alpha_{\text{GaIn}} = a + bx_{\text{Ga}} + c/T + dx_{\text{Ga}}/T \quad (1)$$

Utilizing a least square fit on the data obtained from the emf measurements gives:

$$\alpha_{\text{GaIn}} = 0.2862 + 0.0352x_{\text{Ga}} + 398.3/T + 220.0x_{\text{Ga}}/T \quad (2)$$

The rms deviation of data from this equation is ± 0.016 for the range $0.05 < x_{\text{Ga}} < 0.40$ (see Fig. 2). The activities of Ga at 1223°K are presented graphically in Fig. 3 along with the activities predicted by Eq. (2) and compared to the data of Klinedinst, et al.⁴ Using the Gibbs-Duhem equation and assuming Eq. (2) for the whole composition range, the activities of In were calculated for the experimental compositions and are presented in Table 1.

By using Eq. (2) and fundamental thermodynamic identities, the following equations for $\Delta\bar{H}_{\text{Ga}}$ and $\Delta\bar{S}_{\text{Ga}}^{\text{XS}}$ at 800°C to 950°C are derived from the data of this work:

$$\Delta\bar{H}_{\text{Ga}} = (791.4 + 437.1x_{\text{Ga}})(1 - x_{\text{Ga}})^2 \text{ cal/g-atom} \quad (3a)$$

$$\Delta\bar{S}_{\text{Ga}}^{\text{XS}} = -(0.5687 + 0.0699x_{\text{Ga}})(1 - x_{\text{Ga}})^2 \text{ cal/g-atom} \quad (3b)$$

By extrapolating Eqs. (3) over the whole composition range the following equations are derived, again using the Gibbs-Duhem equation.

$$\Delta H^{\text{M}} = (791.4 + 218.6x_{\text{Ga}}) x_{\text{Ga}}(1 - x_{\text{Ga}}) \quad (4a)$$

$$\Delta S^{\text{XS}} = -(0.5687 + 0.0350x_{\text{Ga}}) x_{\text{Ga}}(1 - x_{\text{Ga}}) \quad (4b)$$

Equation (4a) shows that the integral heat of mixing has a maximum at $x_{\text{Ga}} = 0.53$ with a value of 226 cal/g-atom. $\Delta\bar{H}_{\text{Ga}}$ and ΔH^{M} are plotted in Fig. 4.

Table 1. Experimental emf measurements.

X(GA)	T(K)	EMF(MV)	A(GA)	A(IN)
0.0499	1073.8	73.816	0.0913	0.9514
	1123.2	77.322	0.0910	0.9514
	1174.8	81.532	0.0893	0.9513
	1224.5	85.880	0.0870	0.9513
0.1003	1073.4	53.898	0.1741	0.9048
	1124.4	56.537	0.1737	0.9047
	1174.0	59.495	0.1713	0.9046
	1223.9	62.335	0.1698	0.9045
0.2009	1073.7	35.941	0.3118	0.8182
	1124.2	38.129	0.3070	0.8177
	1174.5	40.316	0.3027	0.8173
	1224.0	42.325	0.3000	0.8169
0.4089	1073.9	19.357	0.5339	0.6573
	1124.2	20.509	0.5299	0.6556
	1174.3	21.629	0.5266	0.6540
	1224.4	22.729	0.5240	0.6526

B. Discussion

The Ga-In system has been investigated by Macur, Edwards, and Wahlbeck using Knudsen effusion,¹ by Bros^{2a} and Bros, Castanet, and Laffitte using microcalorimetry at 150°C,^{2b} by Predel and Stein using microcalorimetry at 350°C,³ and by Klinedinst, Rao and Stevenson using solid electrolyte techniques from 800°C to 950°C.⁴ From their data, Bros et al., conclude that the heats of mixing are symmetrical about $x_{\text{Ga}} = 0.5$. The data of Predel and Stein are not in apparent agreement concerning the symmetry of the results of Bros et al., though the data of Predel and Stein are not as comprehensive as those of Bros et al. The heat of mixing data derived from Gibbs energy measurements by Klinedinst et al., are also not in agreement with the conclusion of Bros et al. However, the scatter in the Gibbs energy data of Klinedinst et al., is such as to render questionable the derived heats of mixing.

The data of Klinedinst were fitted to Eq. (1) giving

$$\alpha_{\text{GaIn}} = 0.1700 - 0.9184x_{\text{Ga}} + 470.5/T + 1186.1x_{\text{Ga}}/T \quad (5)$$

The rms deviation is ± 0.044 for the range $0.05 < x_{\text{Ga}} < 0.80$. From this equation ΔH^{M} is derived:

$$\Delta H^{\text{M}} = (934.9 + 1178.4x_{\text{Ga}}) x_{\text{Ga}} (1 - x_{\text{Ga}}) \quad (6)$$

The conclusions reached from the data of Bros et al., Predel and Stein, and Klinedinst et al., contradict those reached from the data of Macur et al., that the heat of mixing at $x_{\text{Ga}} = 0.5$ is 2200 cal/mole. The heats for $x_{\text{Ga}} = 0.5$ are found by Bros et al., and Predel and Stein

to be 265 cal/mole and 288 cal/mole respectively. The heats calculated from an equation, of the form of Eq. (1) with d set equal to 0, fitted to the data of Klinedinst et al. These values are symmetrical about $x_{\text{Ga}} = 0.5$ with a maximum heat of 472 cal/mole. Relaxing the symmetry requirement gives Eq. (5) which has a maximum of 395 cal/mole at $x_{\text{Ga}} = 0.59$ and which has the value 381 cal/mole at $x_{\text{Ga}} = 0.5$.

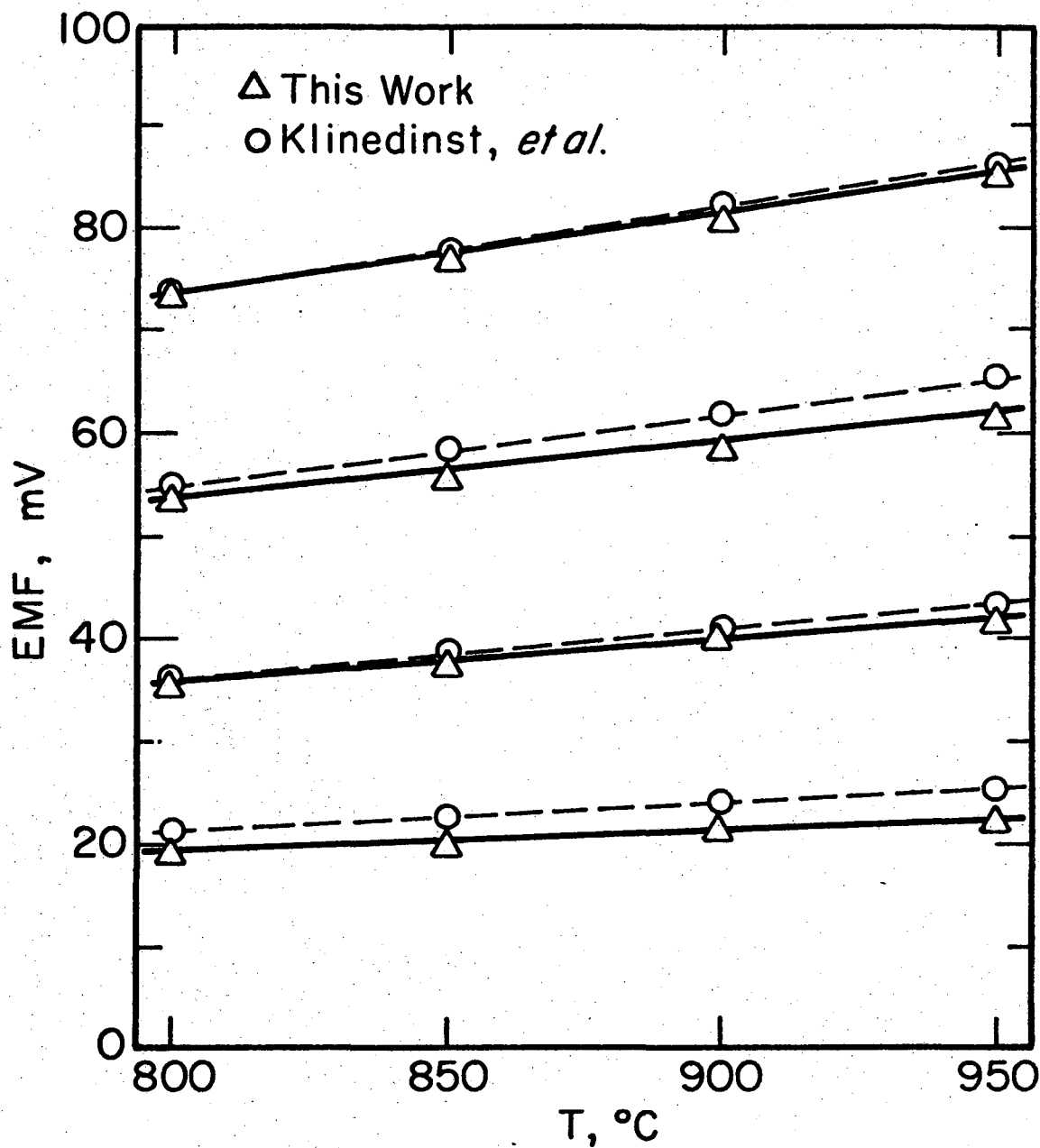
A comparison of heat of mixing data is shown in Fig. 4. Thus, the heats derived from high temperature emf measurements bracket the heats measured at lower temperatures by microcalorimetry. The values at $x = 0.5$ are all in fair agreement except those obtained by Macur et al., 2200 cal/mole, obtained by Knudsen effusion. In addition, the high temperature emf data and the data of Predel and Stein suggest that the maximum heat of mixing is shifted towards the Ga rich side rather than at $x_{\text{Ga}} = 0.5$ as suggested by Bros and by Bros et al.

C. Conclusion

The use of solid oxide electrolytes is quite reproducible. However, derived data are extremely sensitive to the absolute errors in measurement. Nevertheless, the enthalpy of mixing derived from the data of this work is consistent with the data of earlier works. Though, along with the data of two of those works, the data of this work contradicts the conclusion of Bros and Bros et al., that the enthalpy of mixing is symmetric about the composition $x_{\text{Ga}} = 0.5$.

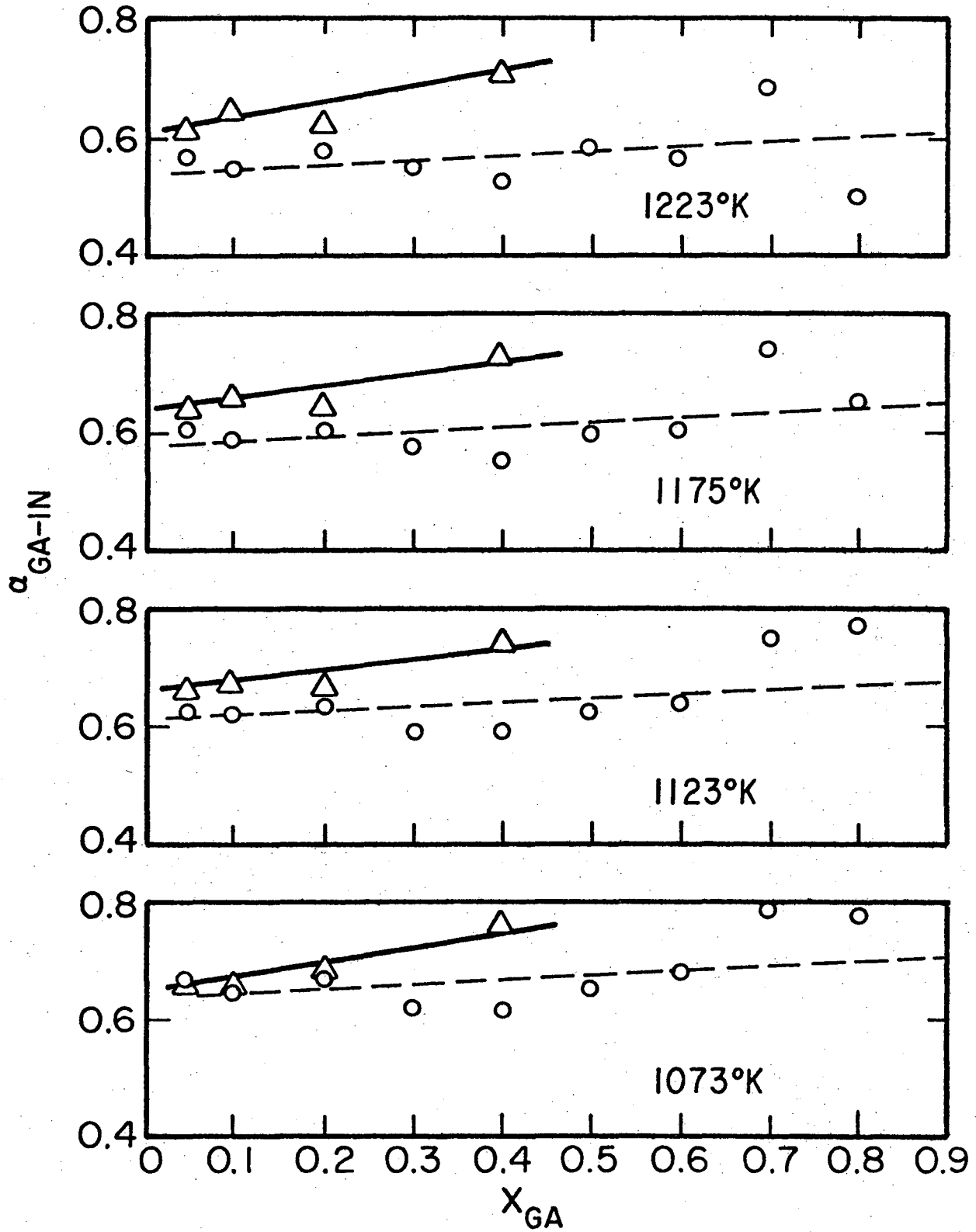
REFERENCES

1. G. J. Macur, R. K. Edwards, P. G. Wahlbeck, J. Phys. Chem. 72, 1047 (1968).
- 2a. Jean-Pierre Bros, C. R. Acad. Sc. Paris, t. 263, Serie C, 977 (1966).
- 2b. J-P Bros, R. Castanet, M. Laffittee, C. R. Acad. Sc. Paris, t. 264, Serie C, 1804 (1967).
3. B. Predel, D. W. Stein, J. Less-Common Metals 18, 49 (1969).
4. K. A. Klinedinst, M. V. Rao, D. A. Stevenson, J. Electrochem. Soc. 119, 1261 (1972).
5. M. V. Rao, W. A. Tiller, J. Mater. Sci. 7, 14 (1972).
6. M. V. Rao, W. A. Tiller, J. Phys. Chem. Solids 31, 191 (1970).
7. J. P. Esdaile, Metallurgical Transactions 2, 2277 (1971).
8. H. K. Hardy, Acta Met. 1, 202 (1953).
9. K. Wahl, Trans. AIChE 42, 215 (1946).



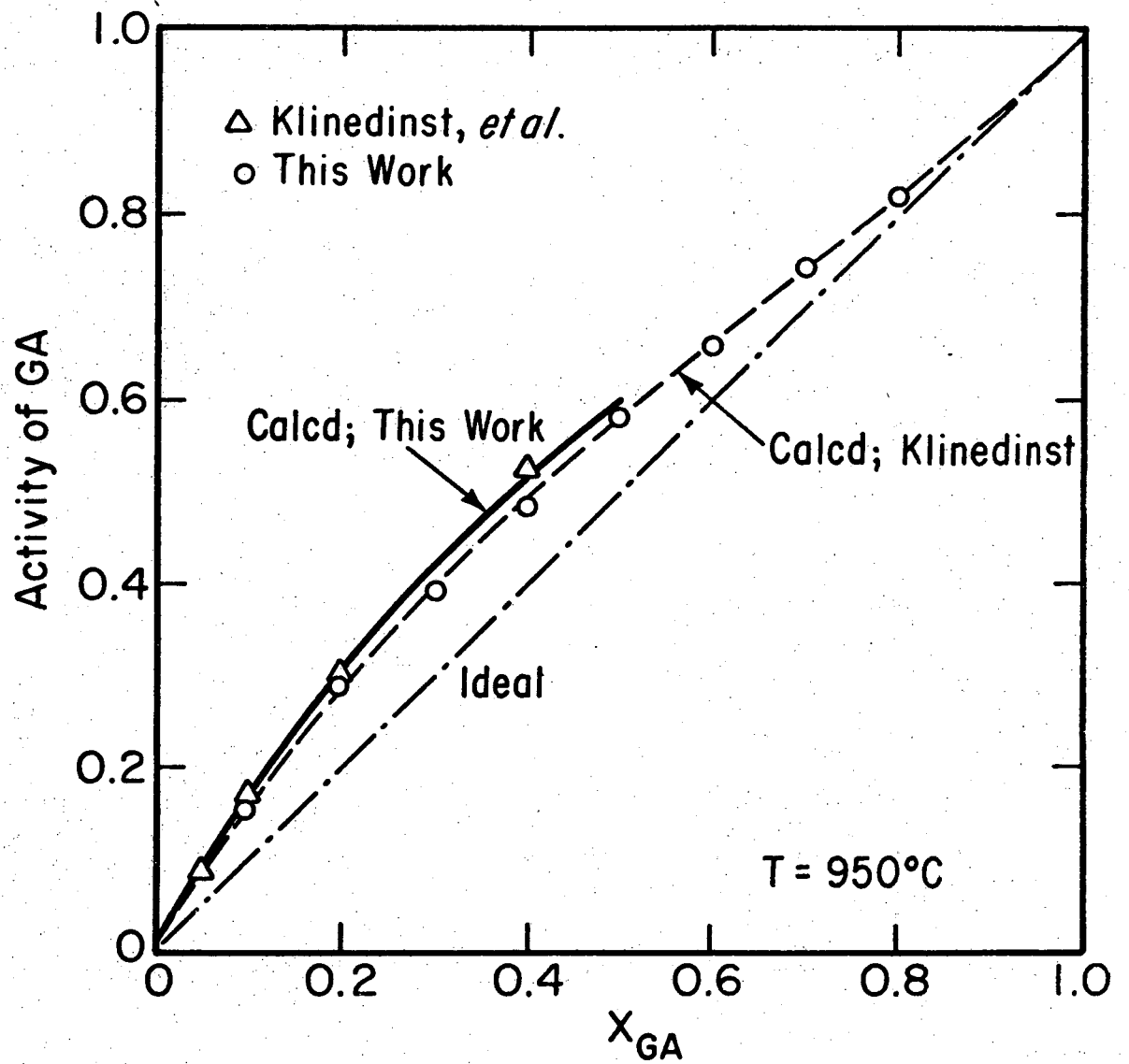
XBL 752-5731

Fig. 1. The experimentally measured Ga-In alloy cell emfs as a function of temperature for several alloy compositions compared to the data of Klinedinst.
- - - - Klinedinst, et al.
_____ This work



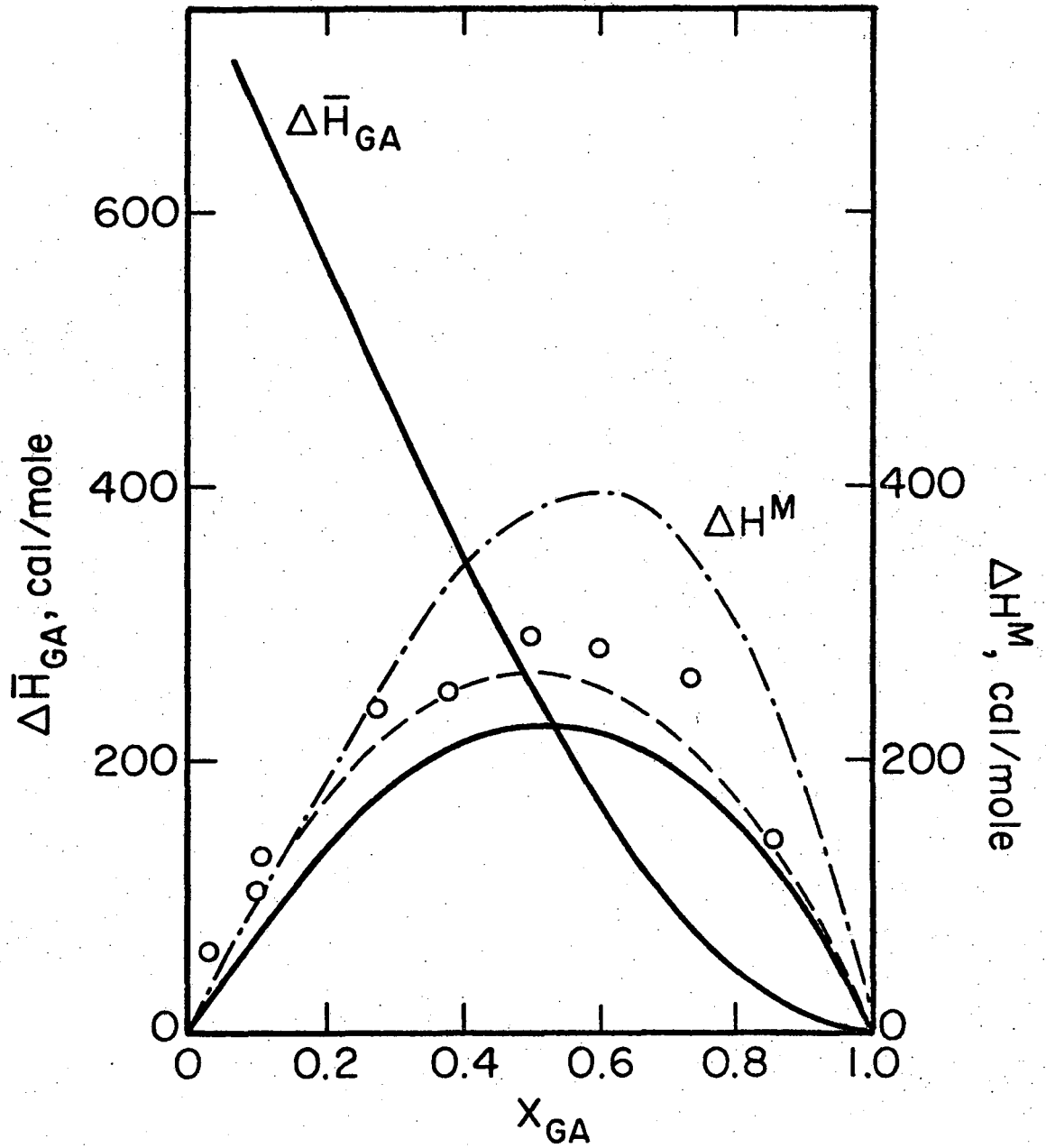
XBL 752-5732

Fig. 2. The $\alpha_{\text{Ga-In}}$ parameters calculated from the emf data of this work and of Klinedinst et al. for several temperatures.



XBL752-5733

Fig. 3. The activity of gallium at 950°C as a function of the Ga-In alloy composition.



XBL 752-5734

Fig. 4. The enthalpies of mixing of Ga-In alloys from several sources:

- This work (800-950°C)
- - - Bros (150°C)
- · - · Klinedinst (800-950°C)
- o Predel and Stein (350°C)

V. THE Ga-Sb SYSTEM

A. Introduction

The study of the Ga-Sb system was motivated by the dearth of thermochemical information on this III-V system. Closer examination of the existing data revealed indirect contradictions in conclusions and derived data. It has been pointed out by Sirota⁴ that the liquid metals in close proximity to the liquidus in compound semiconductor systems exhibit short range order. This observation is contradicted by the low values of heats of mixing selected by Hultgren¹⁰ for the Ga-Sb system, which are more consistent with a more randomly mixed liquid. The derived results of this study show large negative heats of mixing, which are more consistent with liquids with short range order.

The activities in the Ga-Sb system have been previously studied by use of a chloride electrolyte. This technique, as pointed out by Chatterji and Smith,¹ has the disadvantage of being ambiguous with regard to the charge of the ionic carrier in the electrolyte. For the cells of Danilin and Yatsenko³ the ionic carrier can be Ga^{+1} or Ga^{+3} . Thus, the value of "n" in the Nernst equation ($RT \ln a = nFE$) can not be definitely stated. Nevertheless, Danilin and Yatsenko have used $n = 3$, i.e., assumed Ga^{+3} is the ionic carrier, to arrive at the conclusions that the Ga-Sb liquid alloy system has very strong negative deviations from the ideal. This led them to suggest that these deviations can be accounted for by complexes resembling molecules. This conclusion is in contrast to the conclusion of Schottky and Bever⁵ that the system is close to ideal. Schottky and Bever pointed out that the liquidus measured by Köster and Thoma² is very nearly that predicted by an ideal mixing model.

B. Results

The emfs measured as a function of temperature in the Ga-Sb system are given in Table 1 and plotted in Fig. 1 for the compositions investigated. Table 1 also contains the activities and activity coefficients of Ga. Since the emf data were reproducible to 0.5 mV, the error in the activities and activity coefficients are $\pm 2\%$. The activity coefficients are shown in Fig. 2 as a function of composition.

In making these measurements care was taken to remain in the single-phase liquid region. For this reason measurements at the lower temperatures were not made for those compositions near $x_{\text{Ga}} = 0.5$. Furthermore, measurements were not made at temperatures higher than 800°C as Sb has a significant partial pressure for those temperatures.

It is important to note that equilibrium was assumed to have been reached when the emf values remained constant over a period of several hours. The time for initially homogenizing the components of the melt varied from 2 to 5 days. The time constant for equilibration after a temperature change was 1.4 hrs at 997°K and 14 hrs at 922°K . Because of the long equilibration times, at least one data point was repeated for each composition.

It should be pointed out that the depolarization rate is rapid. By passing current through the cell momentarily and watching the emf return to the initial value, it was found that the largest time constant measured was less than 10 min.

Table 1. Experimental data.

x_{Ga}	T (°C)	emf (mV)	a_{Ga}	γ_{Ga}
0.2000	797.9	75.0	0.0873	0.4368
	772.6	77.7	0.0753	0.3767
	747.8	80.0	0.0654	0.3269
	723.1	83.8	0.0534	0.2672
	699.6	88.9	0.0416	0.2078
	676.8	96.2	0.0294	0.1472
0.4000	803.1	40.7	0.2682	0.6706
	775.1	41.5	0.2526	0.6315
	749.7	43.3	0.2292	0.5730
	721.9	47.5	0.1901	0.4751
0.5998	797.0	20.7	0.5101	0.8503
	771.8	21.4	0.4905	0.8178
	749.5	22.5	0.4657	0.7763
0.7998	800.5	8.6	0.7577	0.9474
	775.8	9.3	0.7340	0.9177
	749.7	10.9	0.6905	0.8634
	725.3	12.9	0.6380	0.7677
	700.3	15.8	0.5688	0.7112
	672.8	19.0	0.4967	0.6211
	648.9	23.6	0.4108	0.5136
0.8998	752.8	4.6	0.8555	0.9507
	724.2	4.8	0.8449	0.9390
	699.3	5.5	0.8212	0.9126
	670.5	6.7	0.7816	0.8687
	649.7	8.2	0.7339	0.8156

C. Discussion

The data of this work supports the conclusion that the system is highly nonideal, deviating negatively. However, the agreement with the data of Danilin and Yatsenko is poor. The differences can be attributed to the ambiguity of the ionic carrier in the chloride electrolyte since postulating the Ga^{+1} ion to be the current carrier would result in emf values three times the value that were measured in this work. Thus, the larger emf values of Danilin and Ytsenko can be explained by mixed conduction in the electrolyte by both Ga^{+1} and Ga^{+3} .

As suggested by Danilin and Yatsenko, the data of this work can be explained by postulating molecular complexes. In this case a minimum of three complexes are required. First, let us examine the elements themselves. Gallium are a group III metal with two common valences, +1 and +3. Antimony is a group V metal having three common valencies, -3, +3, and +5. The electron affinities of Ga and Sb are calculated from the electronegativities of Pauling,⁷ which are proportional to the sum of the electron affinity and ionization potential.⁶ These are shown in Table 2. Thus, postulating a valence of -1 is not unreasonable for either Ga or Sb.

Postulating valences of -1 for either Ga or Sb suggests the complexes GaSb_3 and Ga_5Sb in addition to GaSb which follows from the examination of the commonly known valences. Using these species in the chemical theory of Dolezalek requires that the equilibrium constants K_{13} , K_{11} , and K_{51} be defined by

Table 2. Electron affinity calculations.

Element	Electronegativity	Ionization Potential	Electron Affinity
H	2.1	13.598 eV	0 eV
Ga	1.81	5.999 eV	5.7 eV
Sb	1.9	8.641 eV	3.7 eV

*From Pauling.⁷

$$K_{13} = a_{\text{Ga}_1\text{Sb}_3} a_{\text{Ga}}^{-1} a_{\text{Sb}}^{-3}$$

$$K_{11} = a_{\text{Ga}_1\text{Sb}_3} a_{\text{Ga}}^{-1} a_{\text{Sb}}^{-1}$$

$$K_{51} = a_{\text{Ga}_5\text{Sb}_1} a_{\text{Ga}}^{-5} a_{\text{Sb}}^{-1}$$

In the chemical theory the chemical species exhibit ideal behavior, and the deviations from ideality are due to the differences between the "true" and "apparent" mole fractions. Thus, the species activity coefficients are assumed equal to unity, and the "apparent" mole fractions "x" are related to the true mole fractions "z" in the following manner:

$$x_{\text{Ga}} = \frac{z_{\text{Ga}} + z_{\text{GaSb}_3} + z_{\text{GaSb}} + 5z_{\text{Ga}_5\text{Sb}}}{1 + 3z_{\text{GaSb}_3} + z_{\text{GaSb}} + 5z_{\text{Ga}_5\text{Sb}}}$$

$$x_{\text{Sb}} = \frac{z_{\text{Sb}} + 3z_{\text{GaSb}_3} + z_{\text{GaSb}} + z_{\text{Ga}_5\text{Sb}}}{1 + 3z_{\text{GaSb}_3} + z_{\text{GaSb}} + 5z_{\text{Ga}_5\text{Sb}}}$$

Using trial and error to fit the data of this work, the equilibrium constants were determined as a function of temperature and interpreted as Gibbs energy of formation. When these Gibbs energies are assumed to vary linearly with temperature, the enthalpies and entropies of reaction shown in Table 3 result. Using these values, the x_{Ga} were calculated as a function of z_{Ga} and temperature. The activity coefficients $\gamma_{\text{Ga}} = z_{\text{Ga}}/x_{\text{Ga}}$ were calculated for temperatures of 923°K and 1023°K and plotted in Fig. 3.

Notice that the entropies of formation necessary for this model are extremely large. This may be due to the narrow range of temperature measurement.

Table 3. Enthalpy and entropy of formation of melt species necessary to model the data of this work.

Reaction	ΔH^f (kcal/g-atom)	ΔS^f (eu)
$\text{Ga}_l + 3 \text{Sb}_l \rightarrow \text{GaSb}_3$	0	2.1
$\text{Ga}_l + \text{Sb}_l \rightarrow \text{GaSb}_l$	-25.3	-22.5
$5\text{Ga}_l + \text{Sb}_l \rightarrow \text{Ga}_5\text{Sb}_l$	-77.6	-72.3

Table 4. Comparison of enthalpies of mixing.

x_{Ga}	ΔH cal/g-atom According to Hultgren ¹⁰	ΔH cal/g-atom of this Work
0.1	-79	-1554
0.2	-150	-2959
0.3	-206	-4623
0.4	-241	-6024
0.5	-255	-6874
0.6	-244	-7382
0.7	-209	-7712
0.8	-153	-7606
0.9	-81	-5499

The chemical theory assumes that there are no physical interactions between the molecular species, only chemical interactions. Thus, the enthalpy of mixing will be due entirely to the enthalpies of formation. Accordingly, the enthalpies of mixing are calculated for a temperature of 997°K and listed in Table 4 and compared to the enthalpies of mixing of Yazawa et al.,⁹ measured by reaction calorimetry at 1003°K, as revised by Hultgren et al.¹⁰ The more recent work of Predel and Stein¹¹ indicates that $\Delta H = -258$ cal/g-atom at $x_{\text{Ga}} = 0.5$.

There are three main explanations for the great discrepancies: The first is that the chemical theory is at best just a conceptual formalism to account for deviations from ideality, that quantities other than activities cannot be calculated from the equations developed from that formalism. The second explanation is that due to the very slow equilibration of these melts--2 to 5 days at 1073°K for full homogenization of the melt as measured by waiting for the cell emfs to reach steady state values--reaction calorimetry would be very difficult to perform accurately. The third explanation is that a systematic error was introduced by some undetermined cause in the experimental method.

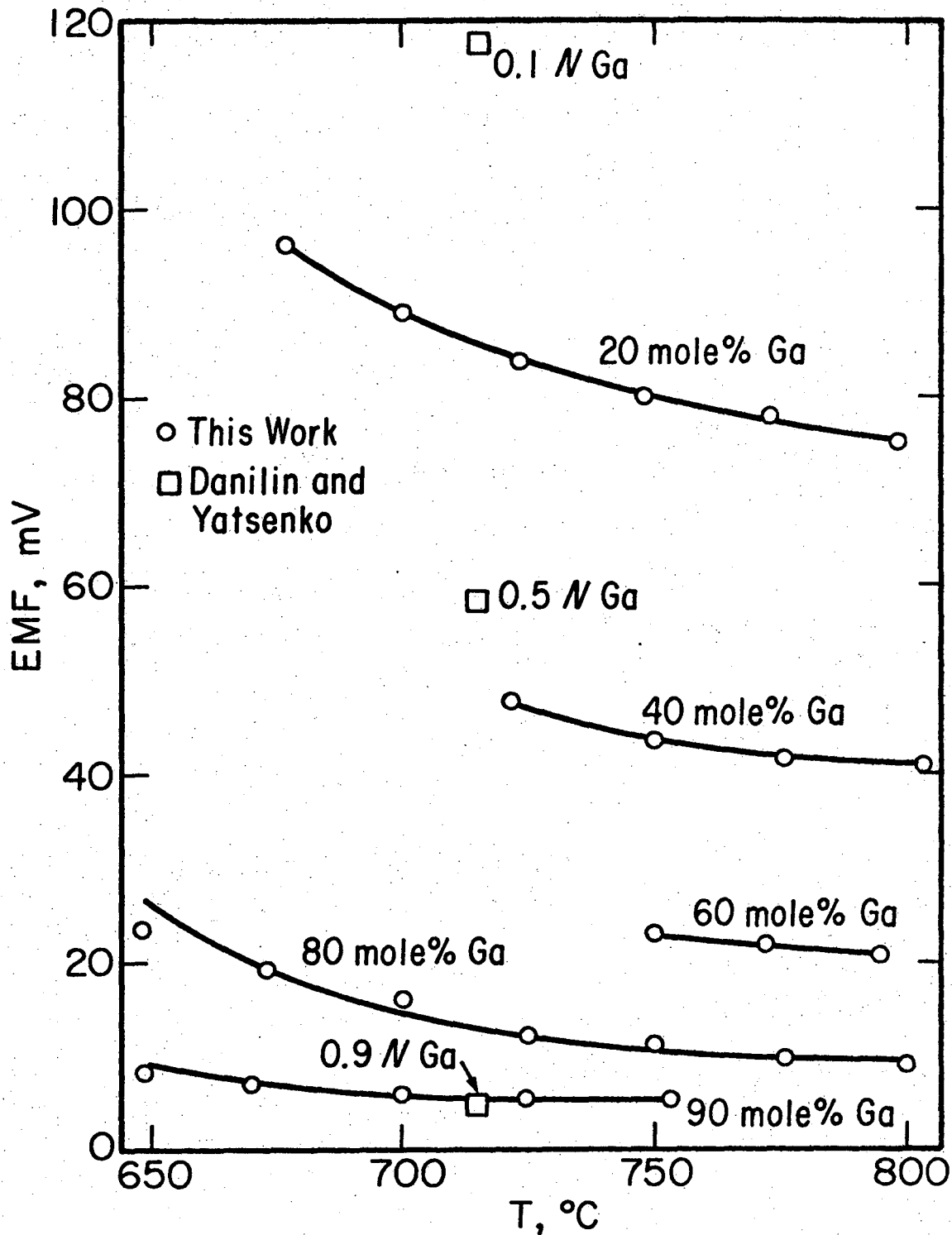
The process of forming the three Ga-Sb complexes would explain the slow equilibration times exhibited by these cells. Since the complexes are larger molecules, the diffusion times necessary for homogenization and equilibration are increased. Another possibility is that the rate of complexing is low so that the rate of equilibration would be slow.

D. Conclusion

The Ga-Sb liquid alloy system shows large negative deviations from the ideal. This can be modeled by postulating complexes of GaSb_3 , GaSb , and Ga_5Sb . In addition, these complexes can explain the short range order of the III-V liquids near the liquidus reported by other observers. However, derived enthalpy of mixing data are much different from those reported earlier and, when coupled with the extremely large hypothesized entropies of formation, casts some doubt as to the validity of the experimental data obtained in this investigation.

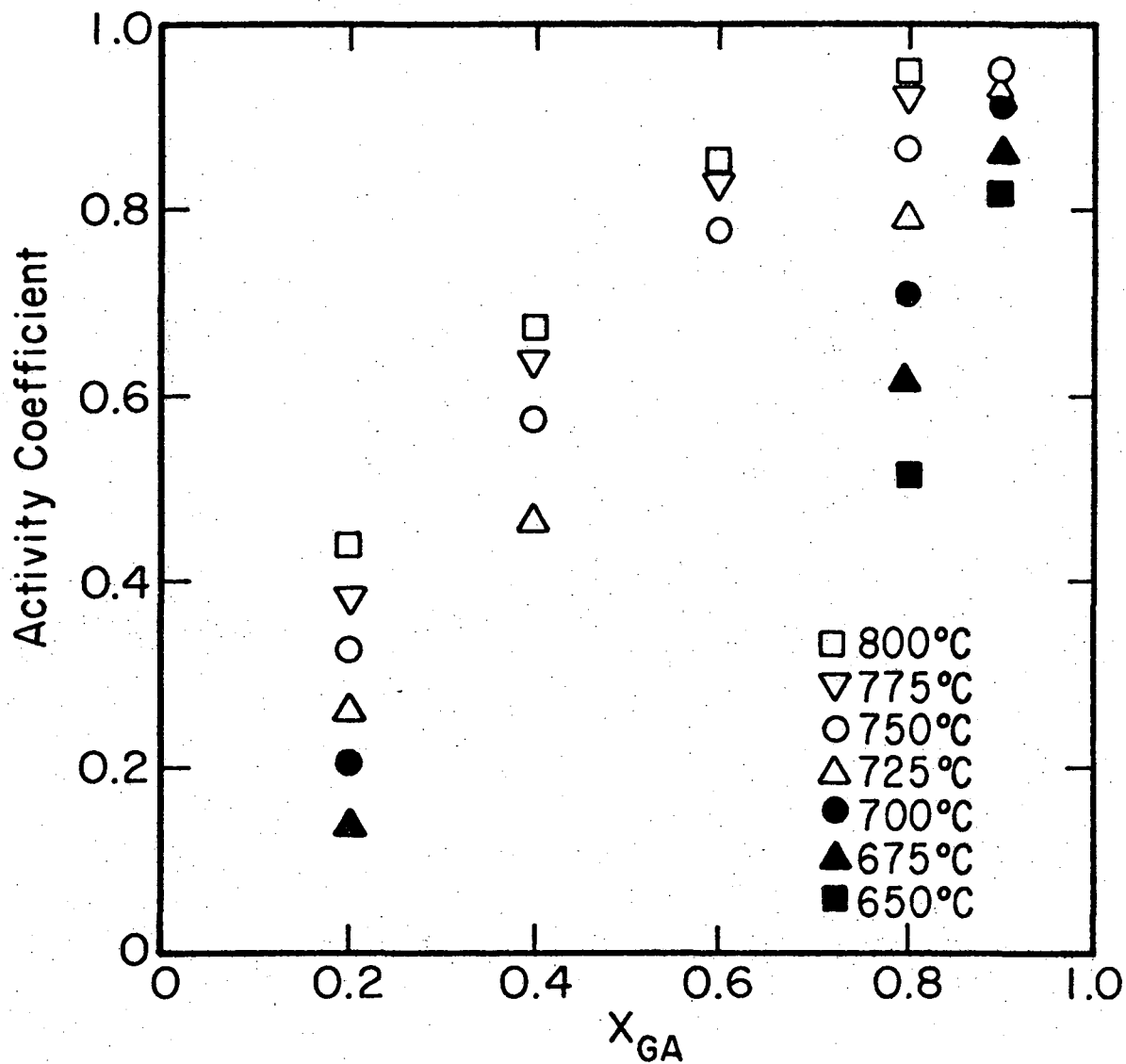
REFERENCES

1. D. Chatterji and J. V. Smith, J. Electrochem. Soc. 120(6), 770 (1973).
3. V. N. Danilin and S. P. Yatsenko, Tr. Inst. Khim., Akad. Nauk SSSR, Ural. Finial No. 20, p. 142-5 (1970).
4. N. N. Sirota, Semiconductors and Semimetals, R. K. Willardson and Albert C. Beer (Academic Press, Inc., N. Y., 1968), Vol. 4, Chapter 2.
5. W. F. Schottky and M. B. Bever, Acta Met. 6, 820 (1958).
6. E. Cartmell and G. W. A. Fowles, Valency and Molecular Structure (D. Van Nostrand Co., Inc., N. J., 1966).
7. L. Pauling, The Nature of the Chemical Bond (Cornell Univ. Press, N. Y., 1960).
8. C. E. Moore, Ionization Potentials and Ionization Limits Derived from the Analyses of Optical Spectra, NSRDS-NBS 34, 1970.
9. A. Yazawa, T. Kawashima, K. Itagaki, J. Japan Inst. Metals 32, 1298-93 (1968).
10. R. Hultgren, P. D. Desai, D. T. Hawkins, M. Gleizer and K. K. Kelley, Selected Values of the Thermodynamic Properties of Binary Alloys (American Society for Metals, Ohio, 1973).
11. B. Predel, and D. W. Stein, J. Less Common Metals 24(4), 391 (1971).



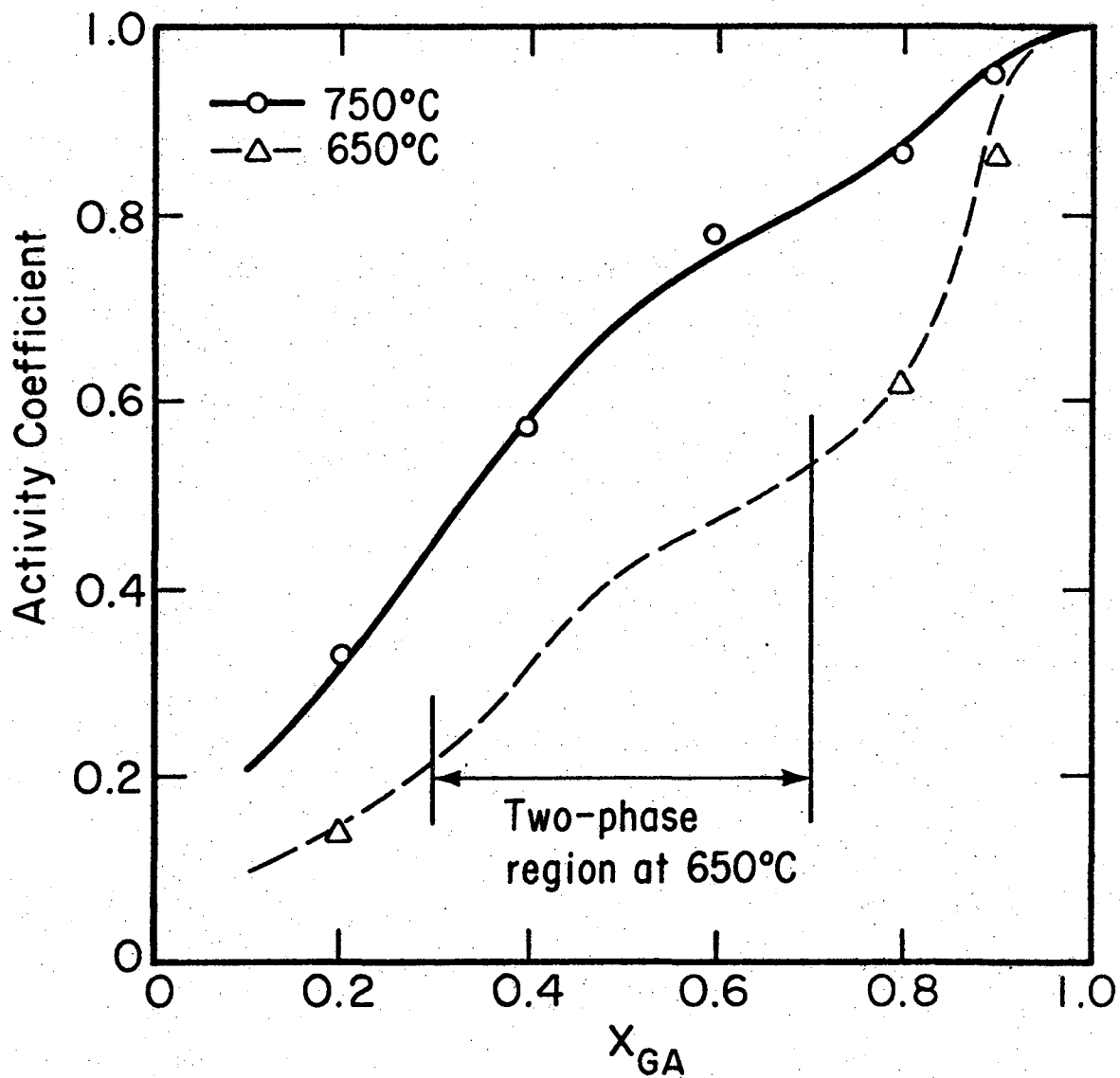
XBL 752-5735

Fig. 1. The measured emfs of various compositions at Ga-Sb alloys contrasted to the data of Danilin and Yatsenko.



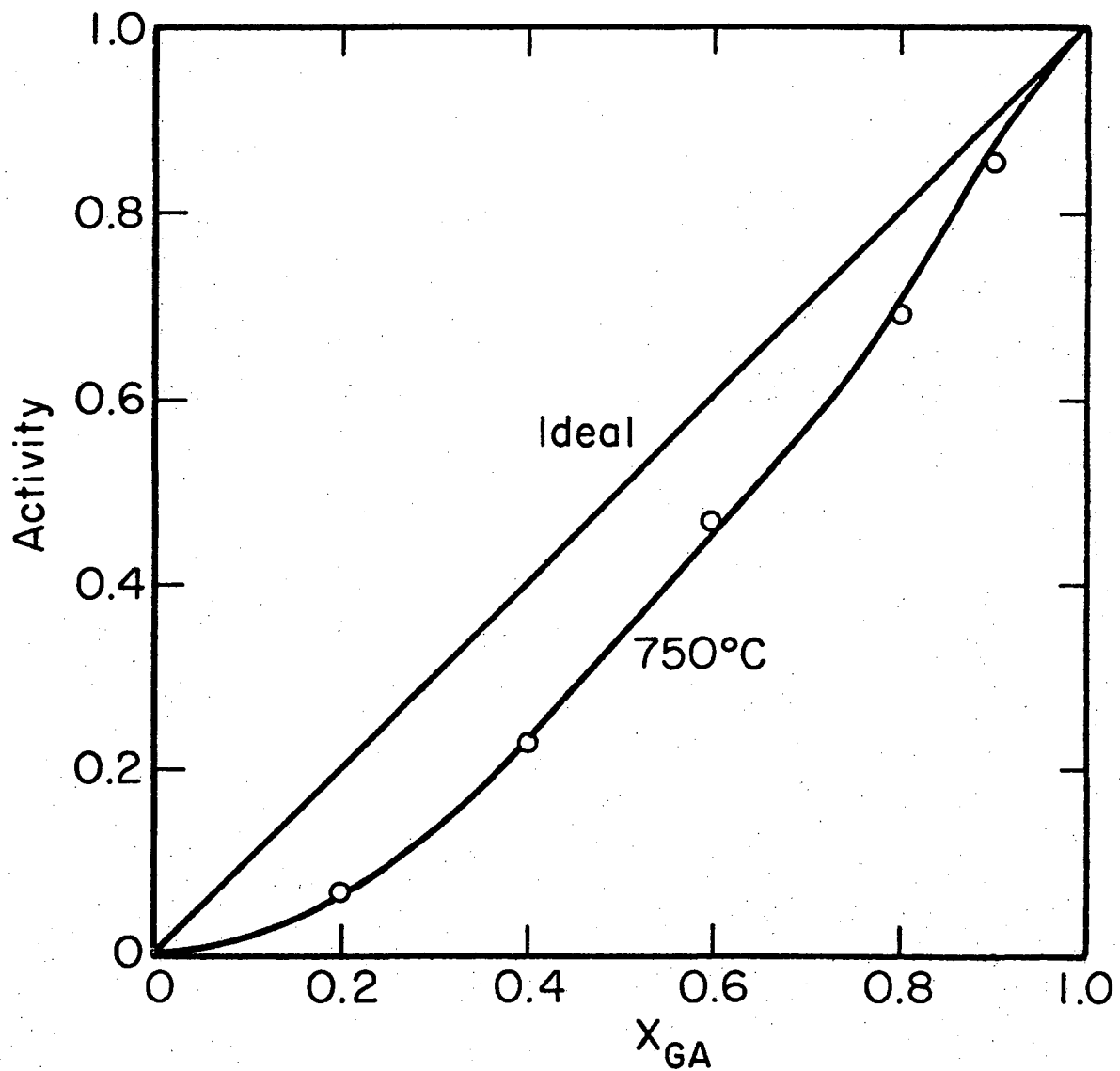
XBL 752-5736

Fig. 2. The measured gallium activity coefficients of various compositions of Ga-Sb alloys of various different temperatures.



XBL 752-5737

Fig. 3. The predicted gallium activity coefficients of various Ga-Sb alloy compositions contrasted with the measured data.



XBL 752-5738

fig. 4. The measured gallium activity compared to the fitted curve from the chemical theory.

VI. THE Ga-In-Sb SYSTEM

A. Results

The activity of gallium in a Ga-In-Sb liquid alloy with composition $x_{\text{Ga}} = 0.708$, $x_{\text{In}} = 0.102$, and $x_{\text{Sb}} = 0.190$ was found to be strongly depressed below that of an ideal liquid alloy, as expected from the results of Ga-Sb alloy melt activity studies. In this preliminary and cursory study of the Ga-In-Sb system, the melt equilibration times were found to be extremely long, as in the Ga-Sb studies. Table 1 gives the measured emfs and calculated activities and activity coefficients of Ga for this cell.

The time constant for the melt to reach full homogenization and equilibration at 800°C was measured to be 3 days.

B. Conclusion

The experimental result is a strongly negative deviation of gallium activity from ideality, which becomes more negative with decreasing temperature.

Table 1. Ga activity data for a Ga-In-Sb alloy.

T(°C)	EMF(V)	a_{Ga}	α_{Ga}
797	11.7	0.681	0.962
772	16.4	0.575	0.813
747	24.8	0.426	0.601

VII. THE QUASI-CHEMICAL MODEL REVISITED

A. Introduction

In the system Ga-Sb, the melts are highly non-ideal at temperatures below 750°C. In order to take into account the non-ideality, the quasi-chemical model was examined. Though this model and its extensions are not applicable to the Ga-Sb system, it is useful in the In-Sb system. The quasi-chemical model was applied to the In-Sb system by Stringfellow and Greene¹ and the data of Hoshino et al.²

In this study, the quasi-chemical model and its extensions are compared to the α -parameter model which Guggenheim³ refers to as the zeroth order approximation and the quasi-chemical model. The α -parameter model is used by Hoshino et al., to correlate their data for the In-Sb system. The data expressed as $\alpha_i = RT \ln \gamma_i / (1 - x_i)^2$ show a fairly linear dependence of α on composition from $x = 1$ to $x = 0.5$ but become highly nonlinear for $x = 0.5$ to $x = 0$. This kind of behavior is expected because the entropy of mixing is ignored in the α -parameter model. The quasi-chemical model takes the entropy of mixing into account so that the dependence of the quasi-chemical parameter ω on x , applied to the In-Sb system, should be less non-linear. As derived by Guggenheim both α and ω represent the same quantity, the atomic interaction energy; this is the energy change which occurs when an atom or molecule A is replaced by an atom or molecule B.

Since the data for the Ga-Sb system were found to be highly non-ideal, this non-ideality was assumed to be due to an interaction of Ga and Sb much in the same manner as in the In-Sb system. At the lower temperatures

the activities of Ga are so depressed, however, that the first order quasi-chemical model cannot be utilized to explain them. Closer examination of the quasi-chemical treatment showed, however, that the extension of the treatment beyond the first order quasi-chemical model might depress the theoretical activities of the quasi-chemical model further.

Guggenheim's extended treatment considers the interaction between next-nearest-neighbors only. For liquid InSb the number of nearest-neighbors derived from X-ray data is 5.6,⁴ implying that the simple cubic lattice is the simplest lattice approximation for that liquid. Thus, the simplest configuration to be considered which would take next-nearest-neighbors into consideration would be the square configuration.

The extended quasichemical treatment of Guggenheim contains a contradiction, which is freely admitted in the presentation. This contradiction leads to the ignoring of 3/4 of the interactions of next-nearest-neighbors. The treatment presented here for the square configurations take into account all of the nearest- and next-nearest-neighbors. This is compared to the treatment and derivation of Guggenheim. Comparison with the Ga-Sb data, however, indicates that theoretical activities are still not sufficiently depressed.

A further extension of the model is to consider third-nearest-neighbor interactions. This corresponds to using a cube configuration for a cubic lattice as the basic unit. This treatment does permit the depression of the activities beyond that experimentally found for Ga in the Ga-Sb system, though the model gives a poor fit to the experimental data.

The effect of such a progression to more complex models is that of approaching more closely the simple α -parameter model, so that for the representation of activity data for small values of the interaction parameter the α -parameter model suffices. However, in order to extract excess Gibbs energy of mixing, or enthalpy of mixing and excess entropy of mixing, using a single parameter model, the more complex quasi-chemical models are suggested.

B. Requirements of Extended Quasi-Chemical Models

The interaction parameter " ω " used by Guggenheim is the same quantity as " Ω " used by Stringfellow and Greene in their recent correlations of thermochemical data on metallic melts using the quasi-chemical model and the same as " α " of the α -parameter correlations in popular use. These parameters are theoretically related to the energy change associated with the substitution of one atom or molecule of species A in a lattice of A with one of species B. Thus, ω/N_{Av} (N_{Av} = Avogadro's number) would be the change in internal energy for the A lattice system with a single B. It is important to note here that these models assume that the sizes of the species considered are not significantly different in order that volume changes due to mixing and variations in the number of nearest neighbors are not significant.

The α -parameter defined by

$$\alpha = RT(\ln \gamma_A)/(1 - x_A)^2$$

is a measure of excess quantities which vary slowly with composition, where γ_A and x_A are the activity coefficient and mole fraction of species A. As pointed out by Guggenheim, when α/RT is less than 1/4, the error incurred

in the excess Gibbs energy by assuming a constant α over the whole composition range is less than 1%. This holds for mixtures for which the species preferentially seek to surround themselves with their own species. The same is true of associating species for which $\alpha/RT > -0.25$. Thus, for values of α/RT between $-1/4$ and $1/4$, the excess Gibbs energies are accurate to within 1%, because the energies for interaction are not sufficiently large to cause large deviations in the entropy from the ideal values for entropy.

For values of the interaction energies such that $|\alpha/(RT)| > 1/4$, the excess entropies of mixing become important. For large negative values of α such as occur in III-V melts, the association of the two species is as to appear to give two distinct regions: (i) $x_A > 0.5$ dominated by A and associated A-B, and (ii) $x_A < 0.5$ dominated by B and associated A-B. Thus, as suggested by Darken and Gurry,⁵ binaries would have to be represented by different linear functions of x_A depending on the range of x_A . Furthermore, once α is made dependent on x_A , one must differentiate between

$$\alpha_{AB} = RT \ln \gamma_A / (1 - x_A)^2$$

and

$$\alpha_{BA} = RT \ln \gamma_B / (x_A)^2$$

These α 's are related through the Gibbs-Duhem equation.

The first order quasi-chemical treatment assumes

$$\bar{x}^2 = (N_A - \bar{x})(N_B - \bar{x}) e^{-2\omega/RT}$$

in contrast with the ideal case, where the total number of nearest dissimilar neighbor pairs, \bar{x} , is given by $\bar{x}^2 = (N_A - \bar{x})(N_B - \bar{x})$. (\bar{x} is the number of pairs composed of dissimilar members. N_A and N_B are the numbers of A and B, respectively in the total solution.) Such a treatment includes an excess entropy of mixing by taking only nearest neighbors into account. The first order quasi-chemical model cannot be used to model systems with highly depressed activities. This can be explained by examining the premise that only nearest neighbors are important. For systems where the nearest neighbor interaction is relatively weak it suffices to ignore the energies of interaction of more distant neighbors. Furthermore, the contribution to the excess entropy by secondary ordering is miniscule. (Secondary ordering is defined as ordering of next-nearest neighbors by the influence of nearest neighbors.) As nearest neighbor interactions become more important, however, so must next-nearest neighbor interactions. Thus, such a treatment need not be dependent on the composition.

Guggenheim's treatment takes into account the effect of next-nearest neighbors. Hill⁶ pointed out a contradiction in Guggenheim's treatment which states that the number of pairs of next-nearest neighbors is $1/4 NZ_1$, whereas the actual number is $1/2 NZ_2$. (N , Z_1 , and Z_2 are the number of atoms or molecules in the solution, the number of nearest neighbors for each atom, and the number of next-nearest neighbors, respectively, ($N = N_A + N_B$.) As the systems of interest here are expected to have $Z_1 = 6$, a cubic lattice will be examined in detail though the treatment could be applied to other lattices as well. Since in the cubic system a set of sites translates into a square with the next-nearest neighbor

interactions corresponding to the square diagonals, a simpler analog would be a two dimensional square lattice. This lattice is also treated below.

1. Square Interaction Model

The treatment by Guggenheim counts the number of pairs of nearest neighbors in the solution, $1/2 NZ_1$, and the number of nearest neighbor pairs associated with a square, 4. The ratio of the two gives the number of squares in the solution, $1/8 NZ_1$. Since each square has two diagonals, the number of next-nearest neighbor pairs must be $1/4 NZ_1$. The two dimensional analog of this is shown in Fig. 1a.

In the two dimensional analog $Z_1 = 4$ and $Z_2 = 4$, giving $2N$ nearest neighbor pairs, $1/2 N$ squares, and N next-nearest neighbor pairs. It is obvious that this counting system for the two dimensional case skips half of the squares and half of the next-nearest neighbor pairs.

This counting problem can be alleviated by noting that each nearest-neighbor pair is shared by two squares. Thus, the average number of nearest-neighbor pairs associated with a square is 2 implying that $(1/2 NZ_1)/2 = N$ squares are associated with the lattice. This leads to $2N$ next-nearest neighbor pairs being associated with the lattice which is equal to $1/2 NZ_2$, the correct value. This sharing of pairs also extends to the sharing of the energy of interactions. Thus, in the two dimensional case, a nearest-neighbor pair contributes $1/2$ its interaction energy to each of the two squares of which it is a part. The energy used in the Boltzmann factor in the partition functions are these shared energies and not the whole energy of interaction. It is to be noted that, since the next-nearest neighbors are not shared, their energies are likewise not shared, and the whole energy of interaction is used in the Boltzmann factor.

In the three dimensional case of a cubic lattice, each nearest-neighbor pair is shared by four squares leading to an average of one nearest neighbor pair associated with each square and giving a total of $3N$ squares associated with the lattice. Since the square diagonals are not shared between squares and there are two diagonals to a square, there must be $6N$ next-nearest neighbor pairs. Since in a cubic lattice, $Z_1 = 6$ and $Z_2 = 12$, the above values are the correct ones.

The equivalent quantities according to Guggenheim's treatment are $3/4 N$ and $3/2 N$ for the number of squares and next-nearest neighbor pairs.

As in the treatment used by Guggenheim let:

$$\eta = e^{\omega_1/Z_1 RT}$$

and

$$\phi = e^{\omega_2/Z_2 RT}$$

where $\omega_1/Z_1 N_{Av}$ and $\omega_2/Z_2 N_{Av}$ are the interaction energies of nearest and next-nearest neighbor pairs of dissimilar atoms. Then the Boltzmann factors associated with single pairs of dissimilar atoms in the Guggenheim treatment are η^{-1} and ϕ^{-1} and in this treatment are $\eta^{-1/4}$ and ϕ^{-1} . The difference in nearest neighbor Boltzmann factors result because only one quarter of the energy of a nearest neighbor pair of dissimilar atoms is associated with any one square.

An immediately obvious point to note is that the excess entropies will be smaller for this treatment than for Guggenheim's treatment because of the larger number of squares being considered, i.e., the randomness will be increased.

Complete derivations of both treatments are found in the Appendixes. In general, the principles set forth by Guggenheim for these derivations are used in the treatment advanced here.

In Table 1 the differences of the bases for the derivations of the two treatments are shown. The number of squares in a particular configuration is broken down into three parts; the total number of squares, the number of orientations of that configuration, and the variable representing the fraction of squares in that particular orientation and configuration.

In order to simplify the expressions that occur in the partition function, Van der Waal's law, $E = E_0/r^6$, is assumed for the interaction energy between dissimilar atoms as a function of distance. Since the separation of next-nearest neighbor pairs is $\sqrt{2}$ times that of nearest neighbor pairs, the associated energies are related by:

$$\omega_2/(Z_2 N_{AV}) = (\omega_1/Z_1 N_{AV})/(\sqrt{2})^6 = \omega_1/(8Z_1 N_{AV})$$

This gives the relation

$$\phi = \eta^{1/8}$$

Furthermore, the energy change of placing a B atom in an A lattice becomes $\omega = \omega_1 + \omega_2 = 1.25 \omega_1$ for a cubic lattice.

These two treatments give different distributions of the configurations. In addition the activity coefficients have different forms. The Guggenheim treatment gives:

$$\gamma_B = \left(\frac{\beta}{x_B} \right)^{3/4}$$

Table 1. Configurational degeneracy and Boltzmann factors for square interactions.

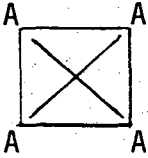
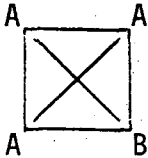
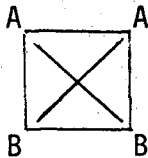
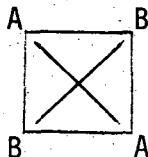
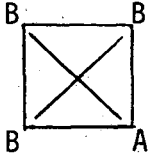
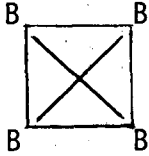
Configuration	Guggenheim's Treatment		This Treatment	
	Number in this Configuration	Boltzmann's Factor in Partition Function	Number in this Configuration	Boltzmann's Factor in Partition Function
	$(3/4)N\alpha$	1	$3N\alpha$	1
	$(3/4)N4\zeta$	$\eta^{-2}\phi^{-1}$	$3N4\zeta$	$\eta^{-2/4}\phi^1$
	$(3/4)N4\nu$	$\eta^{-2}\phi^{-2}$	$3N4\nu$	$\eta^{-2/4}\phi^{-2}$
	$(3/4)N2\nu'$	η^{-4}	$3N2\nu'$	$\eta^{-4/4}$

Table 1. Continued.

Configuration	Guggenheim's Treatment		This Treatment	
	Number in this Configuration	Boltzmann's Factor in Partition Function	Number in this Configuration	Boltzmann's Factor in Partition Function
	$(3/4)N4\xi$	$\eta^{-2}\phi^{-1}$	$3N4\xi$	$\eta^{-2/4}\phi^{-1}$
	$(3/4)N\beta$	1	$3N\beta$	1

and the present model gives

$$\gamma_B = \left(\frac{\beta}{x_B} \right)$$

where β is the fraction of square configurations with all sites occupied by B. Because the β 's have different values between the two treatments, the differences between the two predicted activity coefficients are not very large for ω less than 1/4.

Other thermodynamic quantities can easily be derived for each model, such as ΔG_m and ΔH_m . For example, the Gibbs energy of mixing is given by

$$\Delta G_m = RT(x_B \ln x_B \gamma_B + x_A \ln x_A \gamma_A)$$

The enthalpy of mixing is determined by summing the energies of configurations in the solution.

2. Cube Interaction Model

The counting of the next-nearest neighbor interactions can be extended to include third nearest neighbors in a cubic lattice. The third nearest neighbor pairs span the body diagonals of the cubes.

A cube has 12 edges which represent nearest neighbor pairs. Each edge is shared by 4 cubes so that the average number of nearest neighbor pairs associated with a cube in a lattice is 3. Since the cubic lattice has $3N$ nearest neighbor pairs there must be N cubes. Each cube has 12 face diagonals representing second nearest neighbor. Each face diagonal is shared by 2 cubes implying the total number of second nearest neighbors as $6N$. Body diagonals, representing third nearest neighbor pairs, are not shared. There are four to a cube giving a total of $4N$ third nearest neighbor pairs. Since in a cubic lattice $Z_1 = 6$,

$Z_2 = 12$, and $Z_3 = 8$ (numbers of nearest, next-nearest, and third nearest neighbors, respectively), the values derived are correct.

As before, let

$$\eta = e^{\omega_1 / (Z_1 RT)}$$

$$\phi = e^{\omega_2 / (Z_2 RT)}$$

and

$$\psi = e^{\omega_3 / (Z_3 RT)}$$

where $\omega_3 / (Z_3 N_{AV})$ is the interaction energy of a dissimilar third nearest neighbor pair. Now since nearest neighbor pairs are shared by 4 cubes and next-nearest neighbor pairs by 2 cubes, the energies contributed to a cube are $\omega_1 / (4Z_1 N_{AV})$ and $\omega_2 / (2Z_2 N_{AV})$ by nearest and next-nearest neighbor dissimilar pairs respectively. Consequently the Boltzmann factors associated with these pairs in a cube are $\eta^{-1/4}$ and $\phi^{-1/2}$. Since the third nearest neighbor pairs are not shared among cubes, the interaction energies of such pairs of dissimilar species are contributed wholly to the associated cubic configuration; the Boltzmann factor for such are ψ^{-1} .

The simplification using Van der Waal's model gives

$$\omega_3 / (Z_3 N_{AV}) = \omega_1 / (27 Z_1 N_{AV})$$

since the separation of third nearest neighbor pairs is $\sqrt{3}$ times that of nearest neighbor pairs. Therefore, the functions ψ and η are related by $\psi = \eta^{1/27}$. The total energy of interaction, ω , for placing a B atom in an A lattice is then

$$\omega = \omega_1 + \omega_2 + \omega_3 = \omega_1 \left(1 + \frac{12}{6(8)} + \frac{8}{6(27)} \right).$$

The derivation of the thermodynamic quantities based on this model depends on the solution for values of 23 configurational variables just as the values of 6 configurational variables must be determined in the case of the square configurations. The problem is reduced to one of solving for a value K which is of 4th order in an equation in the square cases and 8th order in the cubic case. Once determined, K is used to calculate the values of the configurational variables. The details of this derivation are in the Appendix.

The activity coefficient as derived from this model is given by

$$\gamma_B = \left(\frac{\beta}{x_B} \right)$$

where β represents the fraction of cubic configurations with all of the sites occupied by B.

C. Evaluation of the Models

To evaluate the usefulness of these models in systems with highly depressed activities, the limiting values of the activity coefficients are plotted in Fig. 2. The limiting values were attained by allowing ω to approach $-\infty$. Granted, for values of ω very large and negative, the assumption that the only significant interactions are those of nearest neighbors is false. The assumptions that only next and third nearest neighbors in the square and cube models need be considered are also false for large negative values of ω . Yet such an examination can provide insight into the properties of a model compared to other models.

Note that the α -parameter model predicts $\gamma = 0$ for all x as ω (or α) $\rightarrow -\infty$. The progression from 1st order to square and cube quasi-chemical models suggests that as one considers interactions of ever more distantly separated pairs the more closely the predictions for the activities will approach those predictions of the α -parameter model.

Guggenheim has shown that the 1st order model reduces to the α -parameter model when the number of nearest neighbors Z_1 approaches infinity. In the situation encountered here as $\omega \rightarrow -\infty$ the dependence of the interaction energy on distance effectively disappears. Thus, by increasing the complexity of the approximation by including the interaction with more distant atoms, the effect of ω approaching $-\infty$ is to increase the effective number of nearest neighbors.

This trend is reflected by the activity coefficients of the different models for finite values of ω . Figures 3 and 4 demonstrate this by comparing the activities computed from the 1st order and the square models to those computed from the α -parameter model for $\frac{\omega}{RT} = -3.0$. A plot of the activity coefficients computed from the cube model would be indistinguishable from the plot of the square model. This indicates that though the more complex models tend to approach the predictions of the α -parameter model, they do not become identical with it for the case of infinite complexity and finite values of ω .

Further, since the energy of interaction is assumed to drop off as r^{-6} , the energies of interaction become small compared to thermal energies and do not make significant contributions to the energy of mixing or to the ordering of the species. Since, this is to be applied to liquids, thermal motion would certainly randomize the pairs interacting over

large distances, obliterating any order due to interaction over large distances. Thus, to consider more complex systems than second order would be of little value. The complexity of the computations do not justify the small gain in accuracy.

Though the activity coefficients do not differ greatly between the 1st order and the square models, the difference between the enthalpies of mixing is considerable. Again, the effect of the difference is a tendency to approach the values predicted by the α -parameter model. This can be seen by comparing Figs. 6 and 7. As before, the plot of the enthalpy of mixing calculated from the cube model is indistinguishable from that derived from the square.

This difference in the enthalpy can be seen to a much smaller extent in the entropies. The 1st order model considers the interaction energies of nearest neighbors and the ordering of nearest neighbors. It does not take into account the secondary ordering of next nearest neighbors by the nearest neighbors preferentially pairing with its other nearest neighbors.

In order to explore the implications of secondary ordering, consider a system consisting of A and B and assume that only nearest neighbor interactions exist and that the interaction parameter is positive so that at temperature T_c (consolute temperature) the solution separates into two phases below T_c and remains a single solution above T_c . Now given ω , the α -parameter model predicts $T_c = \frac{\omega}{2R}$, and the 1st order model predicts $T_c = \frac{\omega}{2.453R}$ for $Z_1 = 6$. Suppose that the ordering of next-nearest neighbors in a 1st order liquid solution is allowed to take

place due to the nearest neighbors, A_2 and A_1 , of A_1 . Then the next nearest neighbor of A_1 preferentially will be A_1 and not B_1 , since B_1 will be repelled away by A_2 and A_1 . What this will do is make A associate more preferentially with A and likewise B with B despite thermal action to randomize the solution. Therefore, the consolute temperature must be greater than $T_c = \frac{\omega}{2.433R}$ for $Z_1 > 6$. In general, then, T_c should be greater than that predicted by the 1st order quasi-chemical model. Inclusion of energies of interaction for next and third nearest neighbors was considered. These energies can only make more probable that B will not be a neighbor to A. Thus, the thermal action to randomize the solution is again thwarted, making the predicted consolute temperature higher. The effect of these considerations is less because of the complex routine for influencing that neighbor. Relations between T_c and ω given by the different models are summarized in Table 2.

In Figs. 9 and 10, activity coefficient data for the In-Sb system at 900°K as taken by Terpilowski⁷ and Hoshino et al.,² are plotted. Plotted on the same graphs are the activity coefficient curves as predicted by the 1st order and square models and fitted to minimize the error. The Terpilowski data fit well with both the 1st order model and the square model, though the square model may have a slightly better fit to the data. The data of Hoshino et al., do not fit well with either model at low In mole fractions. However, the square model does obviously fit better than the 1st order quasi-chemical model.

Table 2. The ratio of the interaction energy ω and the consolute temperature as predicted by the various revised quasi-chemical models.

Model	$\frac{\omega}{RT_c}$
1st order quasi-chemical	2.433
Square model	
Nearest neighbor interactions only	2.088
Include next nearest neighbor interactions	2.065
Cube model	
Nearest neighbor-interactions only	2.089
Include next nearest neighbor interactions	2.062
Include third nearest neighbor interactions	2.058
α -Parameter model	2.000

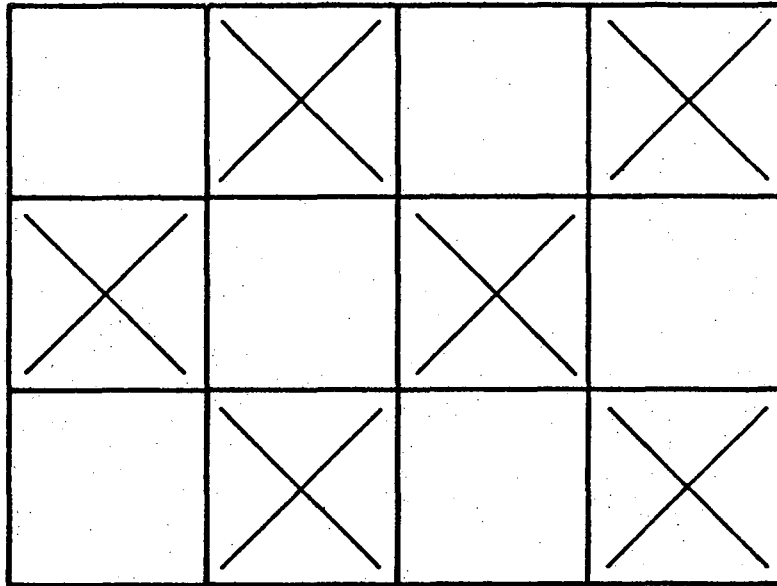
D. Conclusions

Guggenheim's derivation for the second order quasi-chemical models is found to be neglecting three quarters of the second order interactions. A method has been proposed to correct this for the specific case of cubic lattices.

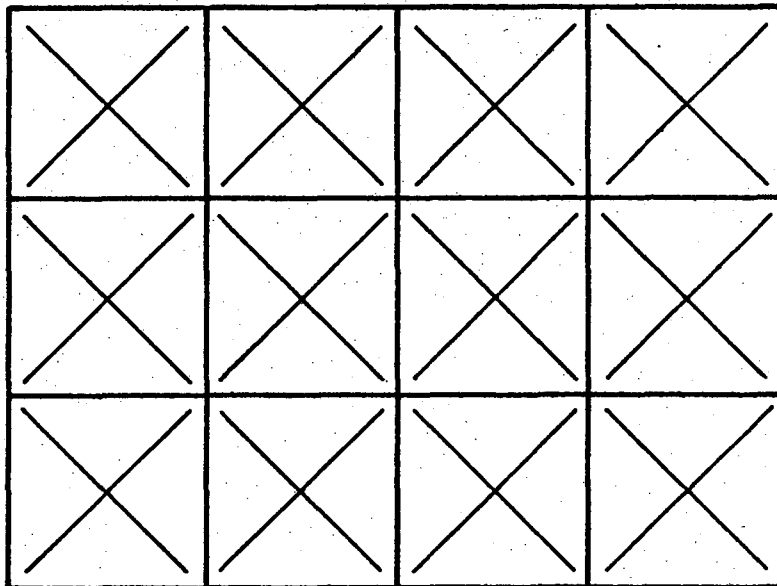
In addition, the higher order quasi-chemical models are found to give a better fit to the available data on the In-Sb alloy melt system than the first order quasi-chemical model. These higher order models give calculated activities quite similar to those predicted by the α -parameter model. Due to the complexity of those higher order models the α -parameter model is preferred for the calculation of activities. Enthalpies and entropies of mixing, however, should be calculated by the higher order quasi-chemical models.

REFERENCES

1. G. B. Stringfellow and P. E. Greene, *J. Phys. Chem. Sol.* 30, 1779 (1969).
2. H. Hoshino, Y. Nakamura, M. Shimoji and K. Niwa, *Berichte der Bunsengesellschaft* 69, 114 (1965).
3. E. A. Guggenheim, *Mixtures* (Clarendon Press, Oxford, 1952), Chapters IV and V.
4. R. Buschert, I. G. Geib and K. Lark-Horowitz, *Bull. Am. phys. Soc.* 1, 111 (1956).
5. L. S. Darken and R. W. Gurry, *Physical Chemistry of Metals* (McGraw Hill, N. Y., 1953), p. 49, p. 271.
6. Hill, *J. Chem. Phys.* 18, 988 (1950).
7. J. Terpilowski, *Archiwum Hutnictwa* 4, 555 (1956).



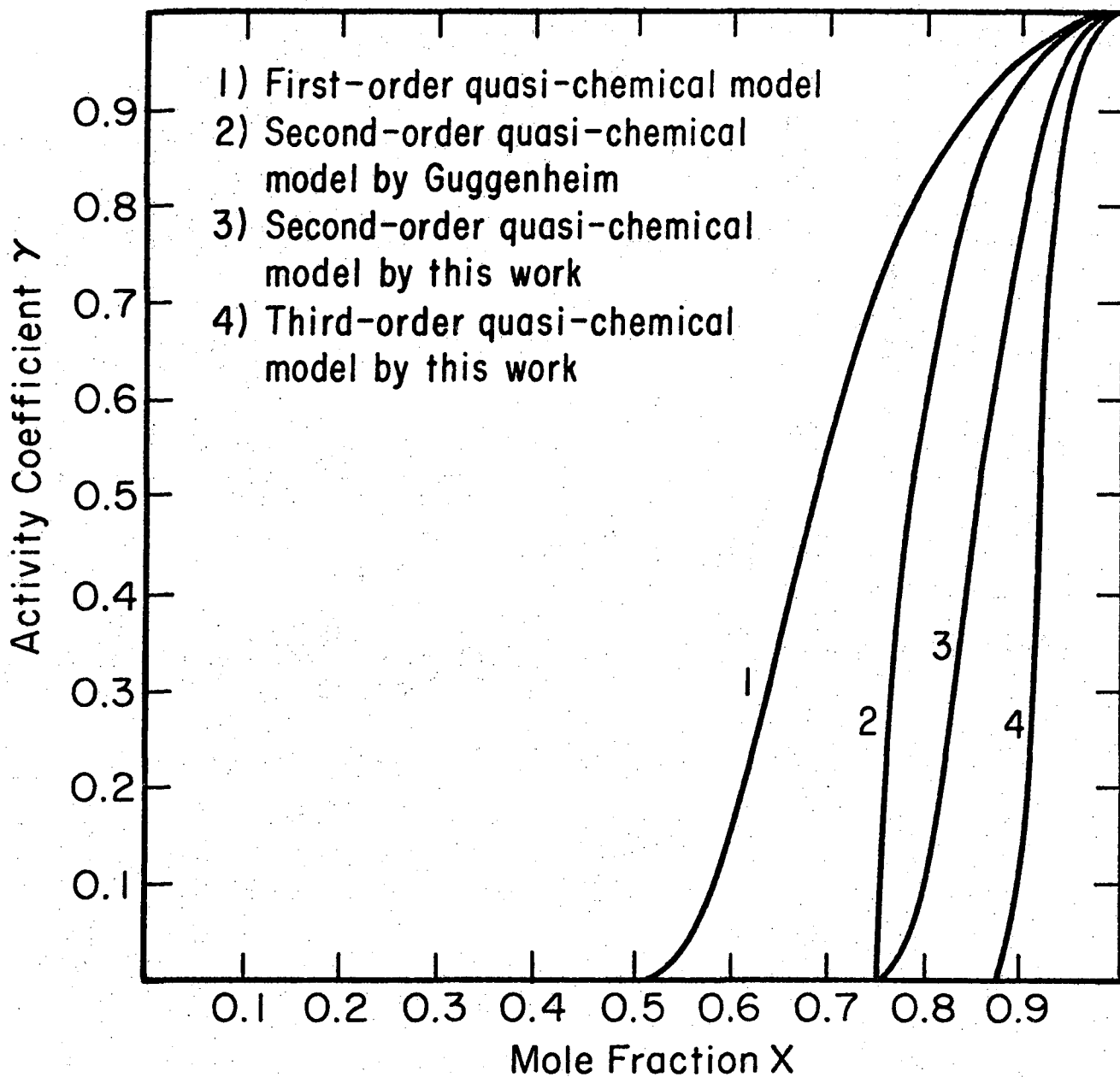
(a)



(b)

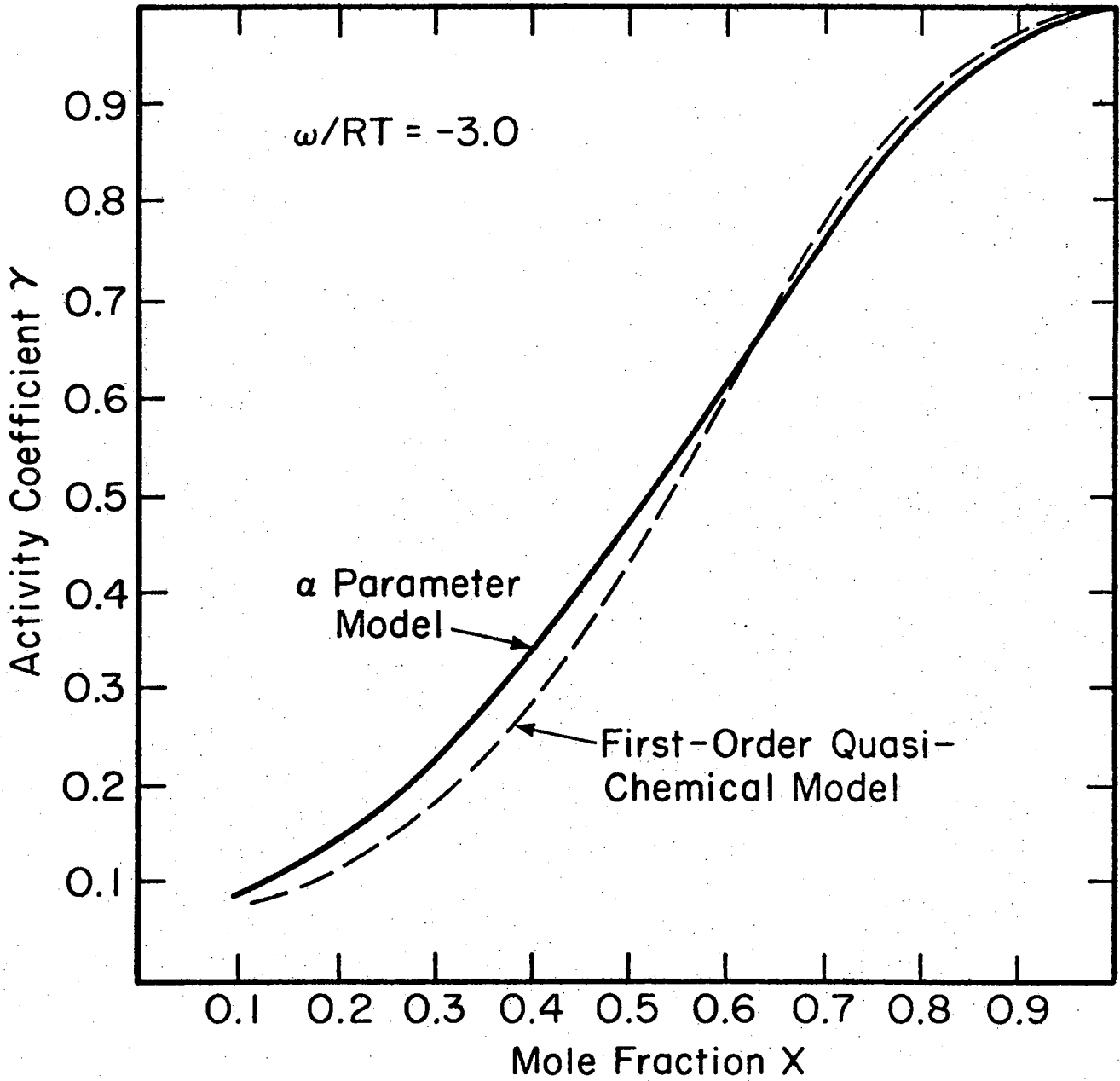
XBL 752-5739

Fig. 1. (a) This is the two dimensional analog of Guggenheim's quasi-chemical treatment for counting second nearest neighbor pairs. (b) This is the two dimensional analog of the counting treatment advanced here.



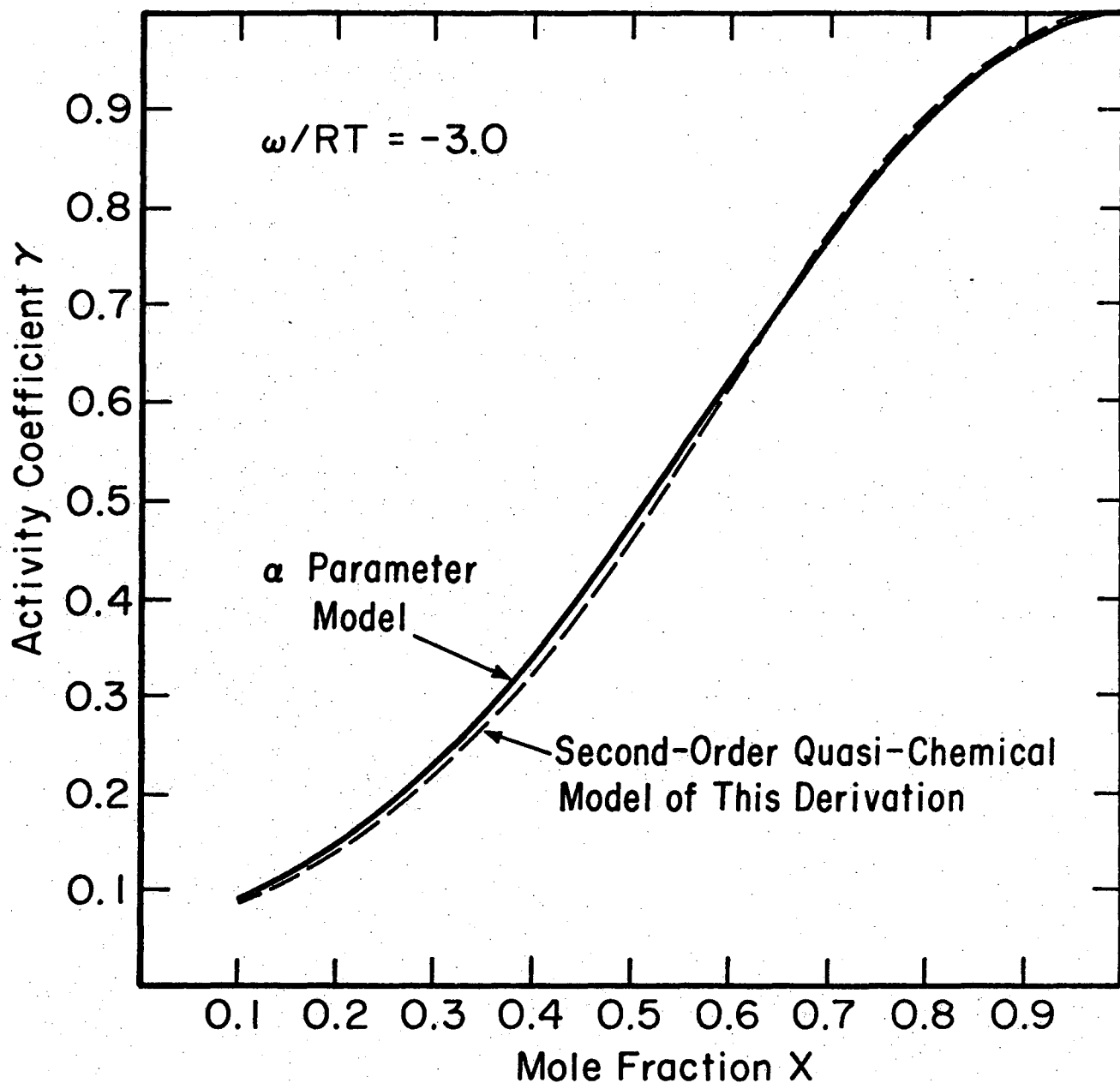
XBL 752-5740

Fig. 2. The limiting activity coefficients for various models for increasingly large negative interaction parameters.



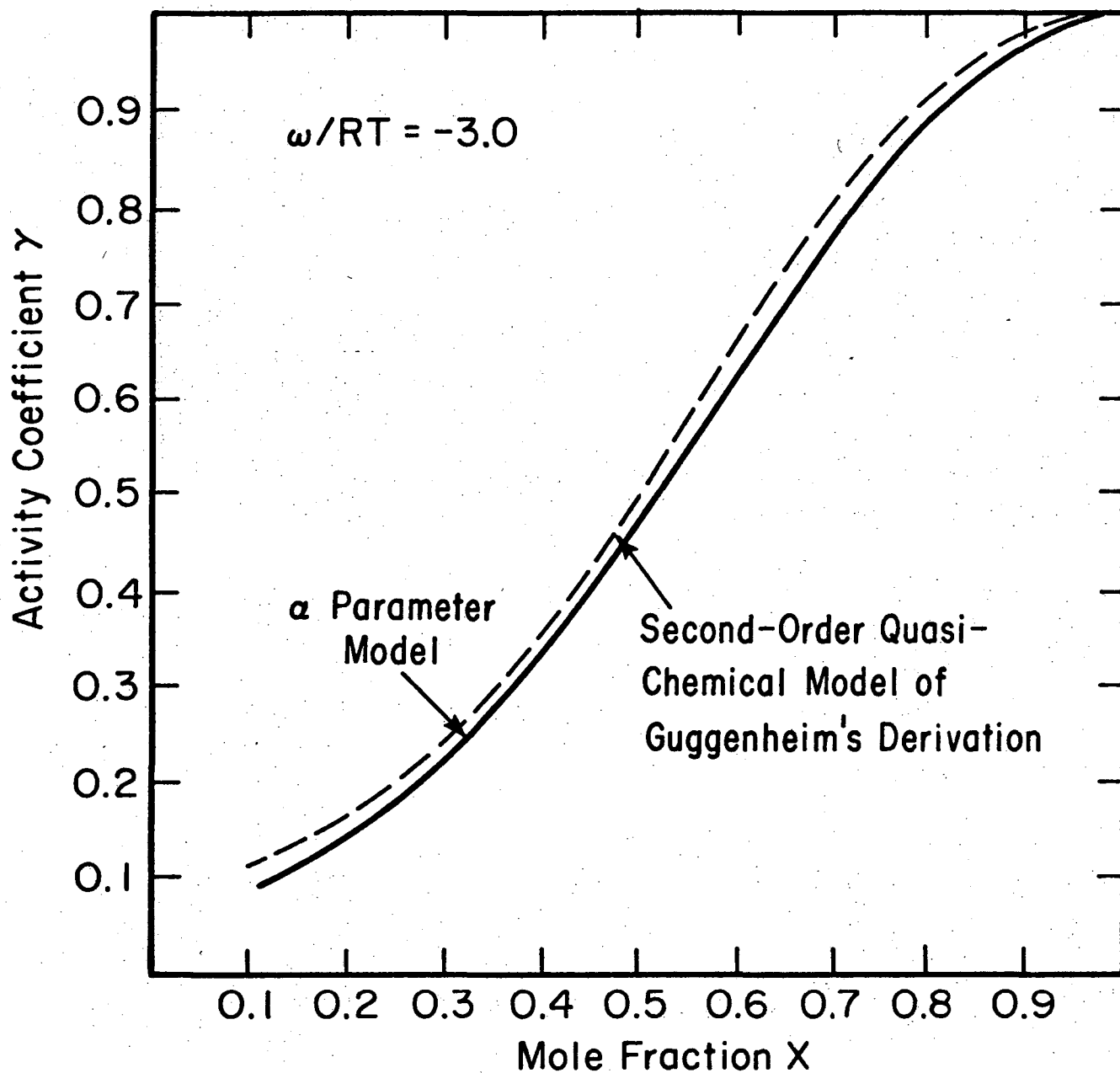
XBL 752-5741

Fig. 3. The activity coefficient predictions of the α parameter and the quasi-chemical (first order) models are compared for $\omega/RT = -3.0$.



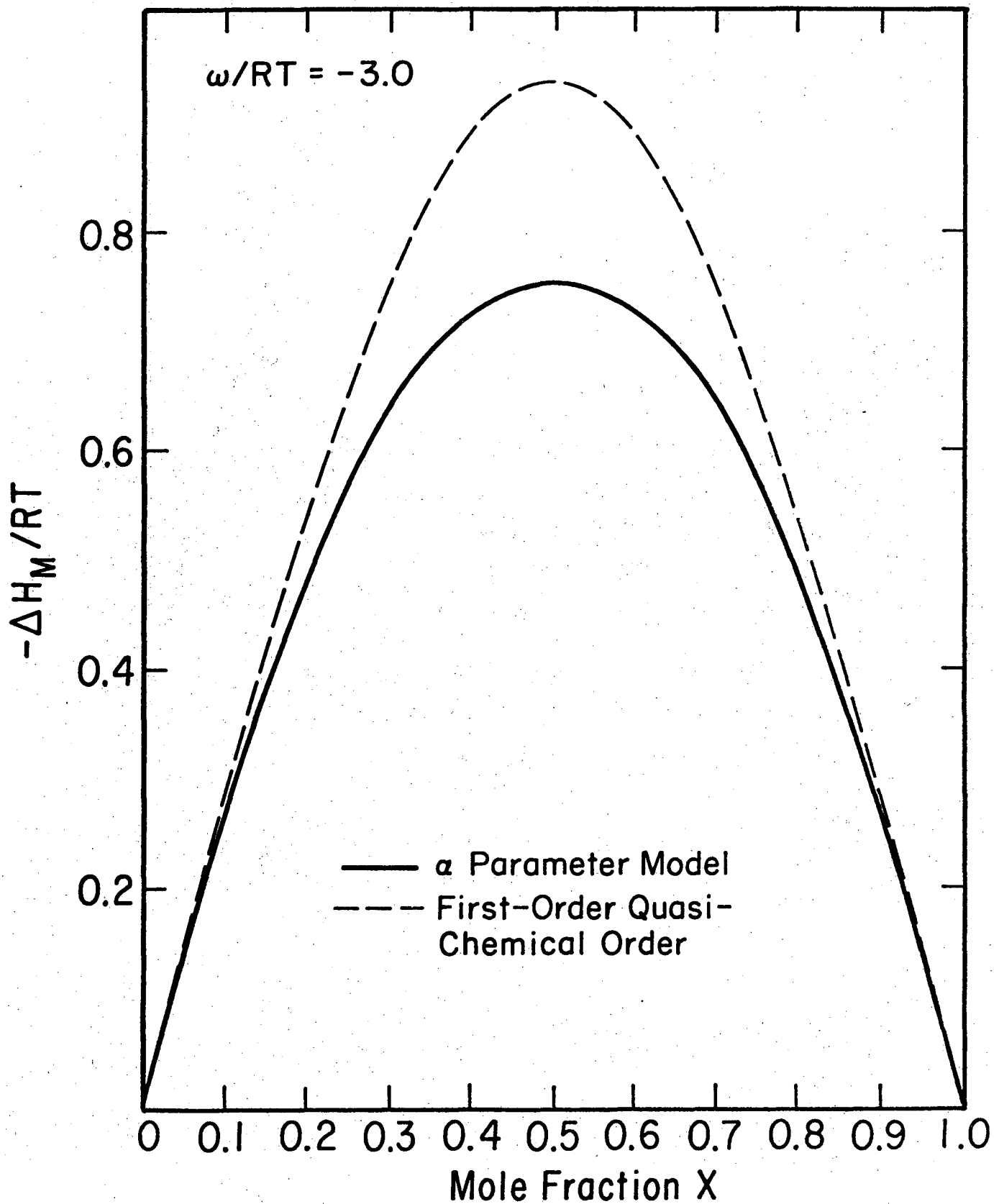
XBL 752-5742

Fig. 4. The activity coefficient predictions of the α parameter and the quasi-chemical (second order, this derivation) models are compared for $\omega/RT = -3.0$.



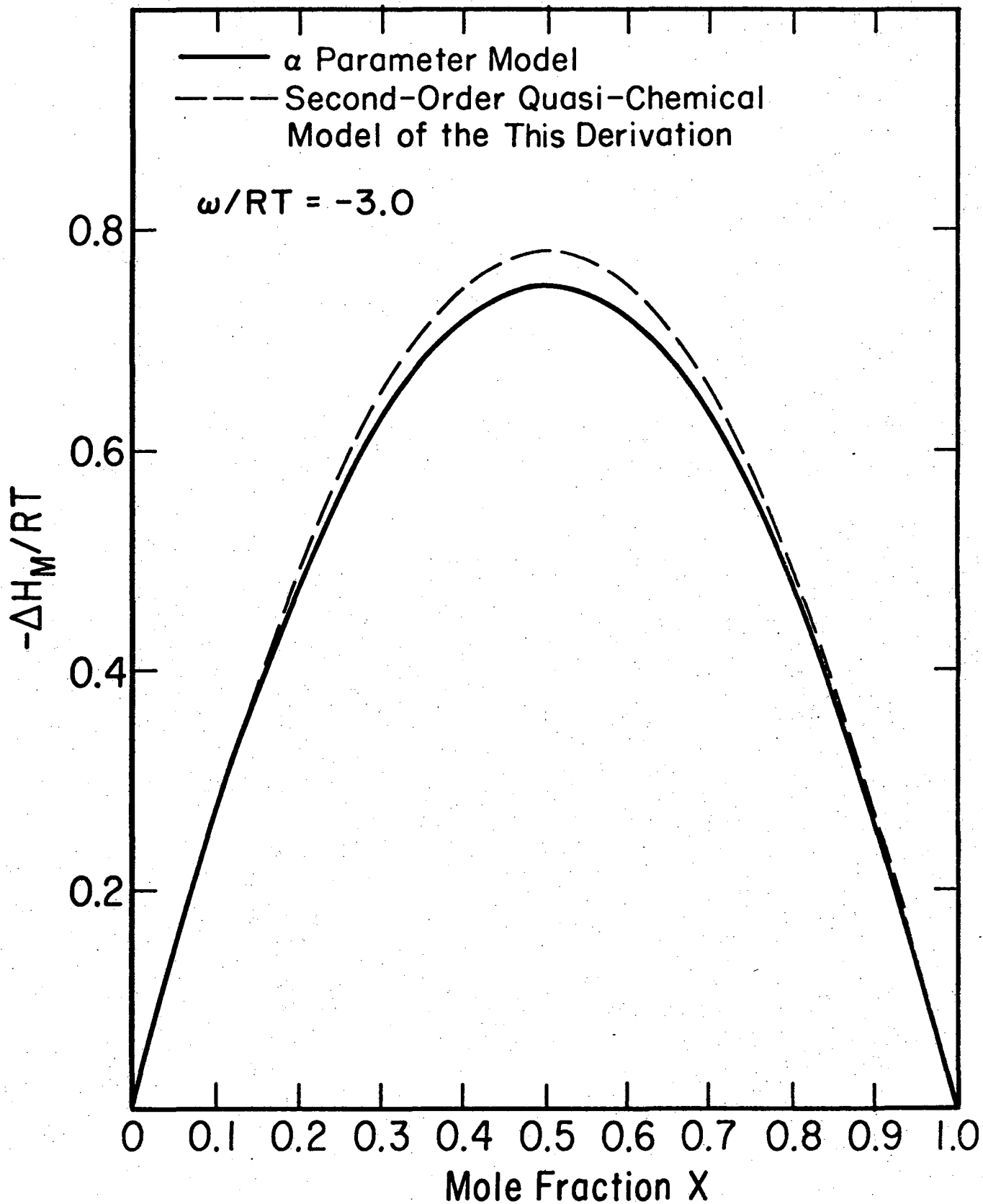
XBL 752-5743

Fig. 5. The activity coefficient predictions of the α parameter and the quasi-chemical (second order, Guggenheim's derivation) models are compared for $\omega/RT = -3.0$.



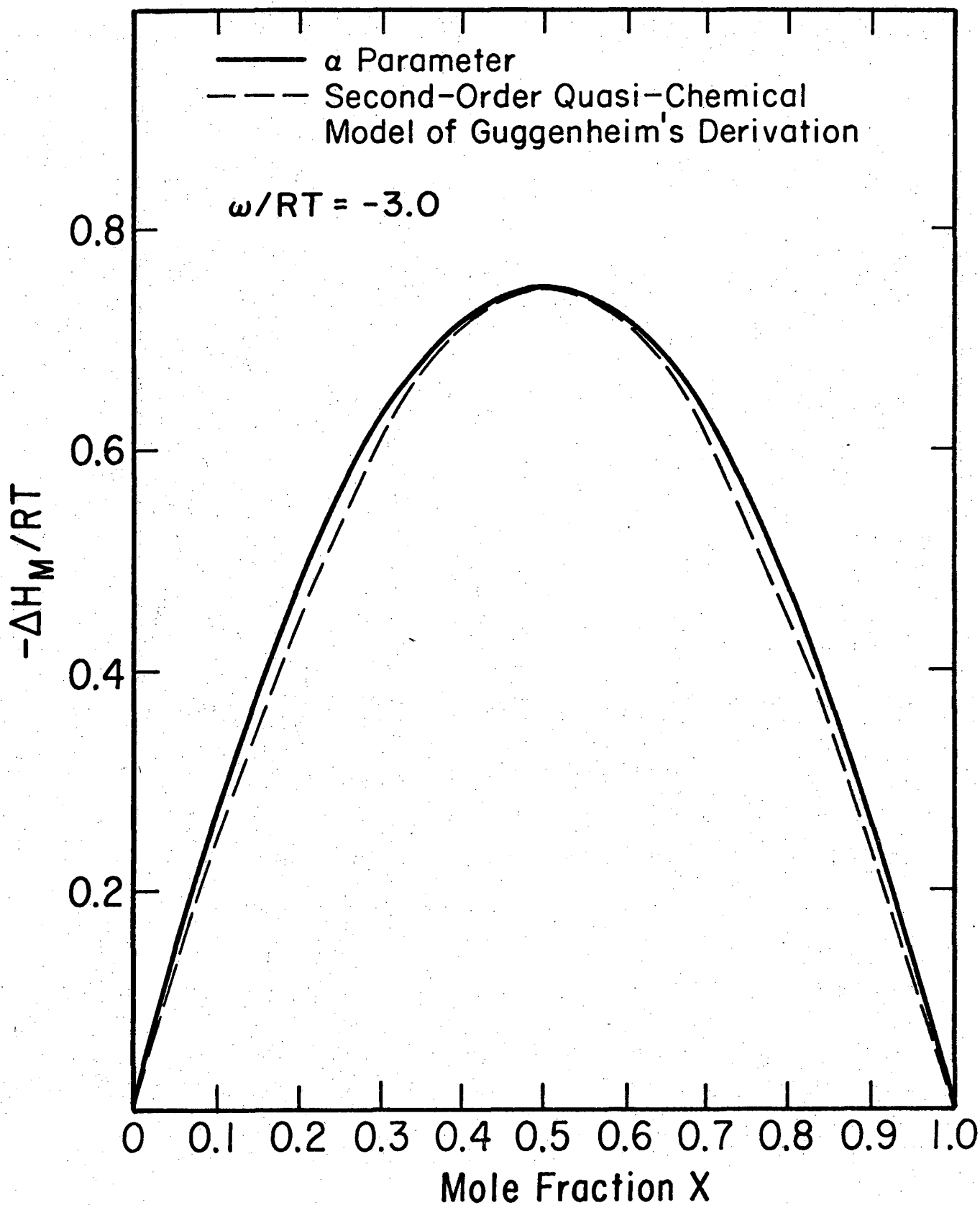
XBL 752-5744

Fig. 6. The enthalpy of mixing predictions of the α parameter and the quasi-chemical (first order) models are compared for $\omega/RT = -3.0$.



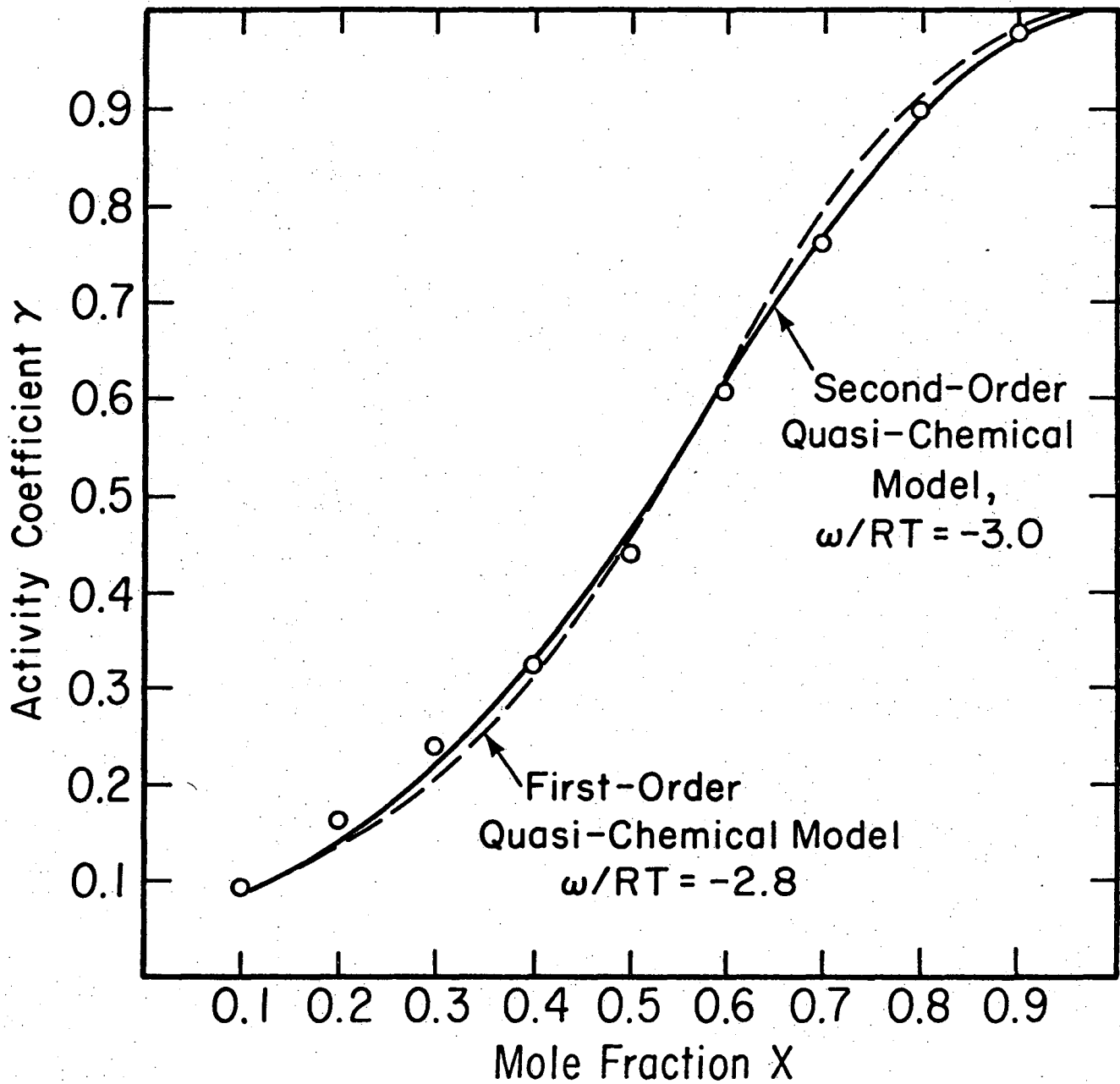
XBL 752-5745

Fig. 7. The enthalpy of mixing predictions of the α parameter and the quasi-chemical (second order, this derivation) models are compared for $\omega/RT = -3.0$.



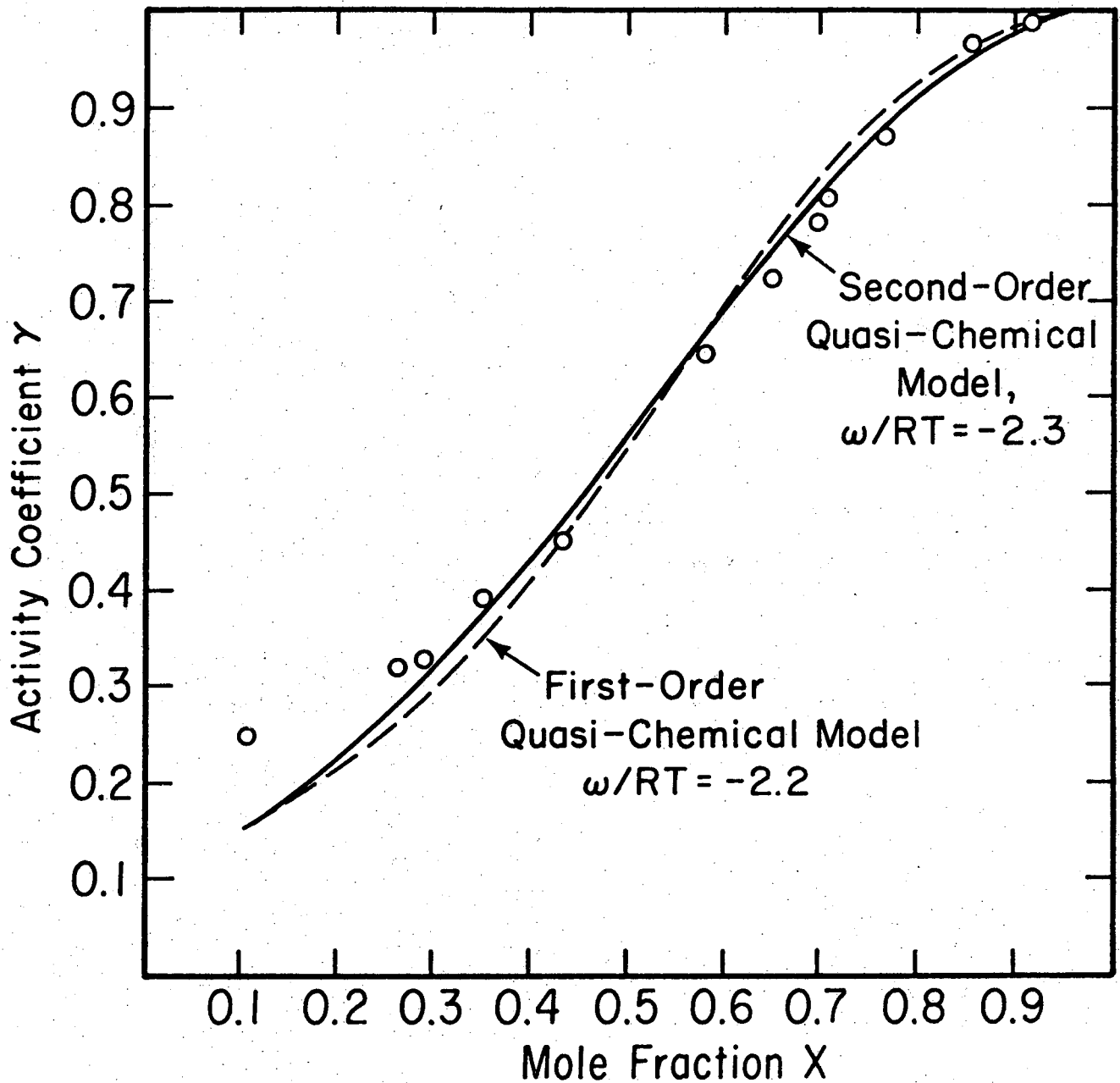
XBL 752-5746

Fig. 8. The enthalpy of mixing predictions of the α parameter and the quasi-chemical (second order, Guggenheim's derivation) models are compared for $\omega/RT = -3.0$.



XBL752-5747

Fig. 9. The activity coefficient data of Terpilowsky for In-Sb alloy melts at 900°K compared with the first order quasi-chemical predictions for $\omega/RT = -2.8$ and compared with the second order (this derivation) quasi-chemical predictions for $\omega/RT = -3.0$.



XBL 752-5748

Fig. 10. The activity coefficient data of Hoshino et al., for In-Sb alloy melts at 900°K compared with the first order quasi-chemical predictions for $\omega/RT = -2.2$ and compared with the second order (this derivation) quasi-chemical predictions for $\omega/RT = -2.3$.

VIII. GENERAL CONCLUSIONS

The use of oxide electrolytes, calcia stabilized zirconia and yttria doped thoria in particular, is shown to be viable for the measurement of Ga activities in Ga-In-Sb liquid alloys by solid state electrochemistry. The activities of Ga in Ga-In alloy melts were measured and used to calculate heats of mixing which correlate quite well with the heats of mixing of Ga-In alloy melts measured by different techniques.

The Ga activity measurements were extended into the Ga-Sb system. The activities of Ga were found to be highly depressed and correlating very well with a model postulating Ga_5Sb , GaSb , and GaSb_3 complexes. The activity coefficients of Ga show a very marked drop at $x_{\text{Ga}} = 0.8$, the reason for postulating Ga_5Sb , and show quite low values at $x_{\text{Ga}} = 0.2$, necessitating the postulation of GaSb_3 . In order to shift the inflection points of the model, the existence in the melt of GaSb was necessary. These complexes together form a system which explains the large negative deviation from Raoult's Law, long equilibration times, and earlier observations by other investigators showing short range order. The ramifications of the model are large negative heats of mixing with a minimum of -7.8 kcal/gram-atom at 997°K for $x_{\text{Ga}} = 0.7$.

Activities of Ga in the ternary alloy Ga-In-Sb melt were then measured for one composition, $x_{\text{Ga}} = 0.7$, $x_{\text{In}} = 0.1$, $x_{\text{Sb}} = 0.2$. The measurements show a depressed Ga activity which decreases rapidly with decreasing temperature.

The higher order extensions of the quasi-chemical model were then examined in relation to the In-Sb alloy melt system. The derivation of Guggenheim for the second order model was modified for a cubic lattice

to account for the second nearest neighbor interactions, which are ignored in that derivation. That derivation ignored 3/4 of those interactions. The modified second order and the derived third order models are found to follow very closely the activity coefficient predictions of the α parameter model, though not exactly. These higher order quasi-chemical models and, thus, the α parameter model, are found to give a closer fit to the measured In activity data for the In-Sb alloy melts than the first order quasi-chemical model.

ACKNOWLEDGEMENTS

I wish to express my appreciation for the financial support of the U. S. Energy Research and Development Administration for my research. I further thank my family and friends for their support and suggestions. I thank Professor L. F. Donaghey for his support and advice during the actual research and during the writing. I extend my appreciation and thanks to Professors L. Brewer and J. Newman for their kindness in agreeing to read this thesis.

APPENDIX: QUASI-CHEMICAL MODELS

A cubic lattice is the simplest structure for which the number of nearest neighbors equals six. Therefore, assume a cubic lattice.

Further, especially for the liquid state, assume Van der Waals forces between atom pairs, i.e., interaction energies proportional to r^{-6} .*

In a cubic lattice, the ratio of next nearest neighbor separation r_2 to nearest neighbor separation r_1 is $r_2/r_1 = \sqrt{2}$, and the ratio of third-nearest neighbor separation r_3 to nearest neighbor separation is $r_3/r_1 = \sqrt{3}$. Therefore, the ratio of next-nearest neighbor interaction energy I_2^0 and nearest neighbor interaction energy I_1^0 is $I_2^0/I_1^0 = 1/(\sqrt{2})^6 = 1/8$. Also, the ratio of the third-nearest neighbor interaction energy I_3 to the nearest neighbor interaction energy is $I_3^0/I_1^0 = 1/(\sqrt{3})^6 = 1/27$. This leads to the following relationships among the Boltzmann factor for nearest neighbors η^{-1} , next nearest neighbors ϕ^{-1} , and third-nearest neighbors ψ^{-1} :

$$\phi = \eta^{1/8} \quad , \quad \psi = \eta^{1/27}$$

The interaction energies above refer to interactions for pairs of atoms of differing species.

Assume now that the atomic radii of the two species are equal so that coordination numbers do not change with composition. Further assume that there is no change in volume with mixing. Then

$$\Delta U_{\text{mixing}} = \Delta H_{\text{mixing}}$$

*It has been suggested that the Leonard-Jones potential would be more appropriate. I agree, but at the time of my original work, I did not think of it.

Now imagine the enthalpy of mixing involved in replacing an atom of species A in a lattice of species A with an atom of species B.

Considering only nearest, next-nearest, and next-next-nearest neighbors:

$\Delta H_{\text{mixing}} = Z_1 I_1^0 + Z_2 I_2^0 + Z_3 I_3^0$, where Z_1 , Z_2 and Z_3 are the numbers of nearest, next-nearest, and third-nearest neighbors, respectively.

Call this enthalpy of mixing Ω , i.e., $\Omega = Z_1 I_1^0 + Z_2 I_2^0 + Z_3 I_3^0$. Thus, a measurement of Ω immediately yields I_1^0 , I_2^0 and I_3^0 , provided Z_1 , Z_2 , Z_3 and the relationships between I_1^0 , I_2^0 and I_3^0 are known. For the case of a cubic lattice $Z_1 = 6$, $Z_2 = 12$, $Z_3 = 8$, $I_2^0/I_1^0 = 1/8$, and $I_3^0/I_1^0 = 1/27$, implying $I_1^0 = \Omega/(6 + 12/8 + 8/27)$. Therefore,

$$\eta = e^{+\Omega/(6+12/8+8/27) RT}$$

when one considers the three nearest levels of neighbors in a cubic lattice.

Now let us consider a cubic lattice as a case of interest since the coordination number of the III-V melt of In-Sb has been measured to be 5.7 or approximately 6, the coordination number of a cubic lattice. The cubic lattice has a unit cell consisting of 8 atoms (in the case of a metallic melt) arranged at the vertices at a cube. Each atom also is at the vertex of 8 cubes or unit cells and, therefore, is shared by 8 unit cells, making the effective number of atoms associated with each unit cell equal to 1. Therefore, for N atoms there are N cubes or unit cells.

Let us now consider the energy contributions of the various interactions to the enthalpy of a cubic cell. Suppose a pair of nearest neighbors consist of atoms of differing species. Then the energy of interaction is I_1 . Now the line connecting the two atoms

is an edge of the cube and is shared with three other cubes. Thus, the energy of interaction of that pair is shared by four unit cells, and the contribution to the unit cell of interest is $I_1/4$, implying that the associated Boltzmann factor is $\eta^{-1/4}$. Similarly, the interaction energy for next nearest neighbors is shared by two unit cells, and the contribution of this interaction to the enthalpy of the unit cell is $I_2/2$; implying that the corresponding Boltzmann factor is $\phi^{-1/2}$. The interaction energy for third-nearest non-identical neighbors is not shared but belongs wholly to the unit cell within which the interaction resides; implying that ψ^{-1} is the associated Boltzmann factor.

Table 1 contains all the different possible configurations for atoms of two species arranged at the vertices of a cube. The second column is a term representing the total number of cubes corresponding to the configuration in the first column. This term is composed of a term N which is the total number of cubes in a cubic matrix. The second term is a variable multiplied by an integer. The variable represents the fraction of cubes in one orientation of the configuration in the first column. The integer is the number of possible orientations of that particular configuration. The third column lists the Boltzmann factor associated with the particular configurations.

The above basis is used to evaluate the thermodynamic properties of a system having a cubic lattice. Several degrees of complexity are used to develop models for which a partition function may be derived.

In order that the partition function be determined, it is necessary to solve for the variables listed in the preceding table using the constraints of the system. One of these constraints is the conservation of species. Let us count the number of B atoms associated with each

Table 1. Boltzmann factors and configurational degeneracies for cubic groups in a binary system.

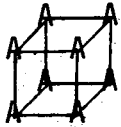
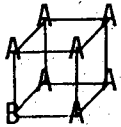
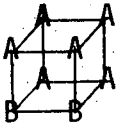
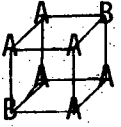
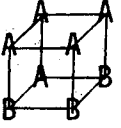
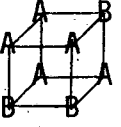
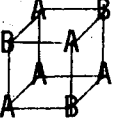
Configuration	Number in this Configuration	Boltzmann Factor
	N_{α}	1
	$N_{8\delta}$	$\eta^{-3/4} \phi^{-3/2} \psi^{-1}$
	$N_{12\zeta_0}$	$\eta^{-4/4} \phi^{-6/2} \psi^{-2}$
	$N_{12\zeta_1}$	$\eta^{-6/4} \phi^{-4/2} \psi^{-2}$
	$N_{4\zeta_2}$	$\eta^{-6/4} \phi^{-6/2}$
	$N_{24\nu_0}$	$\eta^{-5/4} \phi^{-7/2} \psi^{-3}$
	$N_{24\nu_1}$	$\eta^{-7/4} \phi^{-7/2} \psi^{-1}$

Table 1. Continued.

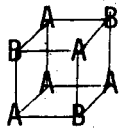
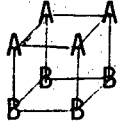
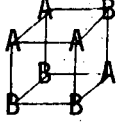
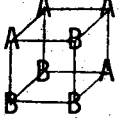
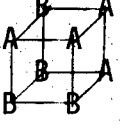
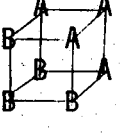
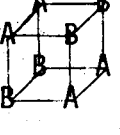
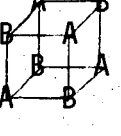
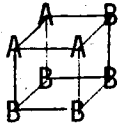
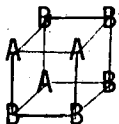
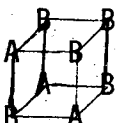
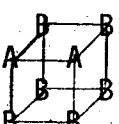
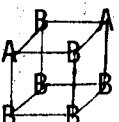
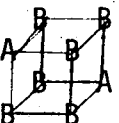
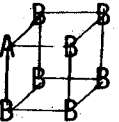
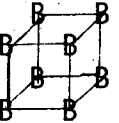
Configuration	Number in this Configuration	Boltzmann Factor
	$N8v_2$	$\eta^{-9/4} \phi^{-3/2} \psi^{-3}$
	$N6\varepsilon_0$	$\eta^{-4/4} \phi^{-8/2} \psi^{-4}$
	$N24\varepsilon_1$	$\eta^{-8/4} \phi^{-6/2} \psi^{-2}$
	$N12\varepsilon_2$	$\eta^{-6/4} \phi^{-8/2} \psi^{-2}$
	$N12\varepsilon_3$	$\eta^{-6/4} \phi^{-8/2} \psi^{-2}$
	$N8\varepsilon_4$	$\eta^{-6/4} \phi^{-6/2} \psi^{-4}$
	$N6\varepsilon_5$	$\eta^{-8/4} \phi^{-8/2}$
	$N2\varepsilon_6$	$\eta^{-12/4} \psi^{-4}$

Table 1. Continued.

Configuration	Number in this Configuration	Boltzmann Factor
	$N24\rho_0$	$\eta^{-5/4}\phi^{-7/2}\psi^{-3}$
	$N24\rho_1$	$\eta^{-7/4}\phi^{-7/2}\psi^{-1}$
	$N8\rho_2$	$\eta^{-9/4}\phi^{-3/2}\psi^{-3}$
	$N12\sigma_0$	$\eta^{-4/4}\phi^{-6/2}\psi^{-2}$
	$N12\sigma_1$	$\eta^{-6/4}\phi^{-4/2}\psi^{-2}$
	$N4\sigma_2$	$\eta^{-6/4}\phi^{-6/2}$
	$N8\tau$	$\eta^{-3/4}\phi^{-3/2}\psi^{-1}$
	NB	1

of the configurations; the total must be N_B . In the accounting we note that the average number of atoms associated with a unit cell is one; therefore, the fraction of B atoms associated with a configuration is equivalent to the average number of B atoms associated with one unit cell of that particular configuration, as shown in Table 2. Thus, we have that:

$$N_B = N\zeta + 3N\zeta_0 + 3N\zeta_1 + N\zeta_2 + 9N\nu_0 + 9N\nu_1 + 3N\nu_2 + 3N\xi_0 + 12N\xi_1 \\ + 6N\xi_2 + 6N\xi_3 + 4N\xi_4 + 3N\xi_5 + N\xi_6 + 15N\rho_0 + 15N\rho_1 + 5N\rho_2 \\ + 9N\sigma_0 + 9N\sigma_1 + 3N\sigma_2 + 7N\tau + N_B$$

or

$$x_B = \zeta + 3\zeta_0 + 3\zeta_1 + \zeta_2 + 9\nu_0 + 9\nu_1 + 3\nu_2 + 3\xi_0 + 12\xi_1 + 6\xi_2 \quad (1) \\ + 6\xi_3 + 4\xi_4 + 3\xi_5 + \xi_6 + 15\rho_0 + 15\rho_1 + 5\rho_2 + 9\sigma_0 + 9\sigma_1 \\ + 3\sigma_2 + 7\tau + \beta$$

Similarly for A:

$$x_A = \alpha + 7\delta + 9\zeta_0 + 9\zeta_1 + 3\zeta_2 + 15\nu_0 + 15\nu_1 + 5\nu_2 + 3\xi_0 + 12\xi_1 \quad (2) \\ + 6\xi_2 + 6\xi_3 + 4\xi_4 + 3\xi_5 + \xi_6 + 9\rho_0 + 9\rho_1 + 3\rho_2 + 3\sigma_0 \\ + 3\sigma_1 + \sigma_2 + \tau$$

Now following the procedure outlined by Guggenheim in Mixtures, we write the approximate partition function and maximize to determine the values of the variables. The partition function is Ω_0 :

Table 2. Fraction of B component in binary configurations of a cubic lattice.

Table Number in Configuration	Number B in Configuration	Total B in Configuration
$N\alpha$	0	0
$N8\zeta$	1/8	$N\zeta$
$N18\zeta_0$	1/4	$N3\zeta_0$
$N12\zeta_1$	1/4	$N3\zeta_1$
$N4\zeta_2$	1/4	$N\zeta$
$N24\nu_0$	3/8	$N9\nu_0$
$N24\nu_1$	3/8	$N9\nu_0$
$N8\nu_2$	3/8	$N3\nu_2$
$N6\varepsilon_0$	1/2	$N3\varepsilon_0$
$N24\varepsilon_1$	1/2	$N12\varepsilon_1$
$N12\varepsilon_2$	1/2	$N6\varepsilon_2$
$N12\varepsilon_3$	1/2	$N6\varepsilon_3$
$N8\varepsilon_4$	1/2	$N4\varepsilon_4$
$N6\varepsilon_5$	1/2	$N3\varepsilon_5$
$N2\varepsilon_6$	1/2	$N\varepsilon_6$
$N24\rho_0$	5/8	$N15\rho_0$
$N24\rho_1$	5/8	$N15\rho_1$
$N8\rho_2$	5/8	$N5\rho_2$
$N12\sigma_0$	3/4	$N9\sigma_0$
$N12\sigma_1$	3/4	$N9\sigma_1$
$N4\sigma_2$	3/4	$N3\sigma_2$
$N8\tau$	7/8	$N7\tau$
$N\rho$	1	$N\beta$

$$\begin{aligned}
 \Omega_0 = & \frac{N!}{N_A! N_B!} \frac{(N\alpha^*)! [(N\delta^*)!]^8 [(N\zeta_0^*)!]^{12} [(N\zeta_1^*)!]^{12} [(N\zeta_2^*)!]^4}{(N\alpha)! [(N\delta)!]^8 [(N\zeta_0)!]^{12} [(N\zeta_1)!]^{12} [(N\zeta_2)!]^4} \quad (3) \\
 & \times \frac{[(N\nu_0^*)!]^{24} [(N\nu_1^*)!]^{24} [(N\nu_2^*)!]^8 [(N\xi_0^*)!]^6 [(N\xi_1^*)!]^{24} [(N\xi_2^*)!]^{12}}{[(N\nu_0)!]^{24} [(N\nu_1)!]^{24} [(N\nu_2)!]^8 [(N\xi_0)!]^6 [(N\xi_1)!]^{24} [(N\xi_2)!]^{12}} \\
 & \times \frac{[(N\xi_3^*)!]^{12} [(N\xi_4^*)!]^8 [(N\xi_5^*)!]^6 [(N\xi_6^*)!]^2 [(N\rho_0^*)!]^{24} [(N\rho_1^*)!]^{24}}{[(N\xi_3)!]^{12} [(N\xi_4)!]^8 [(N\xi_5)!]^6 [(N\xi_6)!]^2 [(N\rho_0)!]^{24} [(N\rho_1)!]^{24}} \\
 & \times \frac{[(N\rho_2^*)!]^8 [(N\sigma_0^*)!]^{12} [(N\sigma_1^*)!]^{12} [(N\sigma_2^*)!]^4 [(N\tau^*)!]^8 (N\beta^*)!}{[(N\rho_2)!]^8 [(N\sigma_0)!]^{12} [(N\sigma_1)!]^{12} [(N\sigma_2)!]^4 [(N\tau)!]^8 (N\beta)!} \\
 & \times \eta^{-z_1 N} \left[\begin{array}{c} \delta + 2\zeta_0 + 3\zeta_1 + \zeta_2 + 5\nu_0 + 7\nu_1 + 3\nu_2 \\ \xi_0 + 8\xi_1 + 3\xi_2 + 3\xi_3 + 2\xi_4 + 2\xi_5 + \xi_6 \\ +5\rho_0 + 7\rho_1 + 3\rho_2 + 2\sigma_0 + 3\sigma_1 + \sigma_2 + \tau \end{array} \right] \\
 & \times \phi^{-z_2 N} \left[\begin{array}{c} \delta + 3\zeta_0 + 2\zeta_1 + \zeta_2 + 7\nu_0 + 7\nu_1 + \nu_2 \\ +2\xi_0 + 6\xi_1 + 4\xi_2 + 4\xi_3 + 2\xi_4 + 2\xi_5 + \\ +7\rho_0 + 7\rho_1 + \rho_2 + 3\sigma_0 + 2\sigma_1 + \sigma_2 + \tau \end{array} \right] \\
 & \times \psi^{-z_3 N} \left[\begin{array}{c} \delta + 3\zeta_0 + 3\zeta_1 + 9\nu_0 + 3\nu_1 + 3\nu_2 \\ +3\xi_0 + 6\xi_1 + 3\xi_2 + 3\xi_3 + 4\xi_4 + \xi_6 \\ +9\rho_0 + 3\rho_1 + 3\rho_2 + 3\sigma_0 + 3\sigma_1 + \tau \end{array} \right]
 \end{aligned}$$

In the partition function the term in front of the Boltzmann factors represents the number of orientations for a given set of values of the configurational variables. The starred configurational variables are the values of these variables in a completely random solution and have

the following values:

$$\alpha^* = x_A^8 = (1-x)^8 \quad (4)$$

$$\delta^* = x_A^7 x_B = x(1-x)^7$$

$$\zeta_0^* = \zeta_1^* = \zeta_2^* = x_A^6 x_B^2 = x^2(1-x)^6$$

$$\nu_0^* = \nu_1^* = \nu_2^* = x_A^5 x_B^3 = x^3(1-x)^5$$

$$\xi_0^* = \xi_1^* = \xi_2^* = \xi_3^* = \xi_4^* = \xi_5^* = \xi_6^* = x_A^4 x_B^4 = x^4(1-x)^4$$

$$\rho_0^* = \rho_1^* = \rho_2^* = x_A^3 x_B^5 = x^5(1-x)^3$$

$$\sigma_0^* = \sigma_1^* = \sigma_2^* = x_A^2 x_B^6 = x^6(1-x)^2$$

$$\tau^* = x_A x_B^7 = x^7(1-x)$$

$$\beta^* = x_B^8 = x^8$$

Note now that there are 23 configurational variables. Equations (1) and (2) are two constraints so that there are now 21 independent variables (provided $z_1, z_2, z_3, \eta, \phi$ and ψ are known). To specify completely the state of equilibrium we must minimize the Gibbs energy with respect to the 21 independent variables, the configurational variables excluding α and β . An equivalent operation is the minimization of the total Gibbs energy of mixing or $RT \ln \Omega_0$. Therefore, it suffices to minimize $\ln \Omega_0$ with respect to the independent variables. Utilizing the Stirling approximation we obtain:

I	$\frac{\partial \ln \Omega_0}{\partial I} = 0$
δ	$\alpha_{\beta}^7 / \zeta^8 = \eta \phi^z \psi^z$
ζ_0	$\alpha_{\beta}^9 / \zeta_0^3 = \eta \phi^{2z_1} \psi^{3z_2} \psi^{3z_3}$
ζ_1	$\alpha_{\beta}^9 / \zeta_1^3 = \eta \phi^{3z_1} \psi^{2z_2} \psi^{3z_3}$
ζ_2	$\alpha_{\beta}^3 / \zeta_2^4 = \eta \phi^{z_1} \psi^{z_2}$
ν_0	$\alpha_{\beta}^{15} / \nu_0^9 = \eta \phi^{5z_1} \psi^{7z_2} \psi^{9z_3}$
ν_1	$\alpha_{\beta}^{15} / \nu_1^9 = \eta \phi^{7z_1} \psi^{7z_2} \psi^{3z_3}$
ν_2	$\alpha_{\beta}^5 / \nu_2^3 = \eta \phi^{3z_1} \psi^{z_2} \psi^{3z_3}$
ξ_0	$\alpha_{\beta}^3 / \xi_0^3 = \eta \phi^{z_1} \psi^{2z_2} \psi^{3z_3}$
ξ_1	$\alpha_{\beta}^{12} / \xi_1^{12} = \eta \phi^{8z_1} \psi^{6z_2} \psi^{6z_3}$
ξ_2	$\alpha_{\beta}^6 / \xi_2^6 = \eta \phi^{3z_1} \psi^{4z_2} \psi^{3z_3}$
ξ_3	$\alpha_{\beta}^6 / \xi_3^6 = \eta \phi^{3z_1} \psi^{4z_2} \psi^{3z_3}$
ξ_4	$\alpha_{\beta}^4 / \xi_4^4 = \eta \phi^{2z_1} \psi^{2z_2} \psi^{4z_3}$
ξ_5	$\alpha_{\beta}^3 / \xi_5^3 = \eta \phi^{2z_1} \psi^{2z_2}$
ξ_6	$\alpha_{\beta} / \xi_6 = \eta \phi^{z_1} \psi^{z_3}$

$$\begin{aligned}
 \rho_0 & \alpha \beta^{9,15} / \rho_0^{24} = \eta^5 \phi^{7z_1} \psi^{7z_2} \psi^{9z_3} \\
 \rho_1 & \alpha \beta^{9,15} / \rho_1^{24} = \eta^7 \phi^{7z_1} \psi^{7z_2} \psi^{3z_3} \\
 \rho_2 & \alpha \beta^{3,5} / \rho_2^8 = \eta^3 \phi^{z_1} \psi^{z_2} \psi^{3z_3} \\
 \sigma_0 & \alpha \beta^{3,9} / \sigma_0^{12} = \eta^{2z_1} \phi^{3z_2} \psi^{3z_3} \\
 \sigma_2 & \alpha \beta^3 / \sigma_2^4 = \eta^{z_1} \phi^{z_2} \\
 \sigma_1 & \alpha \beta^{3,9} / \sigma_1^{12} = \eta^{3z_1} \phi^{2z_2} \psi^{3z_3} \\
 \tau & \alpha \beta^7 / \tau^8 = \eta^{z_1} \phi^{z_2} \psi^{z_3}
 \end{aligned}$$

With appropriate algebraic manipulations and the substitution $\rho_0/v_0 = \kappa^2$, the following relationships can be derived.

$$\begin{aligned}
 \alpha & = \kappa^{-4} \epsilon_0 \eta \phi^2 \psi^4 & \epsilon_3 & = \epsilon_0 \eta^{-1/2} \psi^2 & (5) \\
 \delta & = \kappa^{-3} \epsilon_0 \eta^{1/4} \phi^{5/2} \psi^3 & \epsilon_4 & = \epsilon_0 \eta^{-1/2} \phi \\
 \zeta_0 & = \kappa^{-2} \epsilon_0 \phi \psi^2 & \epsilon_5 & = \epsilon_0 \eta^{-1} \psi^4 \\
 \zeta_1 & = \kappa^{-2} \epsilon_0 \eta^{-1/2} \phi^2 \psi^2 & \epsilon_6 & = \epsilon_0 \eta^{-2} \phi^4 \\
 \epsilon_2 & = \kappa^{-2} \epsilon_0 \eta^{-1/2} \phi \psi^4 & \rho_0 & = \kappa \epsilon_0 \eta^{-1/4} \phi^{1/2} \psi \\
 v_0 & = \kappa^{-1} \epsilon_0 \eta^{-1/4} \phi^{1/2} \psi & \rho_1 & = \kappa \epsilon_0 \eta^{-3/4} \phi^{1/2} \psi^3 \\
 v_1 & = \kappa^{-1} \epsilon_0 \eta^{-3/4} \phi^{1/2} \psi^3 & \rho_2 & = \kappa \epsilon_0 \eta^{-5/4} \phi^{5/2} \\
 v_2 & = \kappa^{-1} \epsilon_0 \eta^{-5/4} \phi^{5/2} \psi & \sigma_0 & = \kappa^2 \epsilon_0 \phi \psi^2
 \end{aligned}$$

$$\xi_0 = \xi_0$$

$$\sigma_1 = K^2 \xi_0 \eta^{-1/2} \phi^2 \psi^2$$

$$\xi_1 = \xi_0 \eta^{-1} \phi \psi^2$$

$$\sigma_2 = K^2 \xi_0 \eta^{-1/2} \phi \psi^4$$

$$\xi_2 = \xi_0 \eta^{-1/2} \phi^0 \psi^2$$

$$\tau = K^3 \xi_0 \eta^{1/4} \phi^{5/2} \psi^3$$

$$\beta = K^4 \xi_0 \eta \phi^4 \psi^4$$

Let us now digress to Eqs. (1) and (2). In order to simplify the mathematics, let I_i represent the i^{th} configurational variable of the 23. Let a_{i1} and a_{i2} represent the corresponding constants of Eqs. (1) and (2), respectively. Thus:

$$x_B = \sum_1^{23} a_{i1} I_i$$

$$x_A = \sum_1^{23} a_{i2} I_i$$

To further simplify, let a_{i3} , a_{i4} , a_{i5} and a_{i6} be the exponents of K , η , ϕ , and ψ in Eqs. (5) for the respective variables. Substituting into Eqs. (1) and (2).

$$x_B = \sum_1^{23} a_{i1} K^{a_{i3}} \eta^{a_{i4}} \phi^{a_{i5}} \psi^{a_{i6}} \quad (1a)$$

$$x_A = \sum_1^{23} a_{i2} K^{a_{i3}} \eta^{a_{i4}} \phi^{a_{i5}} \psi^{a_{i6}} \quad (2a)$$

Factoring out and isolating ξ_0 , we can equate the two equations to obtain

$$x_A \sum_1^{23} a_{i1} K^{a_{i3}} \eta^{a_{i4}} \phi^{a_{i5}} \psi^{a_{i6}} = x_B \sum_1^{23} a_{i2} K^{a_{i3}} \eta^{a_{i4}} \phi^{a_{i5}} \psi^{a_{i6}}$$

or

$$\sum_1^{23} (x_A^{a_{i1}} - x_B^{a_{i2}}) K^{\eta^{a_{i3}} \phi^{a_{i4}} \psi^{a_{i5}}} = 0 \quad .$$

or with $x = x_B$,

$$\sum_1^{23} (a_{i1} - x(a_{i1} + a_{i2})) K^{\eta^{a_{i3}} \phi^{a_{i4}} \psi^{a_{i5}}} = 0 \quad .$$

With η , ϕ , ψ , and x given, it is then possible to solve for K , and then possible to calculate the values of the configurational variables.

Further, simplification can be attained by assuming Van der Waals behavior in which case, as pointed out earlier:

$$\sum_1^{23} (a_{i1} - x(a_{i1} + a_{i2})) K^{\eta^{a_{i3}} \phi^{a_{i4}}} + \frac{a_{i5}}{8} + \frac{a_{i6}}{27} = 0 \quad . \quad (6)$$

Digressing again, let the exponents of the Boltzmann factors in Table 1 be designated by e_{i1} , e_{i2} , e_{i3} for η , ϕ , and ψ respectively for the i^{th} configuration. Let

$$EL_i = e_{i1} + e_{i2}/8 + e_{i3}/27 \quad .$$

Noticing that the number of orientations for each configuration is equal to $a_{i1} + a_{i2}$, we may then write for the molar enthalpy of mixing

$$\Delta H_m = \sum_1^{23} (a_{i1} + a_{i2}) I_i (EL_i) \Omega / \left(6 + \frac{12}{8} + \frac{8}{27} \right) \quad . \quad (7)$$

The molar Gibbs energy of mixing may also be calculated and is given by

$$\Delta G_m = \frac{RT}{N_0} \ln \Omega_0$$

where N_0 is the number of moles used in calculating Ω_0 as contrasted with N , the number of atoms used in calculating Ω_0 . The partial molar Gibbs energy of B is then

$$\overline{\Delta G_B} = \frac{\partial N_0 \Delta G}{\partial N_B} = RT \frac{\partial \ln \Omega_0}{\partial N_B}$$

Now all of the configurational variables starred or unstarred are functions of x or N_B , therefore,

$$\overline{\Delta G_B} = RT \left[\sum_1^{23} \left(\frac{\partial \ln \Omega_0}{\partial I_i^*} \frac{dI_i^*}{dN_B} + \frac{\partial \ln \Omega_0}{\partial I_i} \frac{dI_i}{dN_B} \right) + \frac{\partial \ln \Omega_0}{\partial N} \frac{dN}{dN_B} + \frac{\partial \ln \Omega_0}{\partial N_B} \right]$$

Now assigning values to I_i^* appropriate for a completely random arrangement (regular solution) is equivalent to maximizing Ω . Therefore, for the starred configurational variables excluding α^* and β^* , we find

$$\frac{\partial \ln \Omega_0}{\partial I_i^*} = 0$$

Similarly, in determining the equilibrium values of the unstarred configurational variables, it was necessary to minimize $\ln \Omega$ with respect to these variables excluding α and β , implying

$$\frac{\partial \ln \Omega_0}{\partial I_i} = 0$$

Using Eq. (2) we find that $N\alpha$ and $N\alpha^*$ are functions of N_A and the variables already discussed and, thus, contribute to making those differentials equal to 0. Thus, the only terms not irrelevant are N , N_B , β^* , and β . Performing the indicated operations, we get:

$$\overline{\Delta G}_B = RT \left(\ln x + \ln \frac{\beta}{\beta^*} \right) \quad (8a)$$

Similarly for $\overline{\Delta G}_A$

$$\overline{\Delta G}_A = RT \left[\ln(1 - x) + \ln \frac{\alpha}{\alpha^*} \right] \quad (8b)$$

Thus, a simpler expression for $\overline{\Delta G}_m$ is

$$\Delta G_m = RT \left[x \ln \frac{x\beta}{\beta^*} + (1 - x) \ln \frac{(1 - x)\alpha}{\alpha^*} \right] \quad (9)$$

Substituting for α^* and β^* from Eq. (4) we also obtain

$$\Delta G_m = RT \left[x \ln \frac{\beta}{x^7} + (1 - x) \ln \frac{\alpha}{(1 - x)^7} \right] \quad (9a)$$

Furthermore, the activities and activity coefficients are

$$\begin{aligned} \gamma_A &= \frac{\alpha}{(1 - x)^8} & \gamma_B &= \frac{\beta}{x^8} \\ a_A &= \frac{\alpha}{(1 - x)^7} & a_B &= \frac{\beta}{x^7} \end{aligned} \quad (10)$$

This particular model may be used to evaluate the effect of allowing for third-nearest neighbors. Those terms taking that interaction may be eliminated from this model by just ignoring the interaction energy and its Boltzmann factor for third-nearest neighbors. Then to evaluate the effect of allowing for next-nearest neighbors, their associated interaction energy and Boltzmann factor is just ignored in this model.

Discussion

In principle, in a case of one to one correspondence if, it is possible to calculate some quantity given some initial information, then it must be possible to derive the initial information if the desired quantity is known. That is the case here. The activities have already been calculated for a given Ω . Thus, if the activities are known, Ω may be deduced.

The Initial Model

The method requires that the number of nearest neighbors be established first. If Z_1 is independently determined to be 6, then the equations developed here may be used: one can assume a cubic lattice and a Van der Waals relationship for interaction energy as a function of distance.

Suppose that the activity of B for a given mole fraction of B is known. Then from Eq. (15), β may be calculated,

$$\beta = x^7 a_B$$

But from Eq. (10) we have

$$\beta = K^4 \epsilon_0 \eta \phi^4 \psi^4$$

or

$$\xi_0 = \beta(K^4_{\eta\phi\psi})^{-1} \quad (10a)$$

If we substitute this ξ_0 into Eq. (1a), we obtain

$$xK^4_{\eta\phi\psi}/\beta = \sum_1^{23} a_{i1} K^{a_{i3}\eta a_{i4}\phi a_{i5}\psi a_{i6}}$$

or

$$\sum_1^{22} a_{i1} K^{a_{i3}\eta a_{i4}\phi a_{i5}\psi a_{i6}} + \left(1 - \frac{x}{\beta}\right) K^4_{\eta\phi\psi} = 0$$

or

$$\sum_1^{22} a_{i1} K^{a_{i3}\eta a_{i4}\phi + a_{i5}/8 + a_{i6}/27} + \left(1 - \frac{x}{\beta}\right) K^{4\eta^{1+4/8+4/27}} = 0 \quad (10b)$$

Thus, Eqs. (10b), and (6) are two equations in two unknowns, $K + \eta$. These two equations can be solved simultaneously by numerical techniques to obtain Ω , since $\Omega = (6 + 12/8 + 8/27) RT \ln \eta$.

Square Interaction Model

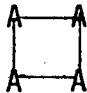
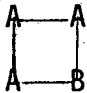
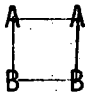
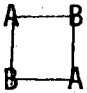
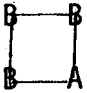
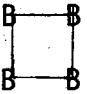
A second model is simpler and allows for the nearest and next-nearest neighbors only. Thus, in this model $I_1^0 = \Omega/(6 + 12/8)$ as is true in all models presented here for the cubic lattice which take only these two interactions into account. This model considers only those atoms at the corners of a square. The number of such squares may be determined by considering the unit cell, a cube. A cube has six square faces; but in a unit cell, each face is shared with another unit cell, implying that each unit cell may be associated with three faces. Now in a cubic lattice, one atom may be associated with each unit cell, implying that for N atoms there are $3N$ squares.

To determine the Boltzmann factors for each configuration, let us consider the relationship of the squares to each other. The edges of the squares represent the nearest neighbor interactions. Each edge is shared by four squares so that the interaction energy of dissimilar atoms is shared by the four squares. Thus, each dissimilar atom's nearest-neighbor interaction contributes 1/4 of the interaction energy of the pair to each of the squares. Thus, the Boltzmann factor for a dissimilar edge pair will be $\eta^{-1/4}$. The diagonals of a square are not shared so that dissimilar diagonal pairs (next nearest neighbors) will contribute the whole of the interaction energy to the associated square. This implies that the associated Boltzmann factor will be ϕ^{-1} .

Table 3 contains all the different possible configurations for the square model. The second column contains terms representing the total number of each configuration. These terms are composed of the total number of squares, $3N$, the number of orientations of the configuration, multiplicative constant, and the variable representing the fraction of squares in one orientation of the corresponding configuration. The third column lists the Boltzmann factors of the configurations.

Thus, we have a total of six configurational variables. It is necessary to develop the relationships between these variables in order to derive meaningful thermodynamic data from this model. The simplest relationships are those of the conservation of the species involved. Together all of the equations of species conservation state implicitly the conservation of mass equation, so that this equation would be dependent on the species conservation equations and, thus, unnecessary. The species conservation equations are

Table 3. Boltzmann factors and configurational Degeneracies for square-grouss in a binary system.

Configuration	Number in this Configuration	Boltzmann
	$3N\alpha$	$\eta^0 \phi^0$
	$3N4\zeta$	$\eta^{-2/4} \phi^{-1}$
	$3N4\nu$	$\eta^{-2/4} \phi^{-2}$
	$3N2\nu'$	$\eta^{-4/4} \phi^0$
	$3N4\xi$	$\eta^{-2/4} \phi^{-1}$
	$3N\beta$	$\eta^0 \phi^0$

$$N_A = N\alpha + 3N\zeta + 2N\nu + N\nu' + N\xi \quad (11a)$$

$$N_B = N\zeta + 2N\nu + N\nu' + 3N\xi + N\beta \quad (11b)$$

or

$$x_A = \alpha + 3\zeta + 2\nu + \nu' + \xi \quad (12a)$$

$$x_B = \zeta + 2\nu + \nu' + 3\xi + \beta \quad (12b)$$

In order to cut down on the writing, let I_i represent the i^{th} configurational variable and a_{i1} and b_{i2} represent the corresponding constants of Eqs. (12a) and (12b), respectively, giving:

$$x_A = \sum_1^6 a_{i1} I_i$$

$$x_B = \sum_1^6 a_{i2} I_i$$

Inspection of Eqs. (11a) and (11b) reveals that two of the six configurations are now no longer independent. For convenience let α and β be the two variables dependent on the other four.

Equations (11a) and (11b) are derived by determining the total effective number of atoms of the respective species in each of the configurations and summing and equating to the total number of each species. For example, consider species B. Each atom is shared by 12 squares in a cubic lattice, therefore, the fraction of that atom which is associated with a single square is 1/12. Therefore, the effective number of B in a particular configuration is the number of B at the corners multiplied by 1/12. Multiplying the effective number of B in a configuration by the total number of squares with that configuration then gives the total effective number of atoms of B associated with that configuration. These values are given in Table 4.

Table 4. Configuration numbers.

Total Number In Configuration	Effective Number B in Configuration	Total Effective B
$3N\alpha$	0	0
$3N4\zeta$	1/12	$N\zeta$
$3N4\nu$	2/12	$2N\nu$
$3N2\nu'$	2/12	$N\nu'$
$3N4\xi$	3/12	$3N\xi$
$3N\beta$	4/12	$N\beta$

In order to derive the relationships between the four presently independent variables, it is necessary to determine the values of these variables when in the state of equilibrium. This is done by determining the minimum Gibbs energy for each variable. With the six variables it is possible to develop an approximate partition function from which the Gibbs energy of mixing is easily obtainable as a continuous function of the four independent variables. Differentiating that function with respect to each of the independent configurational variables and equating with zero will give the remaining relationships between all of the configurational variables at the state of equilibrium.

Keeping in mind that $z_1 = 6$ and $z_2 = 12$, we can write the partition function Ω_0 by following the procedure outlined by Guggenheim in Mixtures and in Table 3, as

$$\Omega_0 = \frac{N!}{N_A! N_B!} \frac{[(3N\alpha^*)!][(3N\zeta^*)!]^4[(3N\nu^*)!]^4[(3N\nu'^*)!]^2[(3N\xi^*)!]^4[(3N\beta^*)!]}{[(3N\alpha)!][(3N\zeta)!]^4[(3N\nu^*)!]^4[(3N\nu')!]^2[(3N\xi)!]^4[(3N\beta)!]} \times \eta^{-z_1 N(\zeta + \nu + \nu' + \xi)} \phi^{-z_2 N(\zeta + 2\nu + \xi)} \quad (13)$$

In the partition function the term in front of the Boltzmann factors represents the number of orientations for a given set of values of the configurational variables. The starred variables are values of the configurational values in a completely random solution and have the following values with $x = x_B$, $1 - x = x_A$:

$$\begin{aligned}
 \alpha^* &= x_A^4 = (1-x)^4 \\
 \zeta^* &= x_A^3 x_B = x(1-x)^3 \\
 \nu^* &= \nu' = x_A^3 x_B^2 = x^2(1-x)^2 \\
 \xi^* &= x_A^1 x_B^3 = x^3(1-x) \\
 \beta^* &= x_B^4 = x^4
 \end{aligned}
 \tag{13a}$$

Now the total Gibbs energy of mixing ΔG_m is given by

$$\Delta G_m = RT \ln \Omega_0$$

Thus, minimizing this function with respect to the independent configurational variables results in

I	$\frac{\partial \ln \Omega_0}{\partial I} = 0$
ζ	$\alpha^3 \beta / \zeta^4 = \eta^2 \phi^4$
ν	$\alpha^2 \beta^2 / \nu^4 = \eta^2 \phi^8$
ν'	$\alpha \beta / \nu'^2 = \eta^2$
ξ	$\alpha \beta^3 / \xi^4 = \eta^2 \phi^4$

With the appropriate algebraic manipulations and the substitution $\xi/\zeta = K^2$, the following relationships can be derived.

$$\begin{aligned}
 \alpha &= K^{-2} \nu \eta^{1/2} \phi^2 \\
 \zeta &= K^{-1} \nu \eta^0 \phi \\
 \nu &= \nu \eta^0 \phi^0 \\
 \nu' &= \nu \eta^{-1/2} \phi^2 \\
 \xi &= K \nu \eta^0 \phi \\
 \beta &= K^2 \nu \eta^{1/2} \phi^2
 \end{aligned}
 \tag{14}$$

Let a_{i3} , a_{i4} , and a_{i5} be the exponents of k , η , and ϕ , respectively, for the i^{th} component of Eq. (14) and substitute Eq. (14) into Eqs. (12a) and (12b).

Then,

$$x_A = \sum_1^6 a_{i1} K^{a_{i3} \eta^{a_{i4}} \phi^{a_{i5}}} \nu$$

$$x_B = \sum_1^6 a_{i2} K^{a_{i3} \eta^{a_{i4}} \phi^{a_{i5}}} \nu$$

Factoring out and isolating ν , we can equate the two equations to obtain

$$x_A \sum_1^6 a_{i2} K^{a_{i3} \eta^{a_{i4}} \phi^{a_{i5}}} = x_B \sum_1^6 a_{i1} K^{a_{i3} \eta^{a_{i4}} \phi^{a_{i5}}}$$

or

$$\sum_1^6 (a_{i2} - x(a_{i1} + a_{i2})) K^{a_{i3} \eta^{a_{i4}} \phi^{a_{i5}}} = 0$$

With η , ϕ , and α given, it is then possible to solve for K , and then possible to calculate the values of the configurational variables.

Further simplification can be attained by assuming Van der Waals behavior, in which case as pointed out earlier:

$$\sum_1^6 [a_{i2} - x(a_{i1} + a_{i2})] K^{a_{i3} \eta^{a_{i4}} + \frac{a_{i5}}{8}} = 0 \quad (15)$$

Now that the configurational variable values have been determined for equilibrium, the enthalpy of mixing may be calculated by summing up all the energies of interaction of differing species. Designating the exponent of η and ϕ under the Boltzmann column of Table 3 as e_{i1} and e_{i2} , respectively, for the i^{th} configuration, we now define E_i as

$$E_i = e_{i1} + e_{i2}/8$$

Noticing that the number of orientations for each configuration is equal to $a_{i1} + a_{i2}$, we may then write for the molar enthalpy of mixing,

$$\Delta H_M = \frac{6}{1} \sum (a_{i1} + a_{i2}) I_i(E_i) \Omega / (6 + 12/8)$$

The molar Gibbs energy of mixing may also be calculated and is given by

$$\Delta G_M = \frac{RT}{N_0} \ln \Omega_0$$

where N_0 is the number of moles used in calculating Ω_0 as contrasted with N , the number of atoms used in calculating Ω_0 . The partial molar Gibbs energy of B is then

$$\overline{\Delta G}_B = \frac{\partial N_0 \Delta G_M}{\partial N_B} = RT \frac{\partial \ln \Omega_0}{\partial N_B}$$

All of the configurational variables starred or unstarred are functions of x or N_B

$$\overline{\Delta G}_B = RT \left[\sum_1^6 \left(\frac{\partial \ln \Omega_0}{\partial I_i^*} \frac{dI_i^*}{N_B} + \frac{\partial \ln \Omega_0}{\partial I_i} \frac{dI_i}{N_B} \right) + \frac{\partial \ln \Omega_0}{\partial N} \frac{dN}{dN_B} + \frac{\partial \ln \Omega_0}{\partial N_B} \right]$$

Now assigning values to I_i^* appropriate for a completely random arrangement (regular solution) is equivalent to maximizing Ω_0 . Therefore,

for the starred configurational variables excluding α^* and β^* which are dependent on the others, we find

$$\frac{\partial \ln \Omega_0}{\partial I_j^*} = 0$$

Similarly, in determining the equilibrium values of the unstarred variables, it was necessary to minimize $\ln \Omega_0$ with respect to these variables implying

$$\frac{\partial \ln \Omega_0}{\partial I_j} = 0$$

such that I_j here does not include α and β . Now by Eq. (11a) it is known that α and α^* are independent of N_B . Therefore,

$$\frac{\partial \ln \Omega_0}{\partial \alpha} = 0$$

and

$$\frac{\partial \ln \Omega_0}{\partial \alpha^*} = 0$$

Thus, the only relevant terms are those involving N , N_B , β^* , and β .

Performing the indicated operations we get:

$$\overline{\Delta G}_B = RT \left[\ln x + \ln \left(\frac{\beta}{\beta^*} \right)^3 \right] \quad (15a)$$

Similarly for $\overline{\Delta G}_A$:

$$\overline{\Delta G}_A = RT \left[\ln(1 - x) + \ln \left(\frac{\alpha}{\alpha^*} \right)^3 \right] \quad (15b)$$

Thus, a simpler expression for ΔG_m is

$$\Delta G_m = RT \left[x \ln x \left(\frac{\beta}{\beta^*} \right)^3 + (1 - x) \ln (1 - x) \left(\frac{\alpha}{\alpha^*} \right)^3 \right] \quad (16)$$

Substituting for α^* and β^* from Eqs. (13a), we find

$$\Delta G_m = RT \left[x \ln x \left(\frac{\beta}{x^4} \right)^3 + (1 - x) \ln (1 - x) \left(\frac{\alpha}{(1 - x)^4} \right)^3 \right] \quad (16a)$$

Furthermore, the activities and activity coefficients are:

$$\gamma_A = \left(\frac{\alpha}{(1 - x)^4} \right)^3 \quad \gamma_B = \left(\frac{\beta}{x^4} \right)^3 \quad (17)$$

$$a_A = (1 - x) \left(\frac{\alpha}{(1 - x)^4} \right)^3 \quad a_B = x \left(\frac{\beta}{x^4} \right)^3$$

These expressions are useful in describing deviations from ideality in liquid alloys known to exhibit square and cube clustering.

LEGAL NOTICE

This report was prepared as an account of work sponsored by the United States Government. Neither the United States nor the United States Energy Research and Development Administration, nor any of their employees, nor any of their contractors, subcontractors, or their employees, makes any warranty, express or implied, or assumes any legal liability or responsibility for the accuracy, completeness or usefulness of any information, apparatus, product or process disclosed, or represents that its use would not infringe privately owned rights.

TECHNICAL INFORMATION DIVISION
LAWRENCE BERKELEY LABORATORY
UNIVERSITY OF CALIFORNIA
BERKELEY, CALIFORNIA 94720